50272-101

REPORT DOCUMENTATION PAGE	1. REPORT NO. MA-RD-940-80056	2.	3. Recipient's Accession No.

4. Title and Subtitle
Ship Springing - An Experimental and Theoretical Study

5. Report Date
May 1980

6.

7. Author(s)
Armin Troesch

8. Performing Organization Rept. No.
219

9. Performing Organization Name and Address
Dept. of Naval Architecture & Marine Engineering
The University of Michigan
Ann Arbor, MI 48109

10. Project/Task/Work Unit No.

11. Contract(C) or Grant(G) No.
(C) 7-38060
(G)

12. Sponsoring Organization Name and Address
The American Bureau of Shipping, 65 Broadway, New York NY 10006
and
Maritime Administration, Office of Commercial Development
Washington, D.C. 20230

13. Type of Report & Period Covered
Final

14.

15. Supplementary Notes

16. Abstract (Limit: 200 words)

The results of an experimental and theoretical study investigating the main hull girder vibrations of Great Lakes ore carriers are presented. The source of excitation is considered to be the incident waves. The emphasis of the work is on the hydrodynamic aspects. Both linear and non-linear springing excitation are considered.

17. Document Analysis a. Descriptors
Wave induced bending moments
Springing
Non-linear ship dynamics
Experimental springing results

b. Identifiers/Open-Ended Terms

c. COSATI Field/Group

18. Availability Statement
Approved for Release
National Technical Information Service
Springfield, Virginia 22151

19. Security Class (This Report) Unclassified

20. Security Class (This Page) Unclassified

21. No. of Pages

22. Price

No. 219
May 1980

SHIP SPRINGING - AN EXPERIMENTAL AND THEORETICAL STUDY

Prepared by:

Armin W. Troesch

January 31, 1980

Co-sponsored by

The American Bureau of Shipping
U.S. Department of Commerce, Maritime Administration
Office of Commercial Development

Department of Naval Architecture
and Marine Engineering
College of Engineering
The University of Michigan
Ann Arbor, Michigan 48109

TABLE OF CONTENTS

PREFACE

The work performed under the ABS-MARAD Springing contract represents the efforts of many individuals. The initial motivation and continuing drive were supplied by the Project Director, T.F. Ogilvie. Professors H. Maeda, M. Ohkusu, and Dr. K. Saito, all Visiting Research Scientists from Japan, provided valuable help and insight to the project. The students of the Department aided in the construction and testing of the model. In particular, Mr. K. Bongort was responsible for much of the computer software used in the data analysis. This broad range of support made the successful completion of the project possible.

LIST OF ILLUSTRATIONS

Introduction

The stated goal of the Ship Springing Project was to understand the fundamental mechanisms of the springing phenomenon. After nearly two years of research during which both theoretical and experimental studies were made, a number of conclusions can be drawn. The primary one is that the nature of Great Lakes springing is at least as complex as originally invisioned.

Many investigators in the past have approached the problem from either a linear or nonlinear bias. The experiments conducted in our tank indicate that both approaches are necessary. A Great Lakes bulk carrier can be excited in the springing mode by both high frequency, short waves, (the linear case) and low frequency, long waves (the nonlinear case). The extent to which one dominates over the other is dependent upon the sea state that the vessel operates in. Based upon the linear theory proposed by either Bishop, et.al. (1977) or Maeda (1979), a reasonable analytical model of a ship operating in short waves may be formulated. However, there currently exists relatively little information in the literature that would help the designer predict the nonlinear response. The one recent publication that shows promise is an article by J. Jensen and P.T. Pedersen (1978). There are a number of difficulties, though, associated with the theory presented in that paper. The effects of the authors' improper handling of the nonlinear free surface condition must be understood before any definite conclusions on the usefulness of the theory can be made.

The work, then, performed under this contract can be separated into two parts: the part addressing the linear model and the part addressing the nonlinear model. Most of the success of the project has been in the linear effort. However, many of the results obtained in that effort, (for example, the added mass and damping coefficients) are directly applicable to the nonlinear analysis.

In this report, the following topics will be discussed: the linear theory of ship springing, short wave experiments, comparison of short wave theory and experiment, long wave experiments, and the nonlinear, long wave theory. Again it should be emphasized that the nonlinear theory part of this project consisted of determining the deficiencies of existing theories. Until these are known, there would be little use in proposing a new approach.

Linear Theory of Ship Springing

There have existed in the past, several strip theories that calculated the springing excitation and motion coefficients based upon a part rational and part intuitive approach. Some of them in this category are Belgova (1962), Goodman (1971), van Gunsteren (1974), and Hoffman and van Hooff (1976). A more analytical method was proposed by Bishop, et.al. (1977) and Maeda (1979). (Some of the practitioners in the field claim this new method is unnecessarily complicated.) The work done by Maeda was performed under this contract.

The approach taken by Bishop, et.al. (1977) and Maeda (1979) was to define the vertical deflection of the ship as the sum of vibratory modes of the vessel in *air*. These are referred to as "dry modes" and should be contrasted with the "wet modes" used in the typical ship vibration problem. While the use of dry modes complicates the problem somewhat, they insure that the derivation is rigorous.

One advantage that Maeda's representation has over Bishop's is found in the form of the generalized exciting force. If one ignores end effects, or has a hull form that is pointed at both ends, then the two are mathematically equivalent. However, Maeda's form is better suited for computation. In particular, a part of the forward speed component of the exciting force as given by the two theories is shown below:

Bishop et.al. (1977) $\psi_k(x) U \frac{d}{dx} [a(x) + \frac{1}{i\omega} b(x)]$

Maeda (1979) $U[a(x) + \frac{1}{i\omega} b(x)] \frac{d}{dx} \psi_k(x)$

where $\psi_k(x)$ is the k mode shape,

U is the ship velocity,

ω is the frequency of encounter,

$a(x)$ is the sectional added mass,

and $b(x)$ is the sectional damping.

The first result requires the differentiation of the sectional added mass and damping, while the second result requires that the mode shape be differentiated. For a typical Great Lakes bulk carrier, the added mass and damping are constants for much of the length. Only in the bow and stern areas are there significant changes in the coefficients. Their derivatives then, are

large in the regions where strip theory is least valid. Conversely, the mode shape for the first few modes is a relatively smooth function with derivatives that change gradually. This implies that the second representation will be less sensitive to the inaccuracies of the sectional added mass and damping predicted by strip theory.

For an example of the longitudinal distribution of added mass and damping in heave, see Figure 1. Here the coefficients are plotted as functions of position along the hull. The three curves shown represent various ways of finding the added mass and damping. The curve labeled "2-D Lewis Forms" is the usual three parameter fit of ship sections. This is the method normally used by the computer program developed for the springing analysis. The curve labeled "2-D Close Fit" is a representation of the hull sections by line segments. The procedure used in this particular program was first formulated by Troesch (1975). It was later modified under this contract to take care of certain eigen frequencies where the coefficients become singular. The method to correct this problem is described by Ogilvie and Shin (1978). The third curve labeled "3-D Solution" is a complete three dimensional solution to the forced oscillation boundary value problem. This program was supported, in part, by the springing project and is described by Shin (1979).

The use of the 2-D Lewis forms is recommended for typical ship design problems. While it is potentially the least accurate of the three methods, it is also the least expensive to run. The more accurate 3-D solution can cost over *one hundred* times as much as the Lewis form program. This large increase in cost does not really justify its use, even though there is an improvement in accuracy.

The calculation of the generalized exciting force involves the product of an oscillatory term, the mode shape (or its derivative), and the added mass, damping and beam. See equations (4-101)and (4-120) in Maeda (1979). The oscillatory term is $\exp(-i\kappa x\cos\beta)$ where κ is the wave number and β is the heading angle. The wave length where springing occurs is small, approximately 1/6 the ship's length. As a result, the integral involving the exciting force oscillates many times between the limits of integration. If a standard integration formula is used, for example, Simpson's Rule, then many stations must be included. However, by incorporating the oscillatory nature of the integral into the quadrature formula (see for example, Tuck (1967)), this can be avoided. It is then only necessary to provide a station spacing that gives

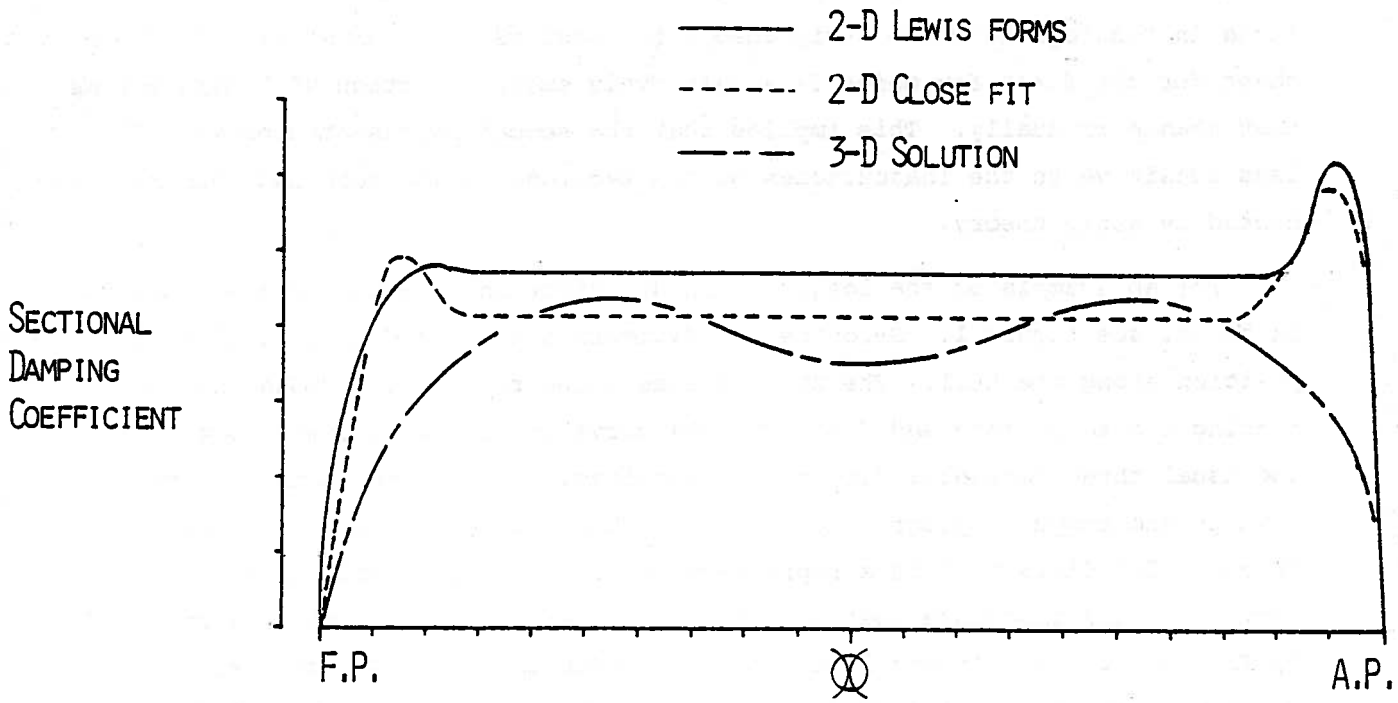

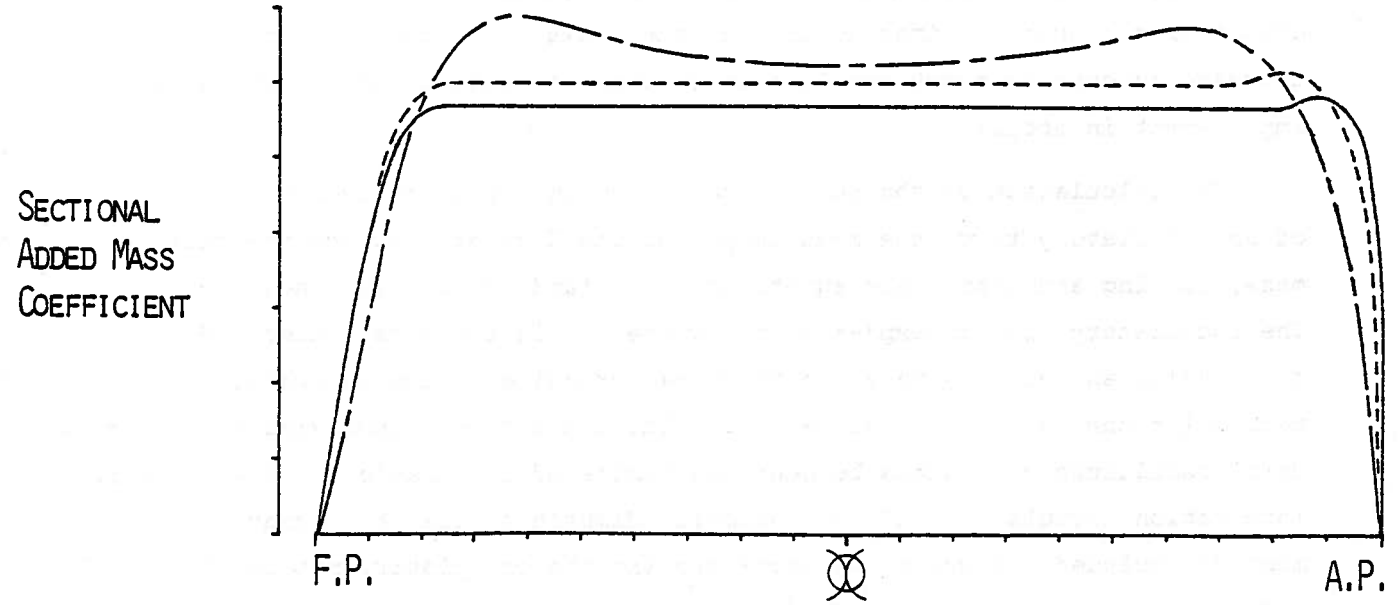

FIGURE 1: SECTIONAL ADDED MASS AND DAMPING FOR THE S.J. CORT
SHIP LENGTH/WAVE LENGTH = 2.0

an adequate representation of the added mass and damping. For Great Lakes bulk carriers, as shown in Figure 1, this means more stations in the bow and stern regions.

The effect of putting more stations in the bow and stern areas is shown in Figure 2. Here the derivatives of the sectional added mass and damping coefficients are plotted as functions of position along the hull. The damping coefficient is represented by the amplitude ratio $\bar{A}(x)$. The total sectional damping, $b(x)$, is given by

$$b(x) = \frac{\rho g^2 \bar{A}^2}{\omega^3}$$

The ship length to wave length ratio for this particular figure is 4.72. Three curves are shown. The first represents the derivatives based upon twenty-one (21) stations spaced equally along the length of the ship. The second is the derivatives based upon forty-one (41) equally spaced stations. The third represents the derivatives based upon thirty-nine (39) stations. However, in this case the ship was divided into three parts and a different station spacing was used in each part. The midship segment had fewer stations while the bow and stern segments had more. If the springing excitation is calculated by the formula given by Bishop et. al. (1977), where the forward speed effect is a function of the longitudinal distribution of the derivatives of the added mass and damping coefficients, then a significantly different answer will be found depending upon which curve is selected. In the springing computer program that compares springing theory with experiments, the third method, the one where the ship is divided into three segments, is the one that is used. Numerical calculations of the exciting force are shown in the section that compares short wave theory with experiments.

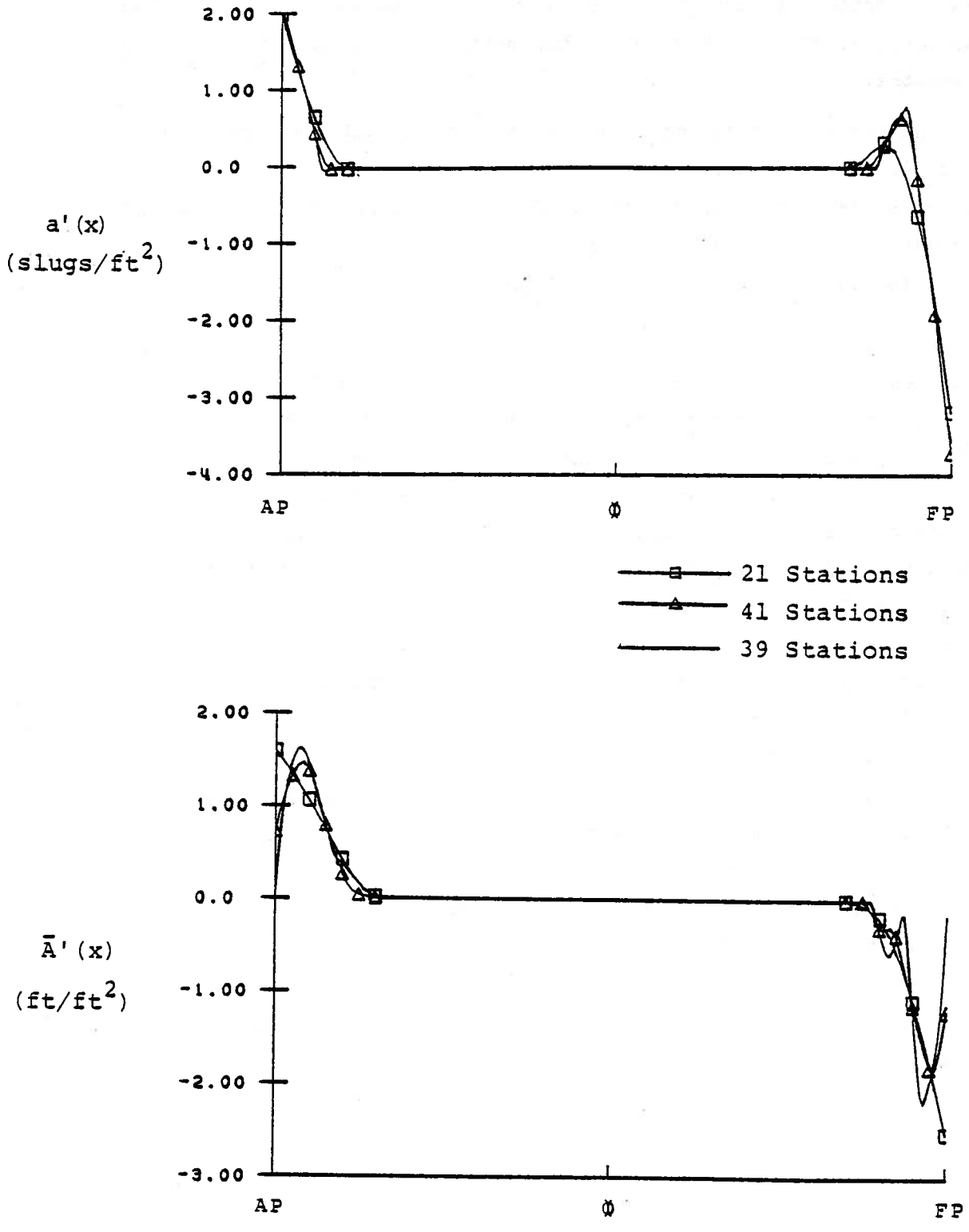

FIGURE 2: LONGITUDINAL DISTRIBUTION OF THE DERIVATIVES OF THE ADDED MASS AND DAMPING FOR THE SPRINGING MODEL. SHIP LENGTH/WAVE LENGTH = 4.72, NO FORWARD SPEED

Short Wave Experiments

A 15 foot fiberglass model of the *S.J. Cort* was constructed for the project. In a manner similar to that described by Hoffman and van Hooff (1976), the model was made in two halves connected by a spring at midships. See Figure 3 for a description of the model and the quantities measured.

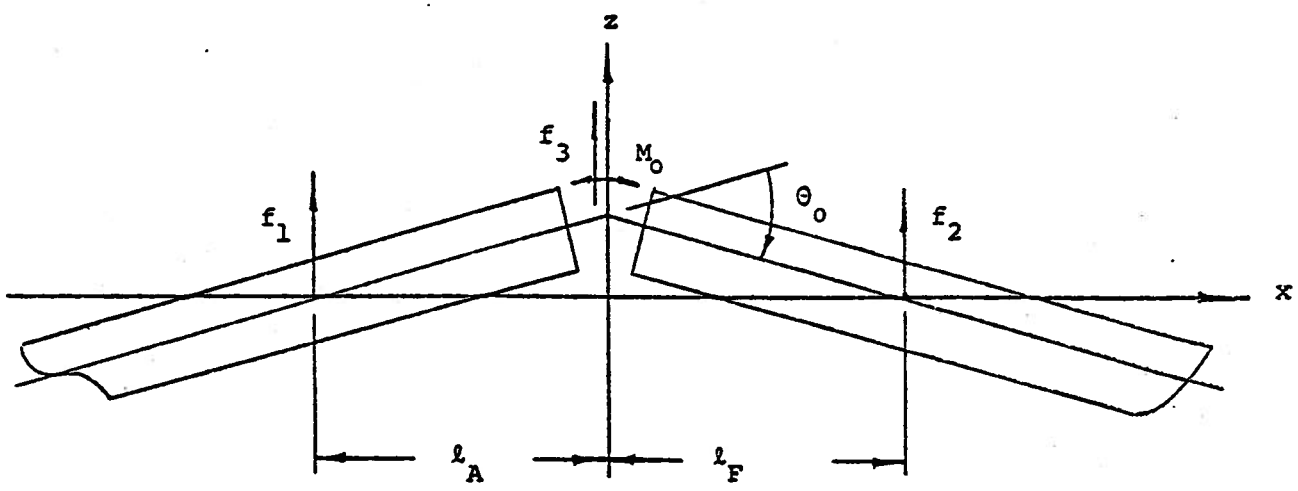

FIGURE 3: SCHEMATIC OF MODEL FOR SPRINGING EXPERIMENTS

In Figure 3, f_1 , f_2 , and f_3 are the measured forces, M_o is the midship bending moment, $\ell_A=-x_{cg_A}$ where x_{cg_A} is the x coordinate of the center of gravity of the after part of the model and $\ell_F=x_{cg_F}$ where x_{cg_F} is the x coordinate of the center of gravity of the forward part of the model.

The model has three degrees of freedom. The normalized linear coupled equations of motion can be written in the following form.

$$\ddot{q}_0(t)a_{00} + \sum_{j=0}^{2} [A_{0j}\,\ddot{q}_j(t) + B_{0j}\,\dot{q}_j(t) + C_{0j}\,q_j(t)] = f_1 + f_2 + f_3 + E_0 \qquad (1)$$

$$\ddot{q}_1(t)a_{11} + \sum_{j=0}^{2} [A_{1j}\,\ddot{q}_j(t) + B_{1j}\,\dot{q}_j(t) + C_{1j}\,q_j(t)] = x_{cg_A}f_1 + x_{cg_A}f_2 + E_1 \qquad (2)$$

$$\ddot{q}_2(t)a_{22} + \dot{q}_2(t)b_{22} + \sum_{j=0}^{2} [A_{2j}\,\ddot{q}_j(t) + B_{2j}\,\dot{q}_j(t) + C_{2j}\,q_j(t)] = -x_{cg_A}f_3 + M_0\left[1 - \frac{x_{cg_A}}{x_{cg_F}}\right] + E_2 \qquad (3)$$

The generalized coordinates are given as

$$q_0(t) = \xi_3 \, e^{i\omega_e t + i\alpha_0}$$

$$q_1(t) = \xi_5 \, e^{i\omega_e t + i\alpha_1}$$

$$q_2(t) = [\theta_0/(1+\ell_A/\ell_F)] \, e^{i\omega_e t + i\alpha_2}$$

where

ξ_3 is the heave amplitude,

ξ_5 is the pitch amplitude,

and θ_0 is the midship deflection angle.

The mode shapes, z_i, are defined as follows:

$$z_0 = 1$$

$$z_1 = x$$

$$z_2 = \begin{cases} \ell_A + x & \text{for } x \leq 0 \\ (\ell_A/\ell_F)(\ell_F - x) & \text{for } x \geq 0 \end{cases}$$

The midship bending moment, M_0, is given as

$$M_0(t) = -K_s(1 + \ell_A/\ell_F) q_2(t)$$

where K_s is a spring constant.

The coefficients have the following forms:

$a_{00} = M$, the mass of the model,

$a_{11} = I$, the mass moment of inertia of the model about midships,

$a_{22} = I_A + \left(\frac{\ell_A}{\ell_F}\right) I_F$ where I_A and I_F are the mass moments of inertias about the centers of gravity of the after part and forward part respectively,

$E_i = \int_L dx \, z_i(x) \, f_e(x,t)$ where f_e is the sectional hydrodynamic exciting force,

and $C_{ij} = \int_L dx\, z_i(x)\, z_j(x) \rho g\, B(x)$ where ρg is the weight density of the fluid and B is the beam of the ship.

Also A_{ij} represents the i-th generalized hydrodynamic force due to an acceleration in the j-th mode,

B_{ij} represents the i-th generalized hydrodynamic force due to a unit velocity in the j-th mode,

and b_{22} represents the springing internal mechanical damping.

Note that f_e represents the hydrodynamic pressures on the hull and may include forward speed effects if the model is moving forward. For the complete theoretical expressions of these coefficients, see the corresponding formulas given by Maeda (1979).

As explained in the linear theory section, the vertical displacements are expanded in terms of the dry modes. For our particular case this is heave, pitch, and springing. These mode shapes must satisfy a condition of orthogonality that requires

$$M_A + M_F = M \ ,$$

$$M_A \ell_A = M_F \ell_F \ ,$$

and

$$I_A = (\ell_A / \ell_F) I_F \ .$$

Here M_A and I_A and M_F and I_F are the mass and mass moment of inertia of the after part and the forward part respectively. Appendix A gives a model body plan and the complete model particulars.

Of the three equations of motion, (3) was the one that we considered as most important. Much of the experimental effort was directed at determining, or at least understanding, the influence of terms in that expression.

The added mass and damping terms in springing, A_{22} and B_{22}, were determined by restraining the model at points ℓ_A and ℓ_F. Springs of different stiffnesses were then put at midships and decrement tests performed. See Figure 4 for a typical record; the vertical scale is proportional to the bending moment and the horizontal scale is the elapsed time in seconds. From these records it is possible to calculate the added mass and damping by assuming

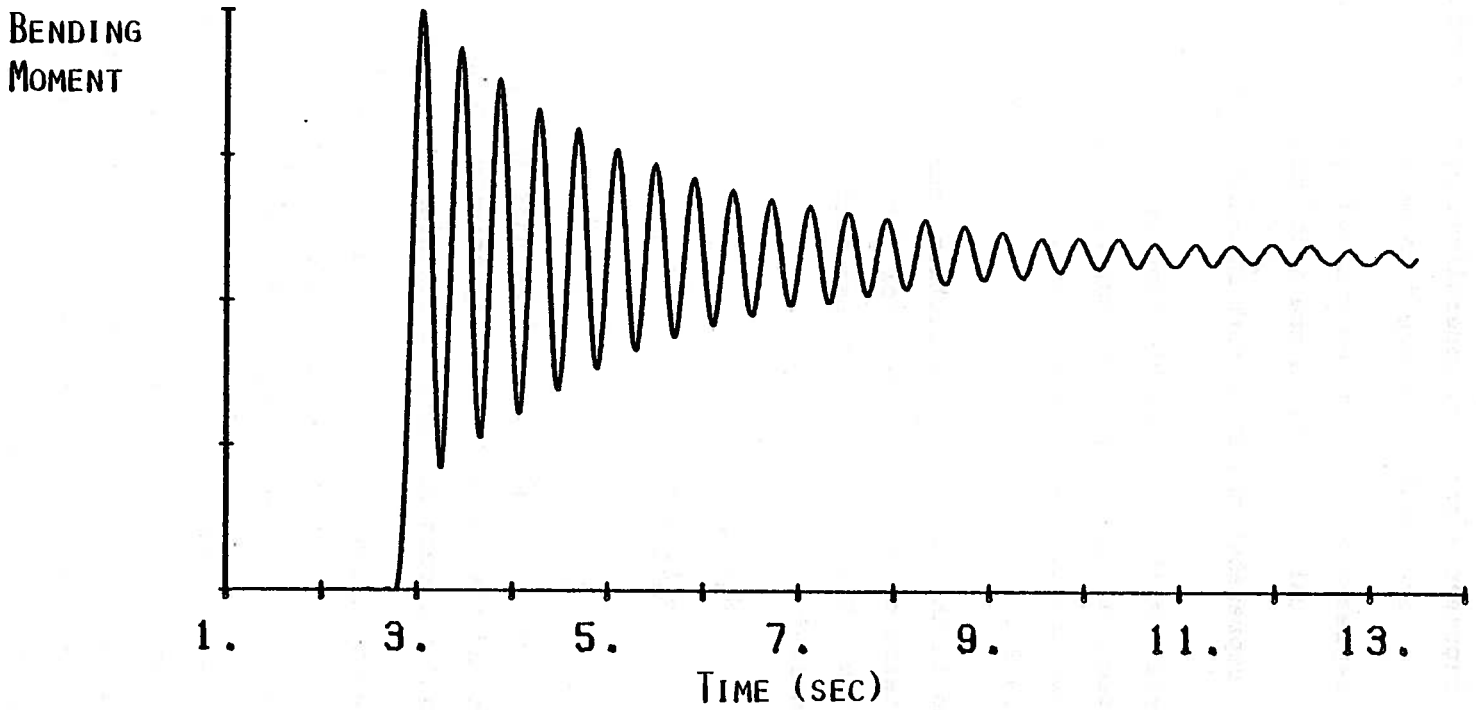

FIGURE 4 : TYPICAL DECREMENT TEST

that the system can be modeled by a second order ordinary differential equation with constant coefficients. (The method is described in Appendix B.) This type of approach ignores the memory effects of the free surface which have been shown to be important in lower frequency, higher damped motions such as heave and pitch. For a discussion of this pheonomenon, see Golovato (1959). To insure that this was not a problem with the springing experiments, a number of decrement records were analyzed using a convolution integral technique described by Freakes and Keay (1966). The results from this limited study indicated that the system had a sufficient lack of damping to make free surface memory effects insignificant.

Figure 5 shows a typical plot of A_{22} and B_{22} as a function of speed for a given frequency of oscillation. The frequency was not fixed for the different speeds shown in the plots, only the spring thickness was. However, one result of the tests is that the frequency and thus the added mass are speed independent. In other words, fixing the spring thickness is equivalent to fixing the natural frequency of the model for any of the speeds tested.

Figure 6 shows a plot of A_{22} and B_{22} as a function of frequency for a Froude number of 0.128. The added mass shows a slight increase with increasing frequency while the damping generally decreases with increasing frequency. The damping at a frequency of 16.1 radians per second appears to be influenced by increased mechanical damping. This may have been caused by some misalignment of the bearings at attachment points ℓ_A and ℓ_F. In order to verify the nature of the damping curve, the decrement tests at this particular Froude number were repeated. This time, however, in addition to using different springs to get a frequency variation, the inertia of the model was also changed by adding and removing ballast weight. The results are shown in Figure 7. The original data is included for reference. As can be seen in the figure, the high damping coefficient at a frequency of 16.1 radians per second was not repeated.

The level of internal damping was estimated for the various springs by hanging the model in air from the attachment points at ℓ_A and ℓ_F, and then displacing the bow and recording the resultant decrement signal. The mechanical damping was typically in the range of 12 to 27 slug-ft^2/sec. Figure 8 shows the air decrement test results for a spring thickness of 0.500 inch. The frequency variation was achieved by moving weights in the model and con-

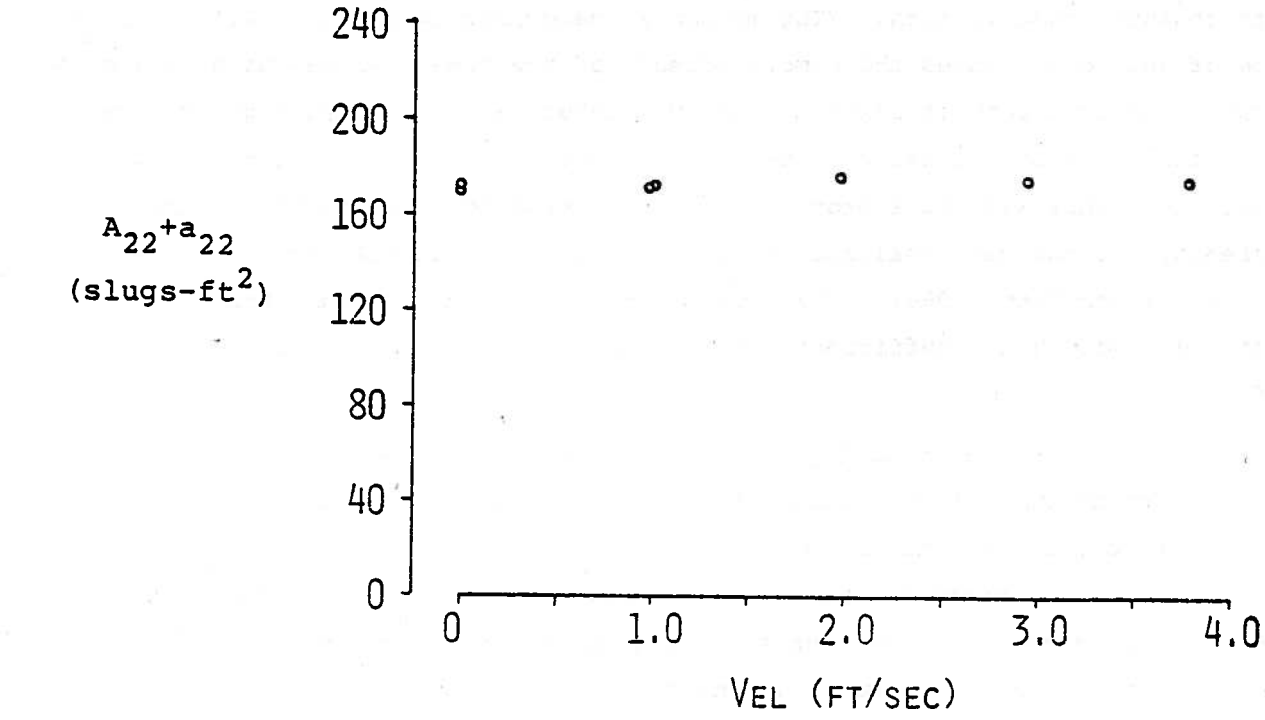

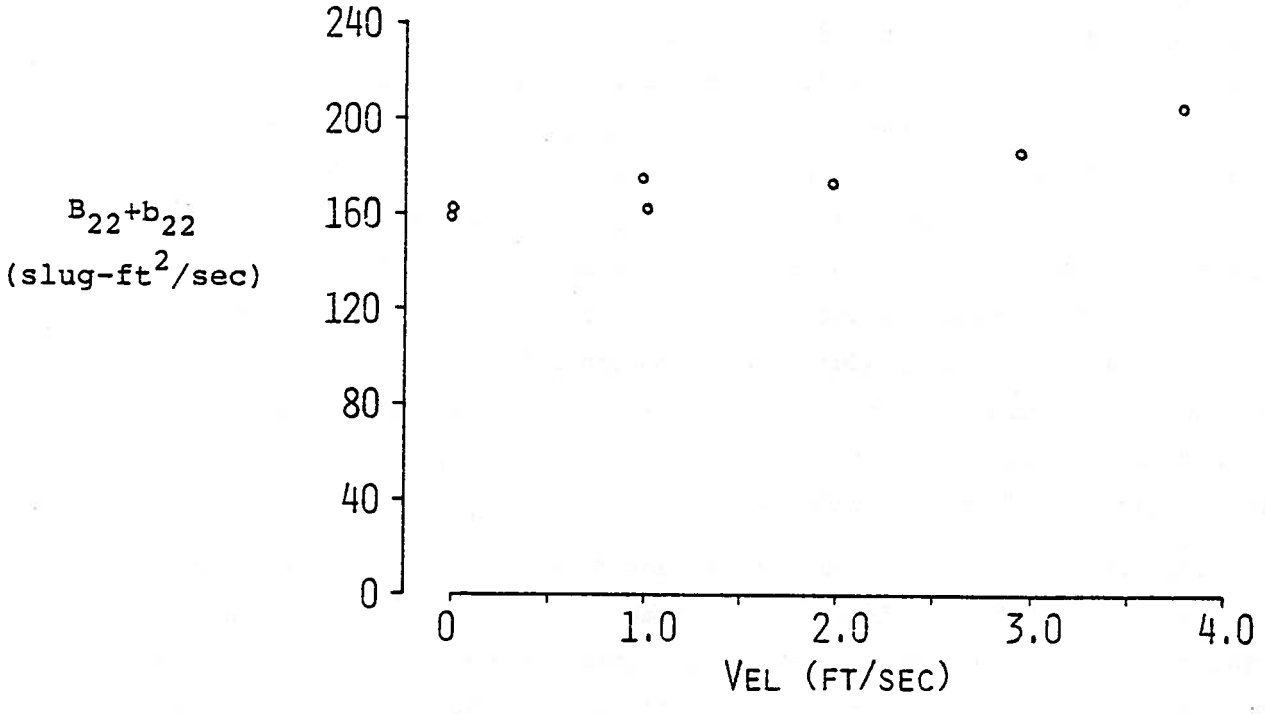

FIGURE 5: MODEL ADDED MASS AND DAMPING AS A FUNCTION OF SPEED. FREQUENCY OF OSCILLATION $\simeq$2.59 CPS. SPRING THICKNESS =.585 IN.

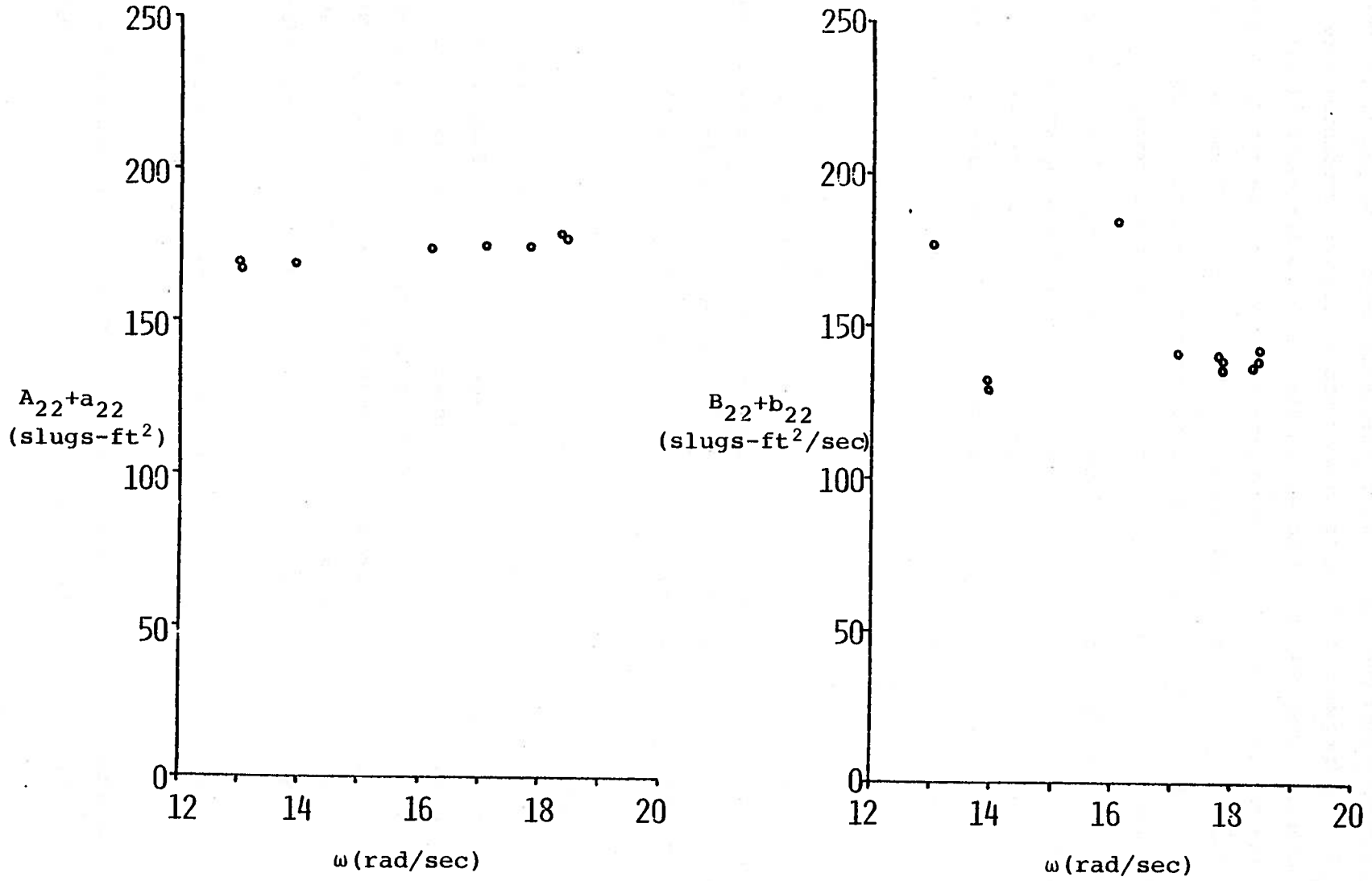

FIGURE 6: MODEL ADDED MASS AND DAMPING AS A FUNCTION OF FREQUENCY. MODEL VELOCITY ≈2.9 FT/SEC

sequently changing the mass moment of inertia. There was a 8% change in the damping coefficient over this limited frequency range. Two points are worth noting. The frequencies at which these tests in air were conducted were considerably higher than the frequencies for the decrement tests in water. Also, the bearings, when in air, were pre-loaded with the weight of the model shell but when in the water, had approximately zero load. These two points raise questions as to the usefulness of subtracting a mechanical damping coefficient determined in air from test results conducted in water.

In order to appreciate the relative magnitude of damping in water of the model (and of the full scale ship), consider the following approximation. Let the springing of the hull be described by a typical spring-mass-dash pot system. For example, let x be the deflection. Then the differential equation governing the motion is

$$m\ddot{x} + c\dot{x} + kx = Fe^{i\omega t}$$

where the dots over the x variable denote differentiation with respect to time and m is the mass, c is the damping that includes both internal and hydrodynamic effects, and k is the spring constant. F, a constant, is the amplitude of the exciting force. A plot of the normalized response (also called the magnification factor) is shown in Figure 9. The critical damping is defined as

$$c_m = 2\sqrt{mk}$$

The model had damping coefficients that averaged .023 c_m, while a typical value for the *S.J. Cort* might be .030 c_m (see Noll (1978)). From the plot, it is clear that the system is lightly damped. At resonance, an oscillatory force will cause a displacement and thus, subsequent stress, that is *seventeen* times larger than the displacement and stress that would exist if the same force were applied in a static, nonoscillating manner. Given this low level of damping, a small excitation at resonance will produce significant deflections.

A description of the added mass and damping tests, along with test results, are given in Appendix B.

To determine the values of the coupling coefficients between springing and heaving and springing and pitching, A_{02} , B_{02} , and A_{12} , B_{12} respec-

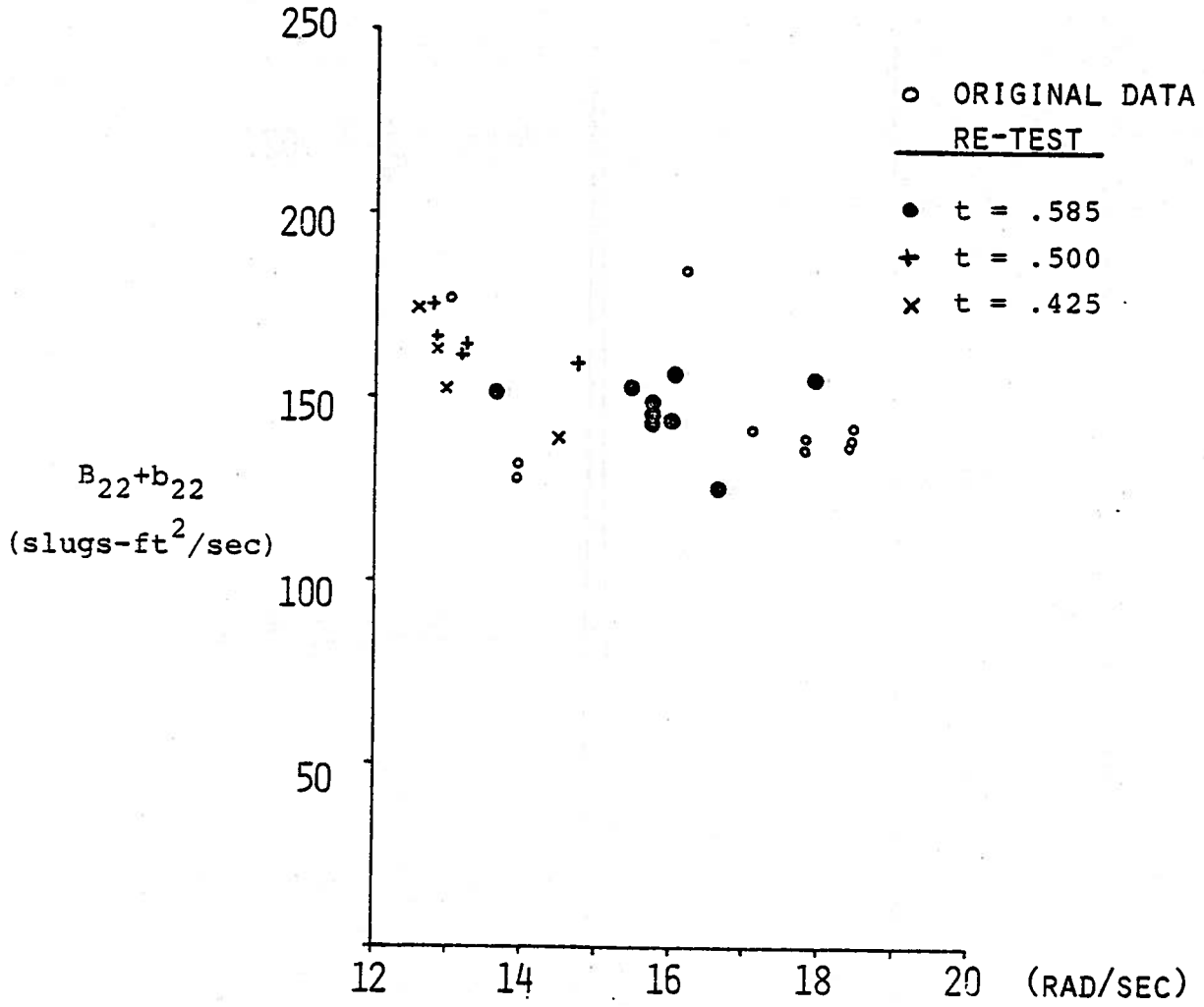

FIGURE 7: MODEL DAMPING AS A FUNCTION OF FREQUENCY RE-TEST. MODEL VELOCITY ≃ 2.9 FT/SEC

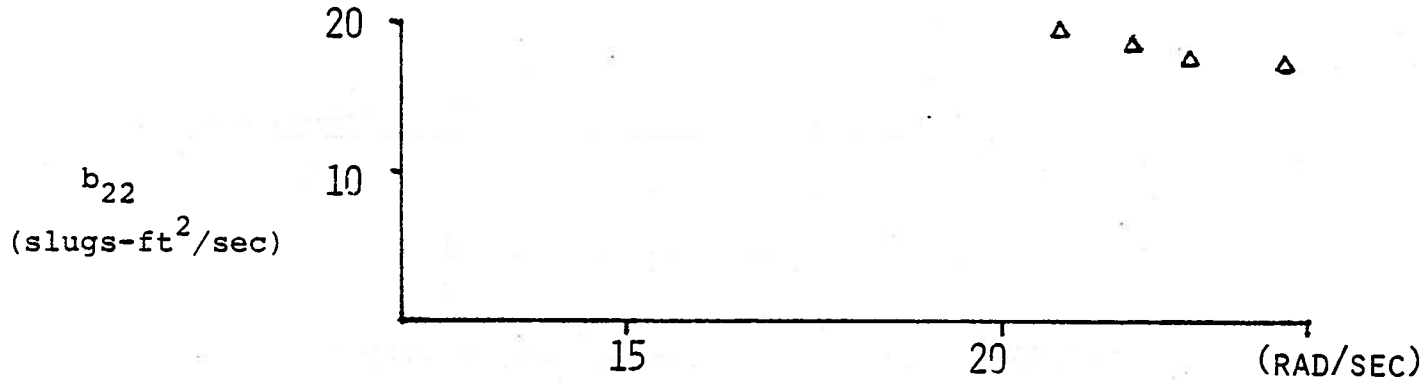

FIGURE 8: INTERNAL MECHANICAL DAMPING AS DETERMINED FROM THE DECREMENT TEST.

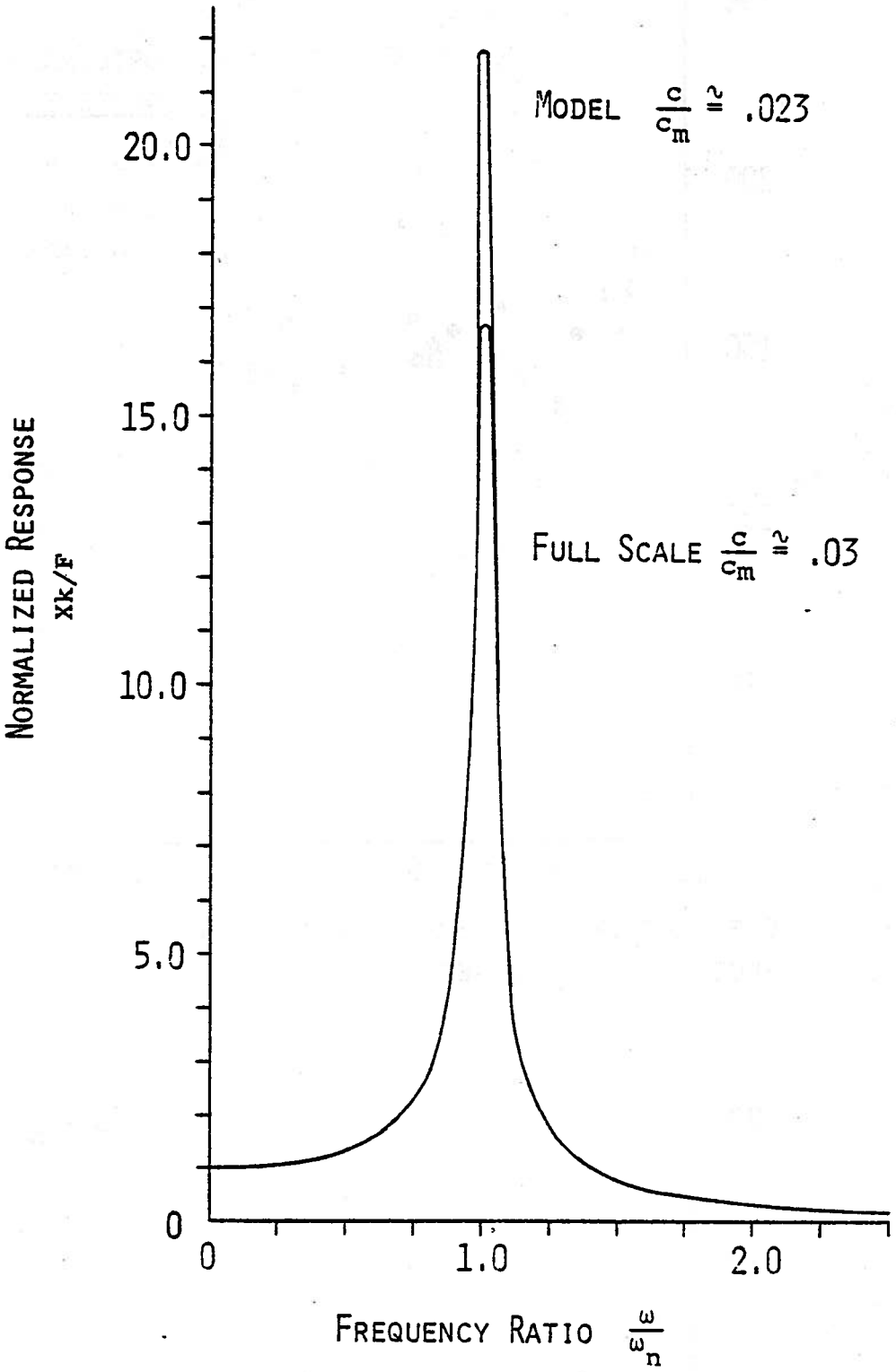

FIGURE 9: RESPONSE OF SPRING-MASS SYSTEM TO UNIT EXCITING FORCE WITH DAMPING FACTORS SIMILAR TO S.J. CORT (MODEL AND FULL SCALE).

tively, the model was to be oscillated at a high frequency and the responses measured. Preliminary tests indicated, however, that the natural frequency of the towing carriage and the shaker mechanism was in the frequency range of interest. Consequently, the carriage dynamics would interfere with the model measurements. Another way to find the effect of the heave and pitch motions on springing is to run the springing tests with the model restrained from heaving and pitching, and then to do the same tests over again with the model unrestrained. This was the procedure used when the springing excitation tests were conducted.

The generalized springing excitation, E_2 in equation (3), was determined by making the spring at midship very stiff and restraining the model from heave and pitch. All the dynamic and static displacement terms of (3), the entire left side, were approximately equal to zero. The model was not attached to the shaker mechanism at midships so f_3 was also zero. The excitation was then directly proportional to the bending moment in the spring. The incident wave and resultant moment were Fourier analyzed by fast Fourier Transforms. In Figure 10, a typical frequency decomposition of the amplitude are shown. The top record is proportional to the incident wave and the bottom record is proportional to the model's response, the bending moment. The horizontal axis is the frequency of encounter in cycles per second. As can be seen from the plots, the input and output at the fundamental frequency of encounter is narrow banded. This particular test, then, yielded accurate results only around that one frequency. Figure 11 shows the model springing excitation as a function of ship length to wave length. The *'s denote the response at ω_0, the fundamental frequency of encounter, and the □'s denote the response at a frequency near ω_0. The Δ's denote separate tests where the plunger amplitude and thus the wave amplitude were increased. This test served as a linearity check. These series of tests are more fully described in Appendix C.

In order to check on the influence of the heave and pitch motions on springing, the tests described in the previous paragraph were conducted a second time. In this series of tests, the model was disconnected from the shaker mechanism and allowed to heave and pitch. The results are shown in Figure 12. Comparing Figure 11 to Figure 12, one can see some differences, par-

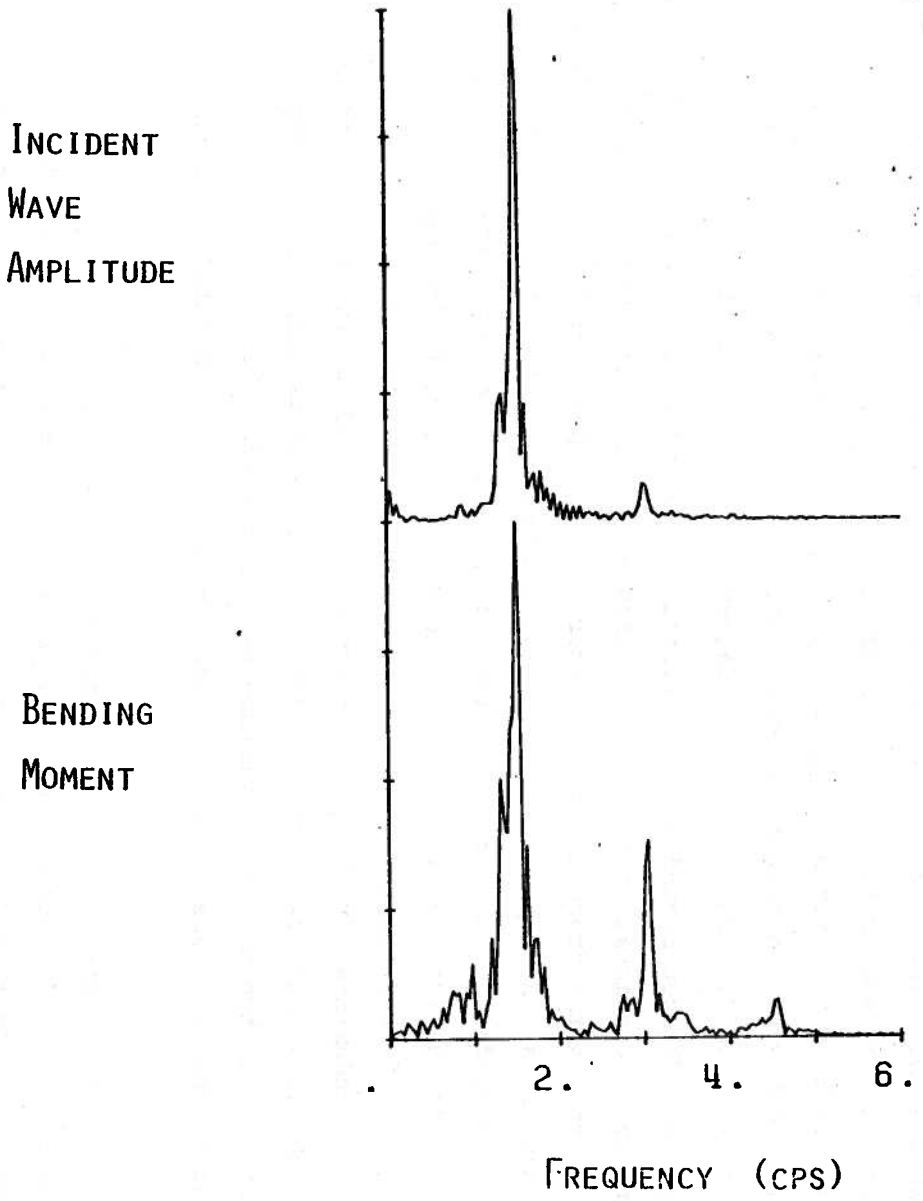

FIGURE 10: TYPICAL MODEL TEST RESULTS USED IN DETERMINING E_2

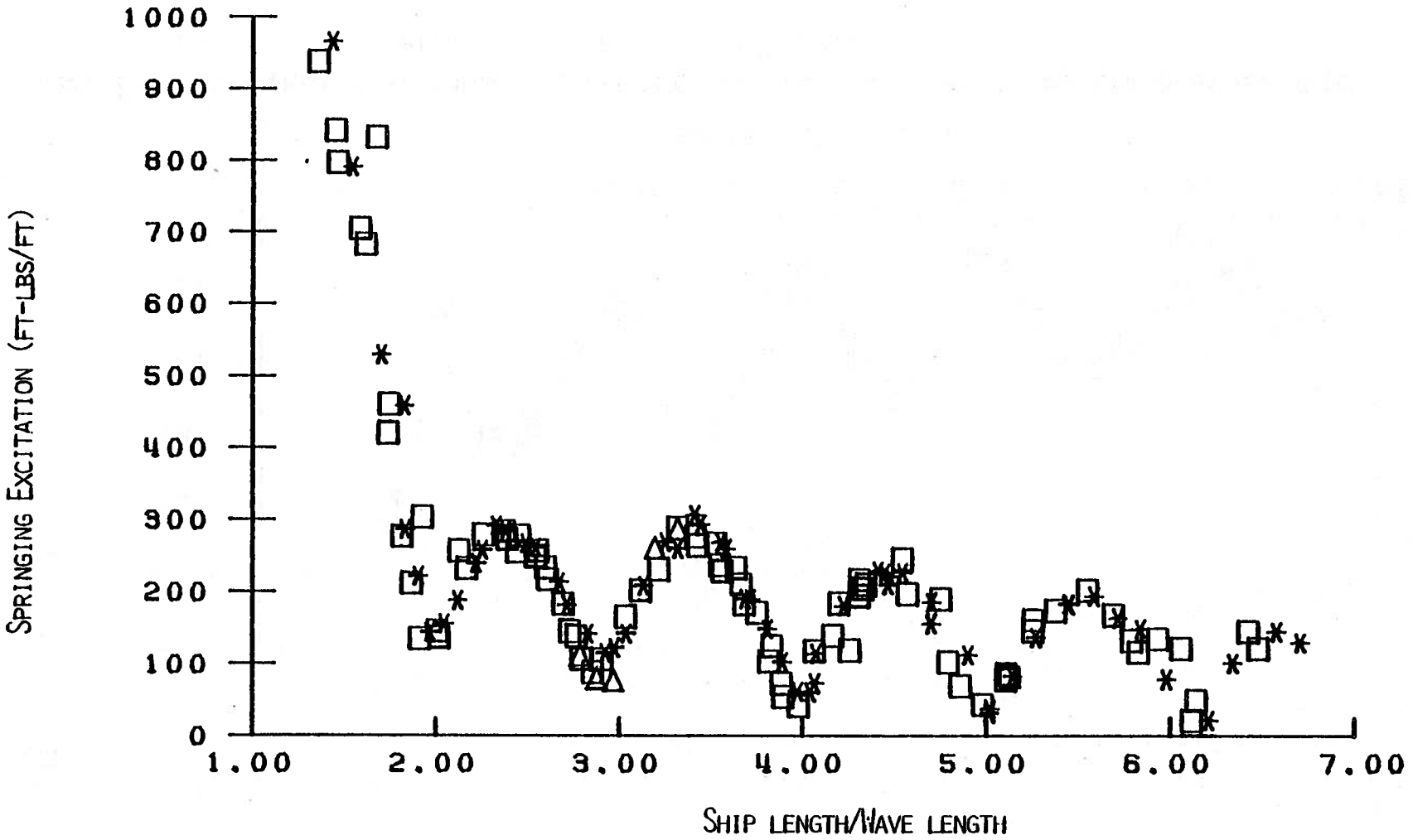

FIGURE 11: EXPERIMENTAL MODEL SPRINGING EXCITATION AS A FUNCTION OF SHIP TO WAVE LENGTH RATIO. MODEL RESTRAINED FROM HEAVE AND PITCH. MODEL VELOCITY $\tilde{}$ 2.9 FT/SEC.

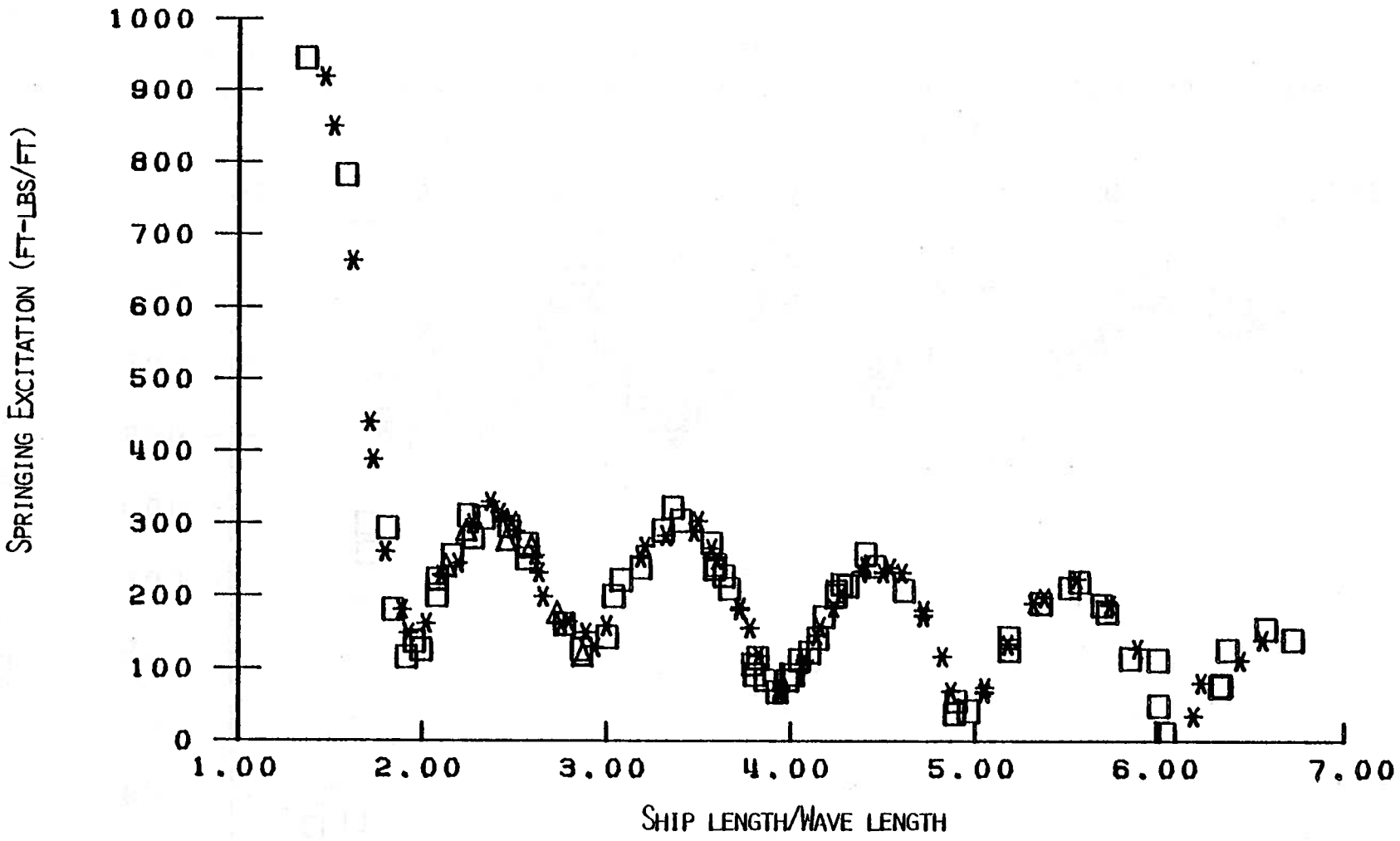

FIGURE 12: EXPERIMENTAL MODEL SPRINGING EXCITATION AS A FUNCTION OF SHIP TO WAVE LENGTH RATIO. MODEL FREE TO HEAVE AND PITCH. MODEL VELOCITY $\simeq$ 2.9 FT/SEC.

ticularly at the longer wave lengths. However, the differences are generally small allowing us to conclude that there is little coupling between springing and heave and pitch in the frequency range where springing is encountered.

Most of the excitation tests were conducted at model speeds that corresponded to the design speed of the *S.J. Cort*. In an effort to see what influence forward speed had on the springing excitation, a limited number of tests were conducted at various forward speeds and wave lengths. The slowest the model could be towed and not be affected by tank wall reflections was 1.3 feet per second. Consequently the model speeds ranged from 1.3 fps to 3.5 fps. The results are shown in Figures 13 and 14. Figure 13 shows the model data for the restrained condition and Figure 14 shows the data for the free condition where heave and pitch were allowed. The solid lines represent curves faired through the experimental data shown in Figures 11 and 12.

The results indicated that there is a slight increase in the springing excitation with forward speed. However, the basic nature of the curve, the hump-hollow behavior, remains unchanged. A conclusion then, is that for a given wave length small changes in the ship's speed do not appreciably alter the level of springing excitation.

The generalized springing response, $q_2(t)$, was measured using two different, relatively soft springs. The stiffer of the two springs produced a springing natural frequency of approximately 2.94 cps. When towing the model at a Froude number of 0.148, resonance was achieved when waves with a ship length to wave length ratio of 6.6 were encountered. The softer of the two springs produced a model natural frequency of 2.48 cps. For a model Froude number of 0.132, resonance occurred when the incident wave had a ship length to wave length ratio of 5.6. Both springs were subjected to waves with encounter frequencies at resonance and off resonance. When the encounter frequency was near the natural frequency of the model, very large responses were measured. Otherwise the response was similar to that shown in Figures 11 and 12. The data records were analyzed in a manner similar to that done for the excitation E_2, i.e. only information obtained near the fundamental frequency of encounter was considered. The results are shown in Figures 15 and 16. The response, q_2, in degrees, has been divided by the

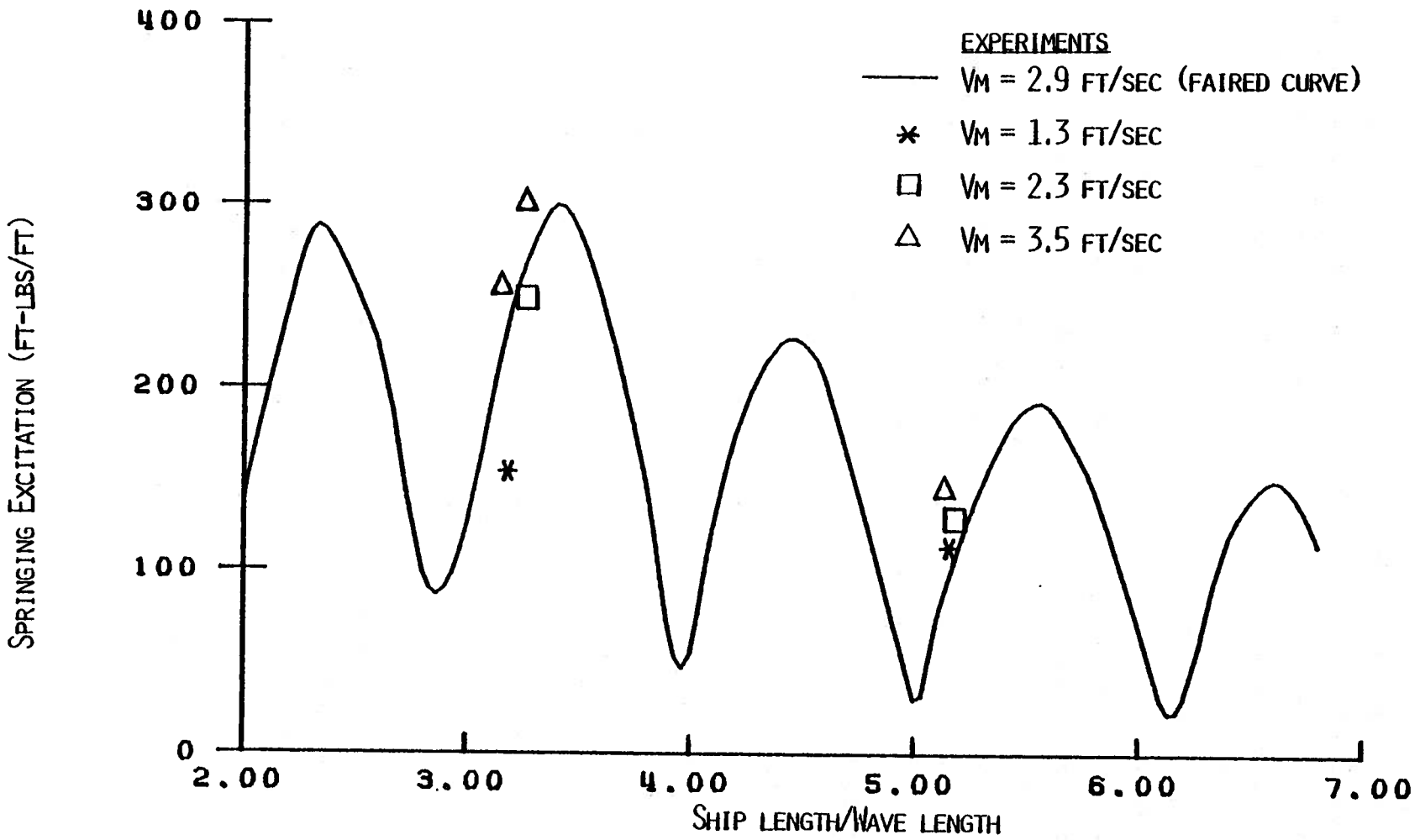

FIGURE 13: SPEED DEPENDENCY OF EXPERIMENTAL SPRINGING EXCITATION. MODEL RESTRAINED FROM HEAVE AND PITCH.

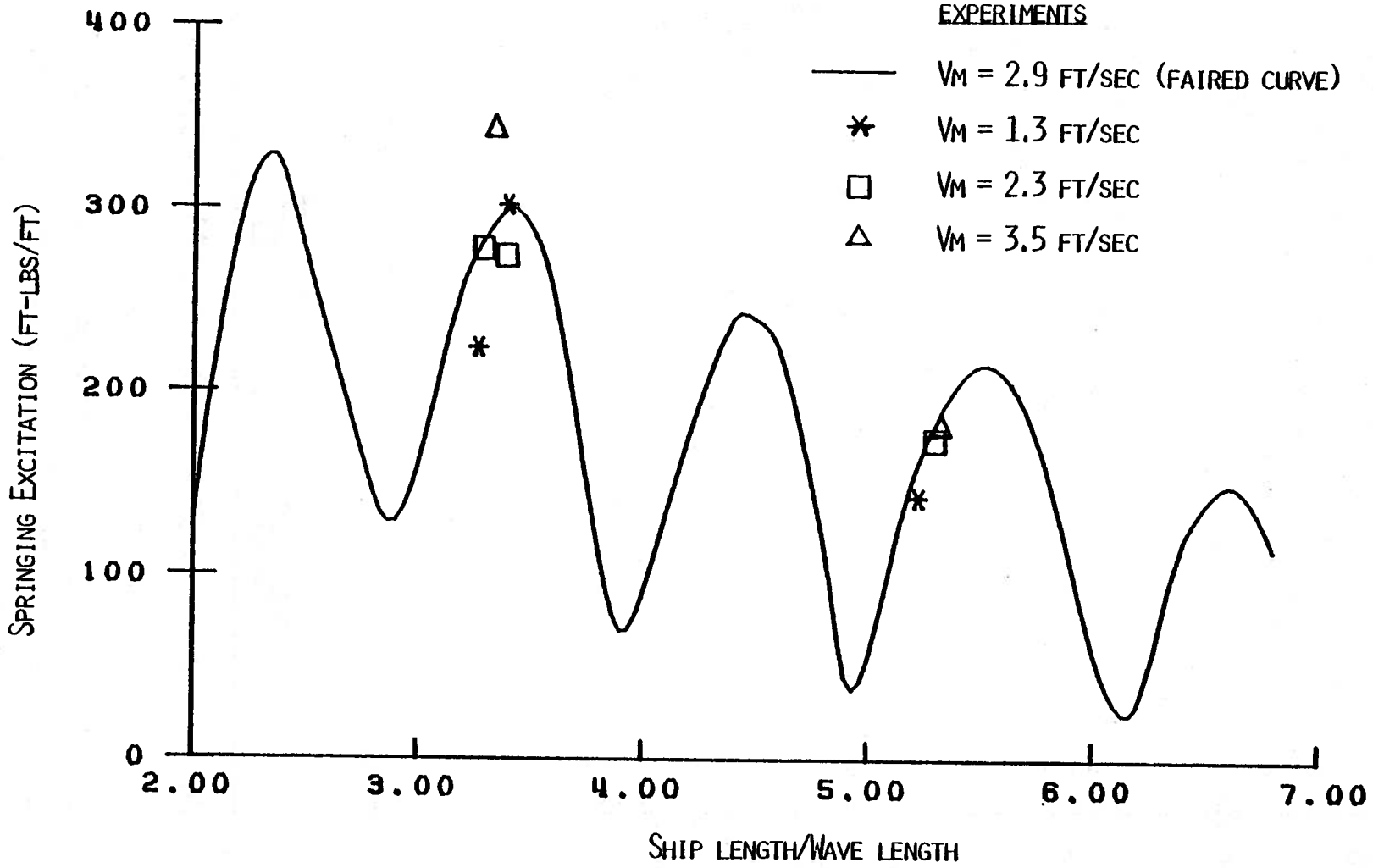

FIGURE 14: SPEED DEPENDENCY OF EXPERIMENTAL SPRINGING EXCITATION MODEL FREE TO HEAVE AND PITCH.

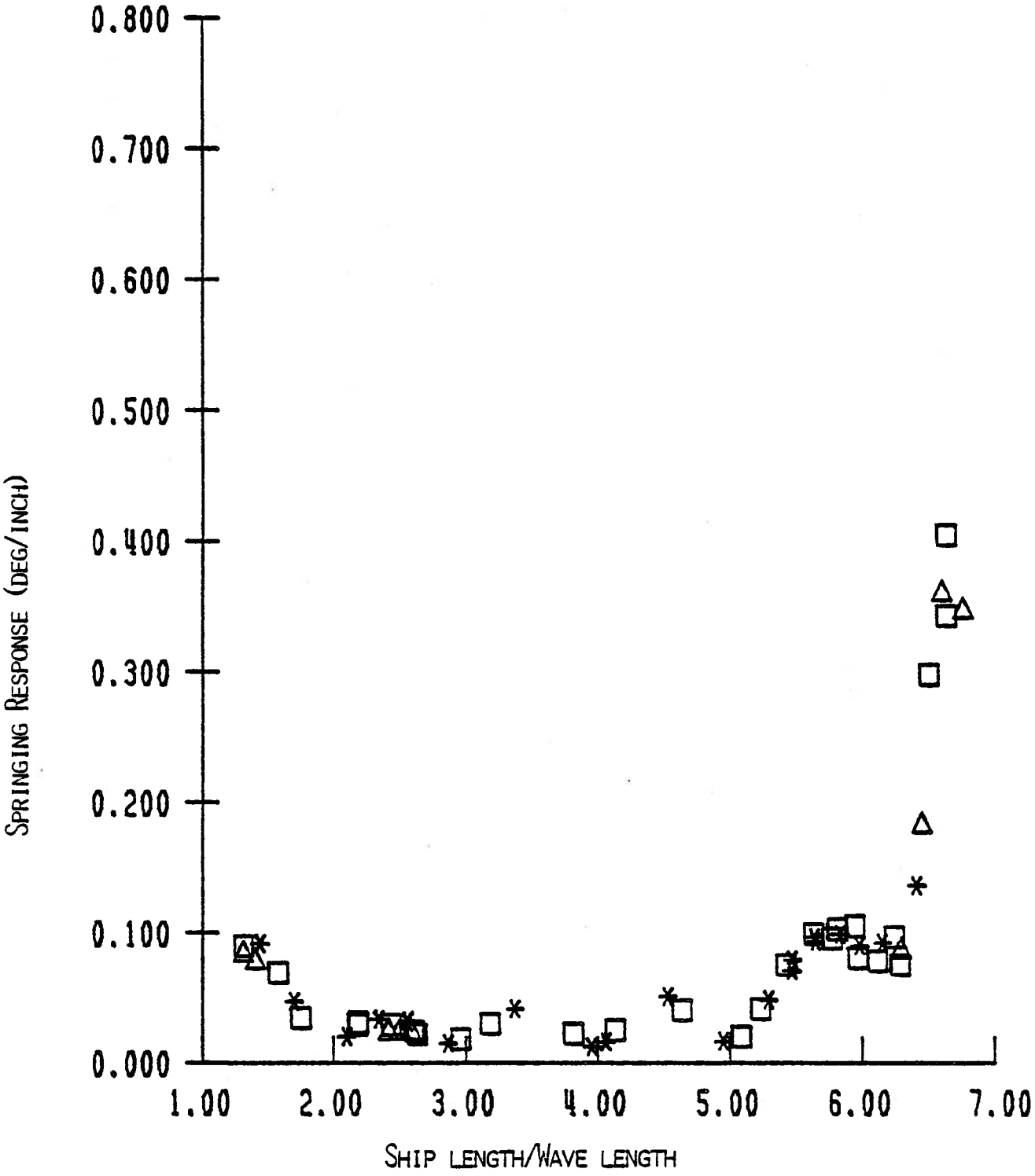

FIGURE 15: EXPERIMENTAL MODEL SPRINGING RESPONSE AS A FUNCTION OF SHIP LENGTH TO MODEL LENGTH. SPRING THICKNESS = .585 IN. MODEL VELOCITY ≃ 3.25 FT/SEC

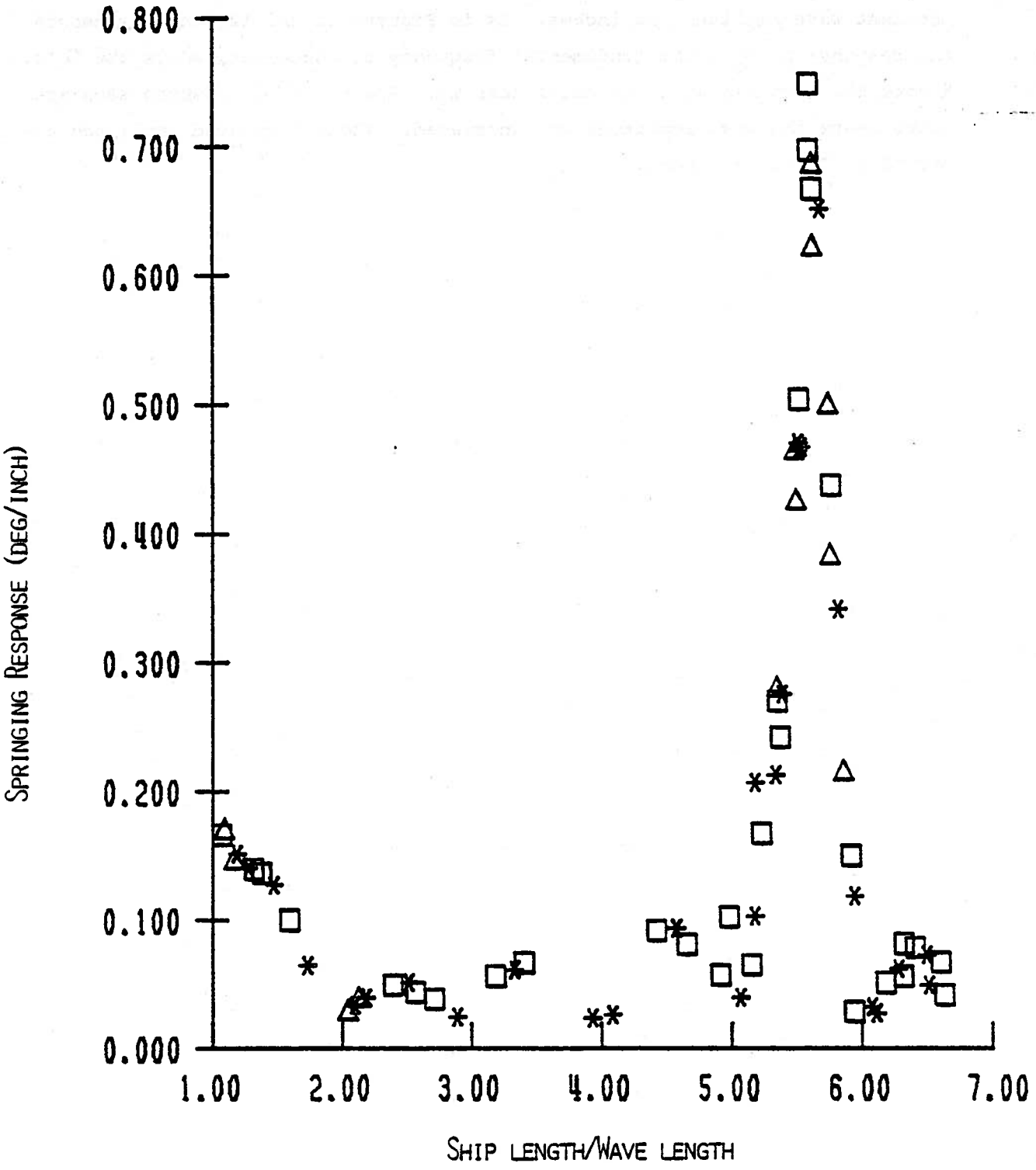

FIGURE 16: EXPERIMENTAL MODEL SPRINGING RESPONSE AS A FUNCTION OF SHIP LENGTH TO MODEL LENGTH. SPRING THICKNESS = .500 IN. MODEL VELOCITY ≃ 2.90 FT/SEC

incident wave amplitude in inches. As in Figures 11 and 12, the *'s denote the response at ω_o , the fundamental frequency of encounter, while the □ 's, denote the response at frequencies near ω_o. Again, the Δ's denote separate tests where the wave amplitude was increased. These increased amplitude tests served as linearity checks.

Comparison of Short Wave Theory and Experiment

The short wave theory is based upon two distinct kinds of assumptions. The first assumes that the springing motion follows a linear relationship. A linear system implies small wave heights, or more specifically, small wave slopes, and small resultant motions. A second set of assumptions is necessary in order to evaluate the various terms in the linear equations of motion. These assumptions deal with the relative ordering of the incident wave length, the hull geometry, and the vessel's speed. They are described completely by Maeda (1979). The comparison between theory and experiment should check both the linearity of system and the validity of the coefficients in the equations of motion.

Consider the form of the equations of motion as shown as equations (1) - (3). The equations are coupled in that they allow for heaving and pitching motion to excite springing. However, in the springing excitation experiments, there was little difference between the restrained model and free model data taken in short waves. Therefore, in the comparison between linear theory and experiment, the springing equation, (3), was assumed to be independent of the other modes of motion. This meant that the coupling coefficients had values of zero. It is possible then to check the form of the governing equation by experimentally measuring the response for a given wave amplitude and wave length and then trying to predict that same response by using the values for the various terms in the equation as determined by experiment. The details on this linearity check are as follows:

- The added mass and damping were determined from decrement tests, such as that shown in Figure 4.
- The heave and pitch coupling coefficients, A_{20}, B_{20}, C_{20}, and A_{21}, B_{21}, C_{21}, respectively, were set equal to zero.
- The springing excitation was estimated from Figure 12.
- The springing response, q_2, was calculated by equation (3) and compared to that measured in the springing response tests shown in Figures 15 and 16.

The results of this comparison are shown in Figures 17 and 18. As can be seen from the plots, the comparison between the measured response and the predicted response is very good. In view of this degree of correlation, there are two points worth emphasizing:

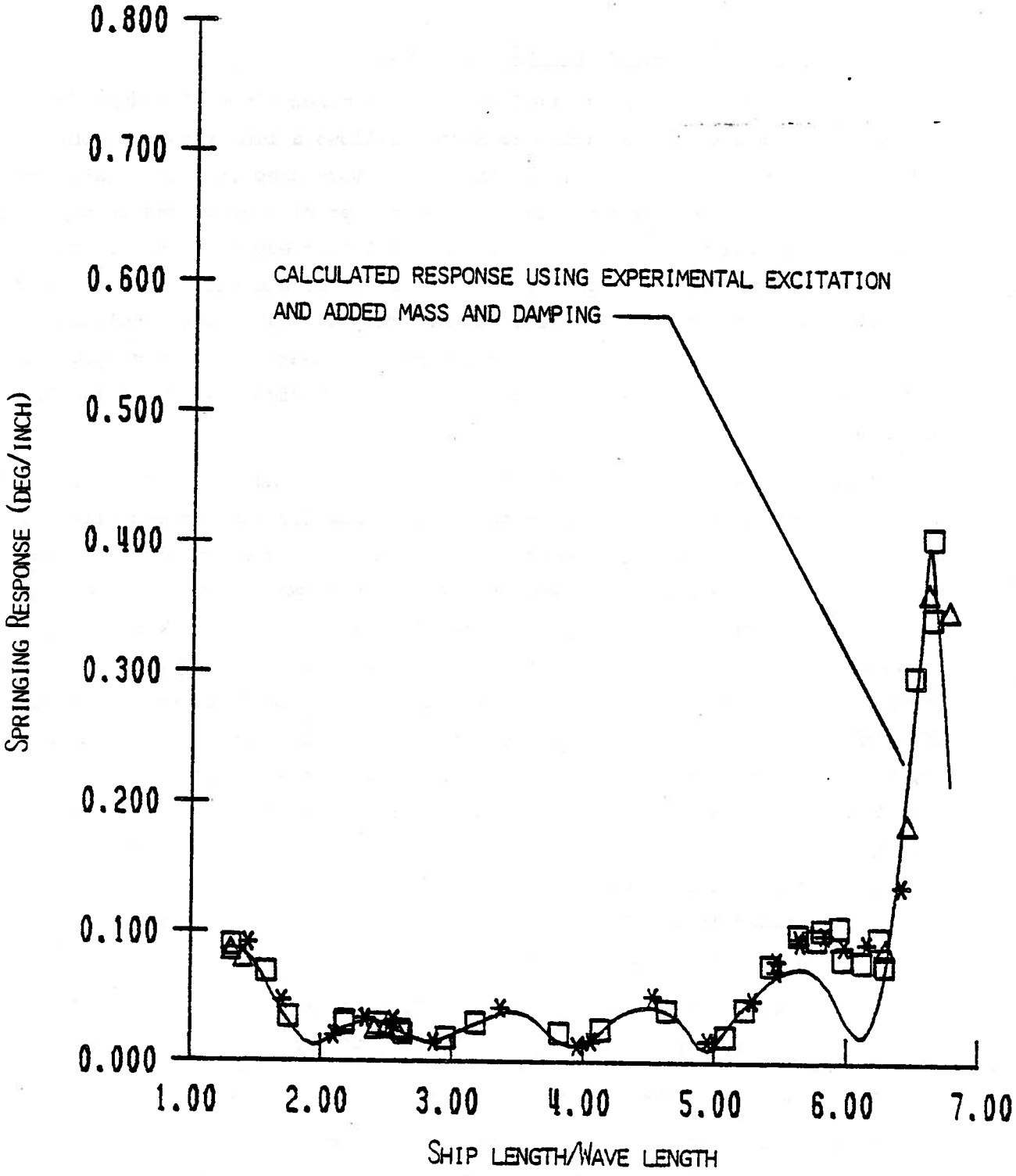

FIGURE 17: COMPARISON BETWEEN MEASURED RESPONSE AND PREDICTED RESPONSE. SPRING THICKNESS = .585 IN. MODEL VELOCITY ≃ 3.25 FT/SEC.

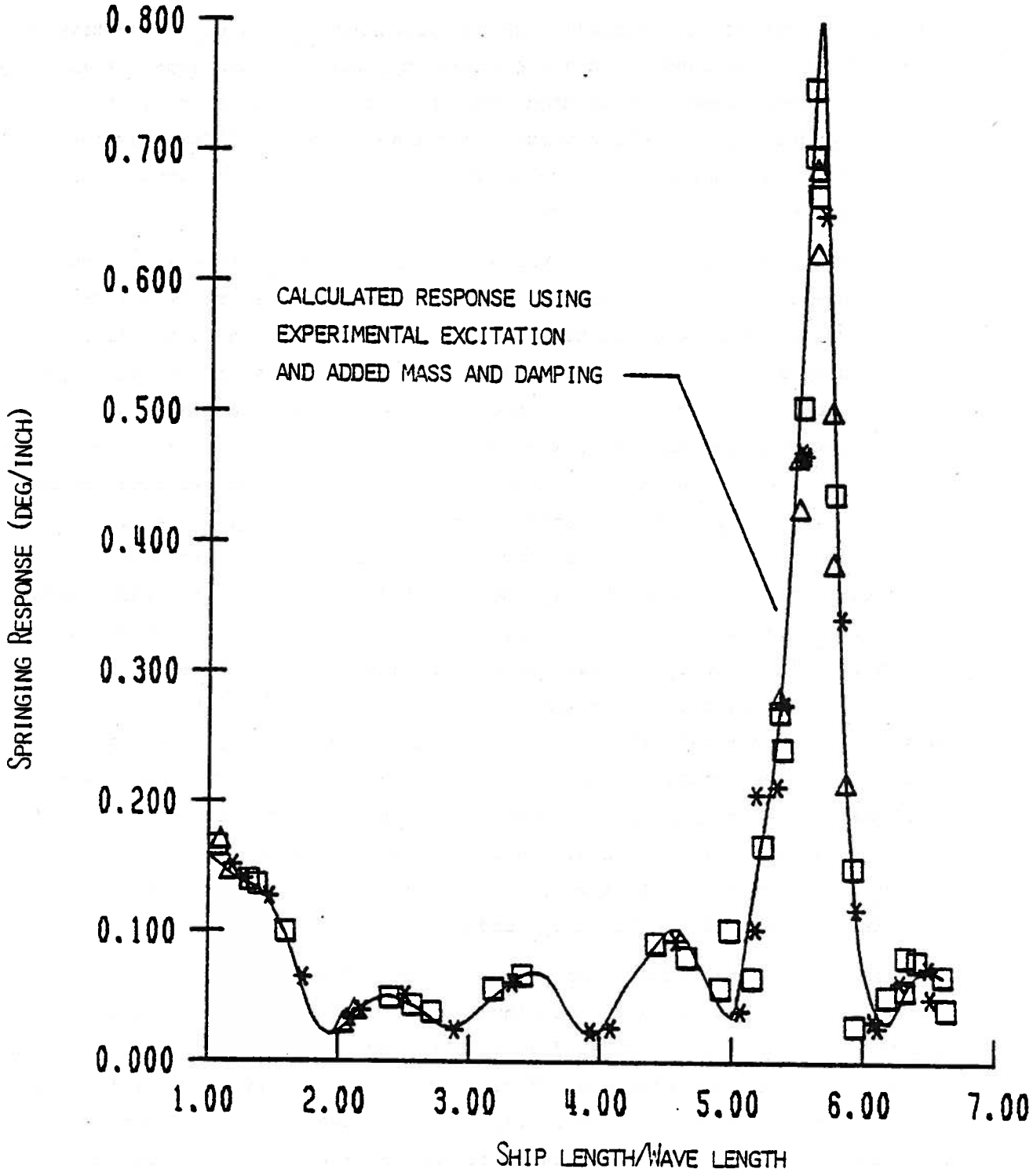

FIGURE 18: COMPARISON BETWEEN MEASURED RESPONSE AND PREDICTED RESPONSE
SPRING THICKNESS =.500 IN. MODEL VELOCITY ≃ 2.90 FT/SEC.

i) The values of the added mass and damping, A_{22} and B_{22} respectively, were determined at only one frequency, that of resonance. These values, however, were used over the entire frequency range to predict q_2. In other words, if the added mass and damping coefficients at resonance are known, they can be used to predict the response at any frequency.

ii) The exciting force, E_2, was experimentally determined at a forward speed of about 2.85 fps. This corresponded to a Froude number of 0.130. The response tests, though, were conducted at two Froude numbers, $F_n \tilde{=} 0.132$ and 0.148. Using the excitation at one Froude number to calculate the response at another and finding that this response compares well with experiment again verifies the conclusion reached on the speed dependency of the generalized exciting force: it has only small variations with changes in forward speed.

One major conclusion of the short wave experiments is that if we can accurately predict E_2, the exciting moment, and A_{22} and B_{22}, the added mass and damping, then equation (3) may be used to calculate $q_2(t)$, the springing response. Unfortunately, linear ideal fluid theory is insufficient in finding B_{22}. Based upon experimental data, the theoretical value of wave damping is approximately 1/3 to 2/3 the actual value measured. See Figure 19 where the experimental damping is compared to theory. Even when the internal mechanical damping of the model is subtracted out, the predicted values fall short of the measured ones. As a consequence, response at resonance will be over predicted. It appears that reasonably accurate values of the total damping can only be found by conducting full scale trials.

The experimental added mass is consistently five to six percent lower than the theoretical values. See Figure 20. The usual ship vibrations problem, where the hull natural frequency is much higher than the Great Lakes ore carriers springing frequency, typically has differences similar to this. That the correlation is not better may indicate that the fluid inertial effects of springing are more closely related to ship vibration than to ship motions. The frequency dependence of the coefficients, though, clearly demonstrates the influence of the free surface.

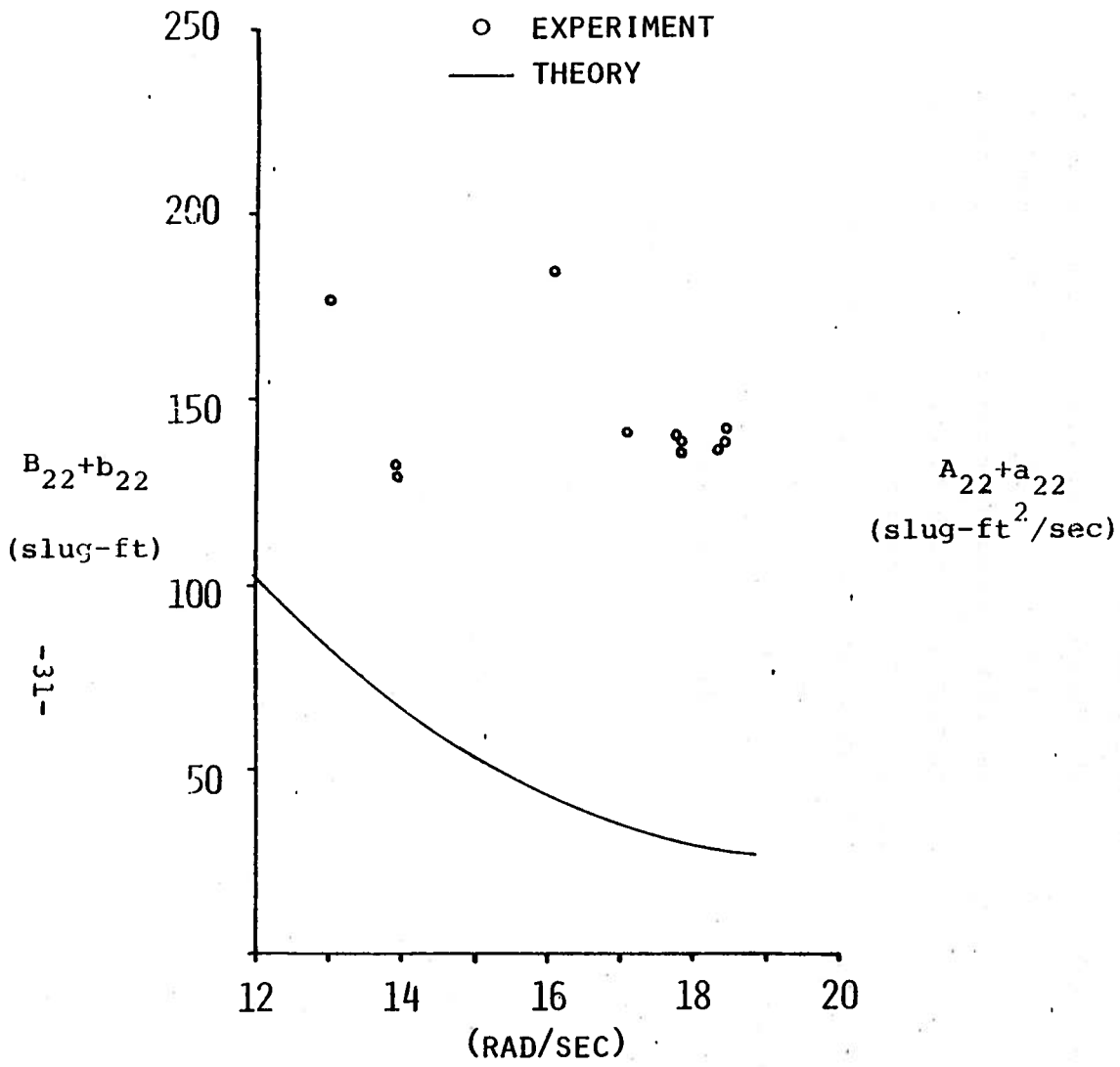

FIGURE 19: COMPARISON BETWEEN EXPERIMENTAL AND THEORETICAL DAMPING COEFFICIENT. MODEL VELOCITY ≃ 2.9 FT/SEC

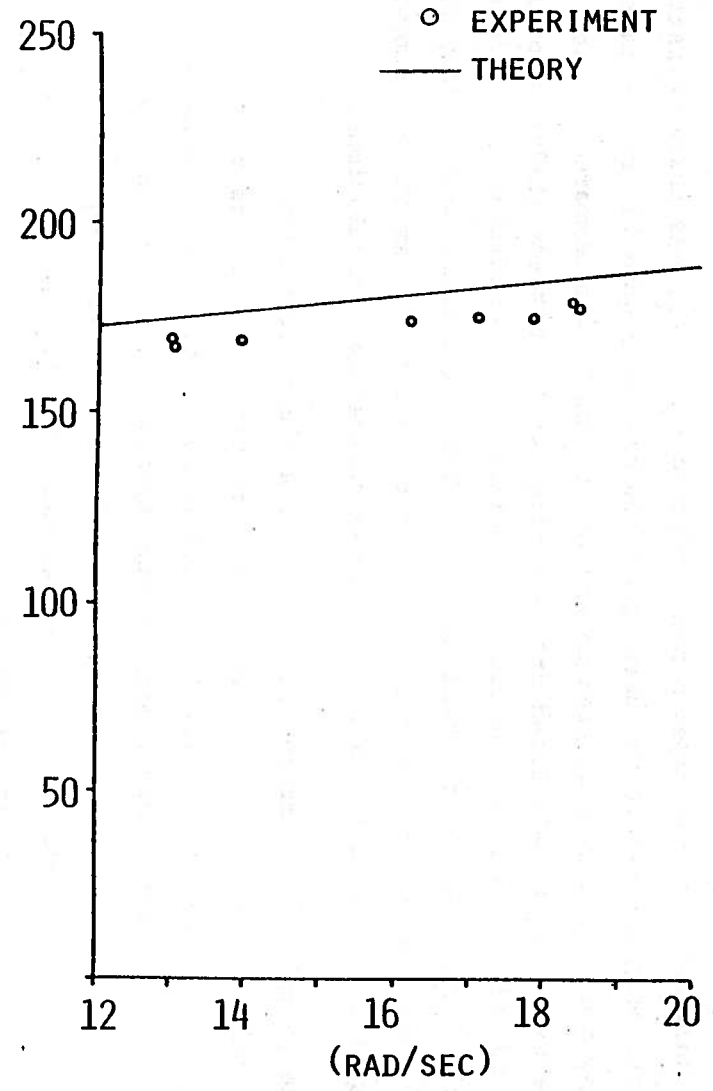

FIGURE 20: COMPARISON BETWEEN EXPERIMENTAL AND THEORETICAL ADDED MASS. MODEL VELOCITY ≃ 2.9 FT/SEC

Qualitatively, the experimental exciting force, E_2, has characteristics that can be predicted by the zero speed theory. In Figure 21, curves representing the faired data plotted in Figures 11 and 12 are compared to the theorectical curve calculated from equation (4-91) in Maeda (1979). Recall that the experimental curves are for a forward speed condition while the theory has the forward speed set equal to zero. When the forward speed theory is compared with experiment, the results are poor. Figure 22 has the experimental values from Figure 12 in addition to three theoretical calculations.

The formulas, as numbered in Figure 22, are described below:

Formula 1) This is the forward speed excitation formula as given by Bishop et. al. (1977) and is described in the section on the linear theory of ship springing. It contains the longitudinal derivatives of the added mass and damping. (Maeda (1977) re-derives this formula. See his equations (4-119) and (4-101).)

Formula 2) This is the forward speed excitation formula as given by Maeda (1979), equation (4-91). Instead of requiring the derivatives of the added mass and damping coefficients, it differentiates the mode shape. For Great Lakes bulk carriers, this should be a much smoother function than the added mass and damping and, at least in principle, should give more accurate results.

Formula 3) This formula represents the zero speed excitation multiplied by a speed dependent factor. Its theoretical basis is given by Faltinsen (1971). The multiplication factor is C where

$$C = \sqrt{1+2\ F_n \sqrt{2\pi}\ \sqrt{L/\lambda}}$$

and F_n is the Froude number

L is the ship length

λ is the incident wave length.

Of the three formulas, 3) seems to be best in describing the forward speed effects in the wave length range where springing occurs. This can possibly be explained by examining the assumptions implicit in the formulas.

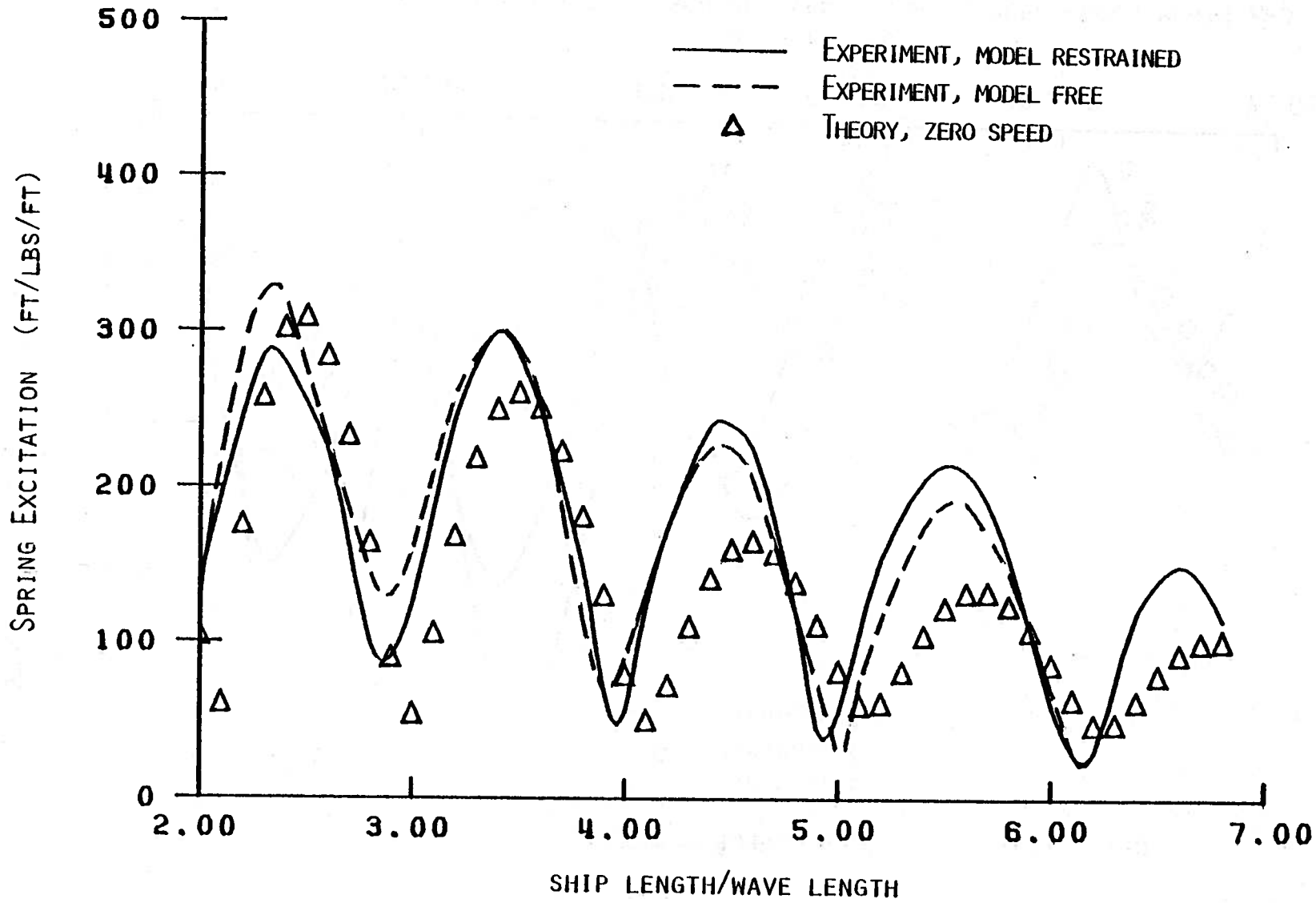

FIGURE 21: SPRINGING EXCITATION - COMPARISON BETWEEN FORWARD SPEED EXPERIMENTS AND ZERO SPEED THEORY. MODEL VELOCITY $\simeq$2.9 FT/SEC.

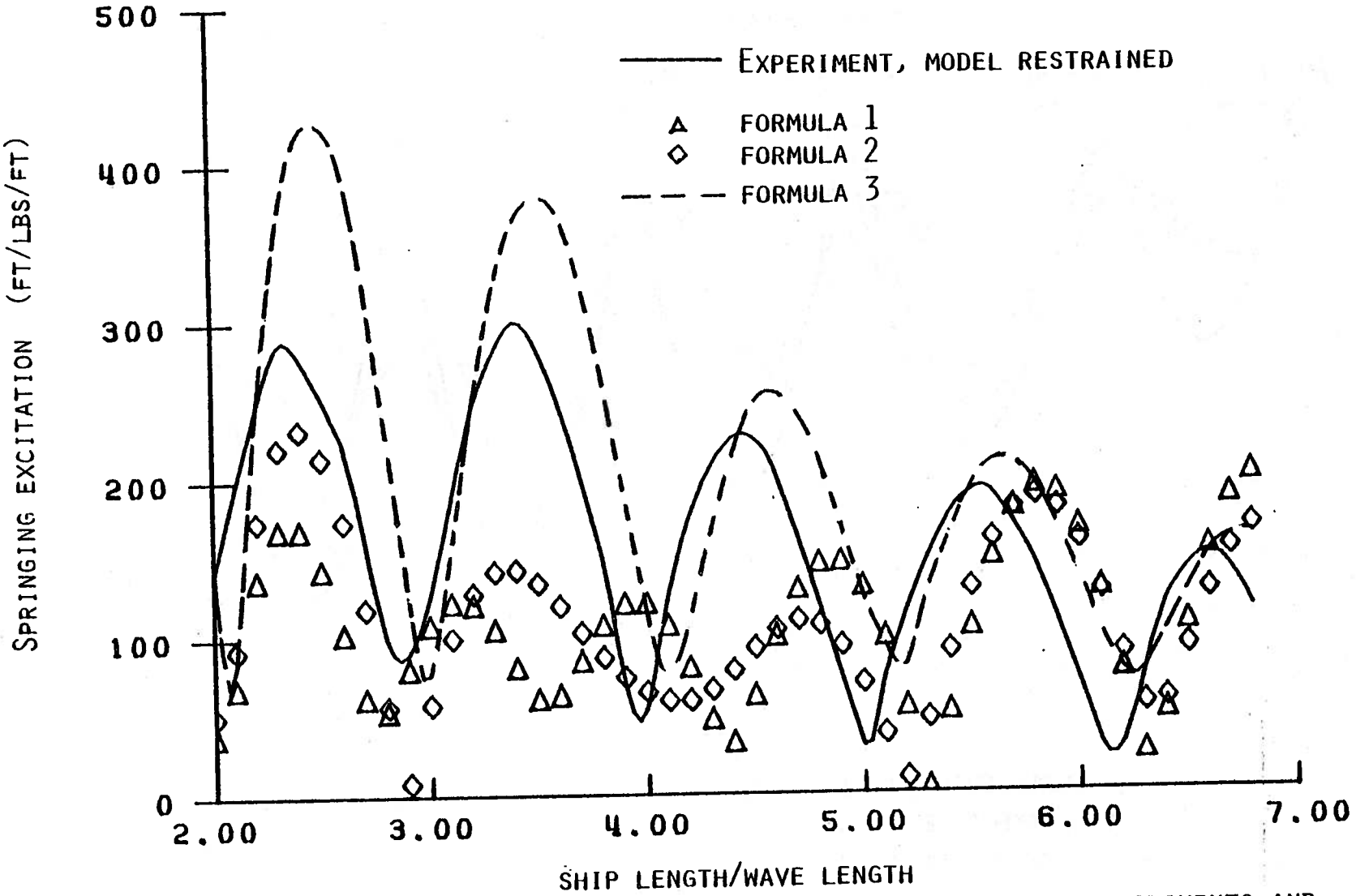

FIGURE 22: SPRINGING EXCITATION - COMPARISON BETWEEN FORWARD SPEED EXPERIMENTS AND FORWARD SPEED THEORY. MODEL VELOCITY ≃ 2.9 FT/SEC .

Formulas 1) and 2) use assumptions on the wave length and frequency of encounter found in the usual ship motions theory. See for example Salvesen, Tuck, and Faltinsen (1970) or Ogilvie and Tuck (1969). Specifically, for zero forward speed the wave length is assumed small, the same order as the beam of the ship. This implies that the wave number, $\kappa(=2\pi/\lambda)$, is large, or in terms of asymptotic expansions, $\kappa = O(\varepsilon^{-1})$. Here ε is a small parameter that describes the slenderness of the vessel. The resulting frequency of encounter, ω_e, which is equal to the incident wave frequency for zero forward speed, has an order of $\omega_e=0(\varepsilon^{-1/2})$. For forward speed, the assumption on the ordering of the frequency of encounter is maintained, implying that the wave number now is $\kappa=0(\varepsilon^{-1/2})$. This is a wave that is longer than the vessel's beam, but shorter than its length. By contrast, Formula 3), represents a short wave theory, even at forward speed. The assumptions used in this theory are described by Faltinsen (1971) or Troesch (1979). Briefly, the incident wave length is assumed to be the same order as the beam, both at zero and forward speed. A result of this assumption is that the forward speed exciting force, in the first approximation, is just the zero speed value. The speed effects only appear in the second order. For head seas, this second order effect is represented by the multiplication factor C described earlier.

It should be emphasized that the asymptotic expressions for the exciting force are only valid in the limit as $\varepsilon\to 0$, or in other words, as the beam and draft of the ship vanish. Since this generally does not happen in practice, the application of the above arguments to real ship shapes is not clear. The two conclusions that can be stated with some level of certainty, though, are that Formula 3) represents a relatively shorter wave length theory, and that the same formula seems to compare better with experiments in the frequency range where springing is likely to occur.

Long-Wave Experiments

Both the springing response and springing excitation experiments were conducted in long waves. In both cases the test records were Fourier analyzed. The magnitude of the response and excitation at harmonics of the frequency of encounter could then be found.

Figure 10 shows a typical excitation record. In that figure, the frequency of encounter was approximately 1.5 cps. The incident wave contained a harmonic component at 3.0 cps. The bending moment had harmonic components at 3.0 cps and at 4.5 cps. To check on the linearity of the system, the bending moment at a harmonic was divided by the wave component at a harmonic and then multiplied by the appropriate scaling factor. This result was then compared with results obtained in other tests where the incident wave frequency of encounter was equal to the aforementioned harmonic frequency. For the particular test shown in Figure 10, this meant that the *harmonic* excitation at 3.0 cps was compared to another test condition where the *fundamental* excitation was 3.0 cps. If the model excitation is linear, the nondimensional form of these two values should be approximately equal. We can now state that there appears to be little or no correlation between the harmonic and fundamental excitation when analyzed in this manner. Figure 23 and 24 show the results for the restrained and free excitation tests respectively. The results obtained from the analysis of the excitation due to the fundamental component of the incident waves are included for comparison. The excitation at the harmonic divided by the component of the incident wave at the harmonic is denoted by $\diamond$. As can be seen by the figures, the data generally has much larger values than might be expected and does not follow a hump-hollow pattern similar to the previous results.

The long wave excitation tests were conducted with the model clamped and also with the model free to heave and pitch. Test results show that non-linear excitation occurs in both instances. This implies that the model motions contributed little to the excitation found at the harmonics. The source, then, appears to be the diffraction of the incident wave by the model's hull.

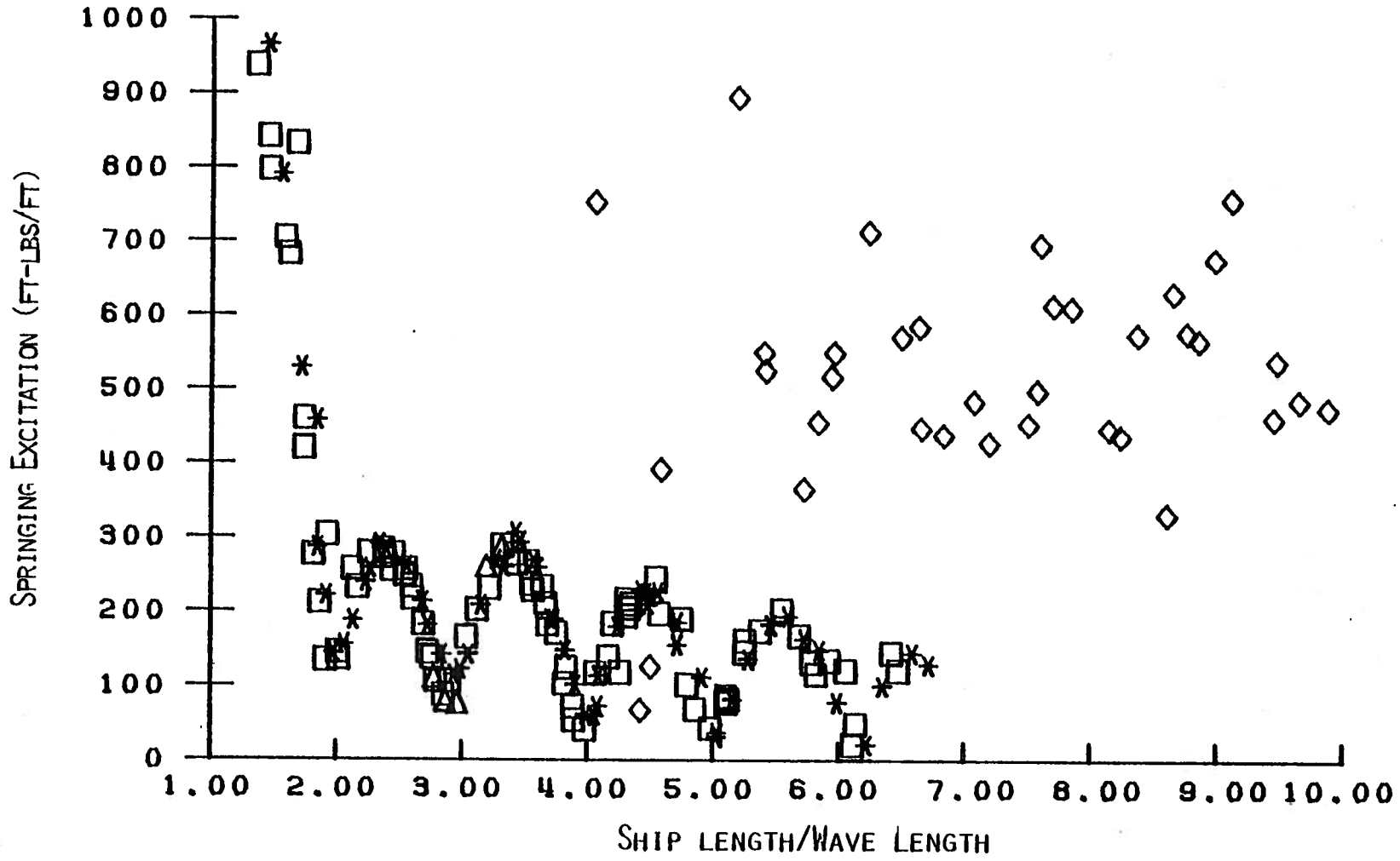

FIGURE 23: EXTENSION OF THE EXPERIMENTAL SPRINGING EXCITATION CURVES BY CONSIDERING HARMONIC EXCITATION. MODEL RESTRAINED FROM HEAVE AND PITCH.

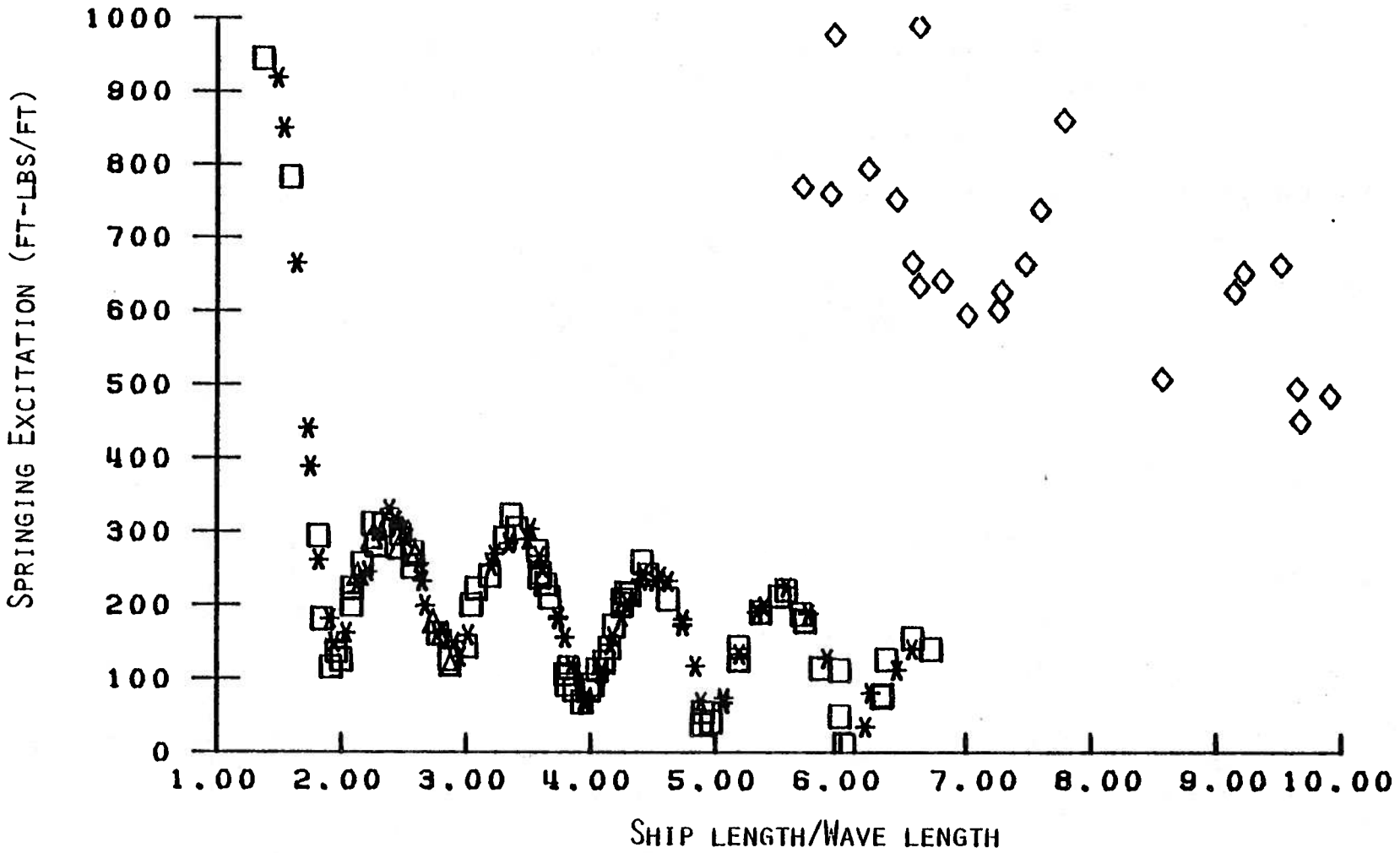

FIGURE 24: EXTENSION OF THE EXPERIMENTAL SPRINGING EXCITATION CURVES BY CONSIDERING HARMONIC EXCITATION. MODEL FREE TO HEAVE AND PITCH.

In an attempt to analyze the non-linear excitation, a number of assumptions about its form were made. First, it was assumed that the harmonic component of the incident wave produced a linear excitation at the harmonic. It could be estimated by using the test results shown in Figures 11 and 12 and from the harmonic computer analysis. (See Appendix C) This linear excitation could be subtracted from the total leaving only the non-linear part. The second assumption was that the resultant non-linear excitation could be scaled by one over the square of the *fundamental* wave component. (This is a standard assumption in the perturbation analysis of finite amplitude waves. See, for example, Longuet-Higgins (1963)). Figure 25 indicates schematically how this was done.

Specifically, assume that the total complex excitation at a harmonic is given as

$$E_2^T e^{i(\omega_n t+\alpha_T)} = E_2^L e^{i(\omega_n t+\alpha_L)} + E_2^{N-L} e^{i(2\omega_e t+\alpha_{N-L})}$$

where E_2^T, E_2^L, and E_2^{N-L} are the amplitudes of the total, linear, and non-linear excitations respectively.

ω_e is the fundamental frequency of encounter (in the case of Figure 25, it would be approximately 1.5 cps),

ω_n is the frequency of encounter corresponding to the harmonic (in the case of Figure 25, it would be approximately 3.0 cps).

and α_T, α_L, and α_{N-L} are the relative phase angles of the total, linear, and non-linear components.

Then the amplitude of non-linear excitation can easily be shown to be

$$E_2^{N-L} = \sqrt{(E_2^T)^2 + (E_2^L)^2 - 2\, E_2^T\, E_2^L \cos(\alpha_T-\alpha_L)}\ .$$

The quantities E_2^T and α_T can be read directly from the computer printout. (See Appendix C). Using a plot of the linear phase angles vs wave length, Figure 12, and the amplitude of the harmonic wave from the computer analysis, E_2^L and α_L at the harmonic (in the case of Figure 25, it would be approximately 3.0 cps) can be estimated. The amplitude of the non-linear excitation can then be calculated and divided by the square of the fundamental wave component. Figure 26 shows the results for the test condition where the model was free to heave and pitch. As before, the *'s represent the excitation at the peak of the harmonic and the Δ's represent tests where the incident

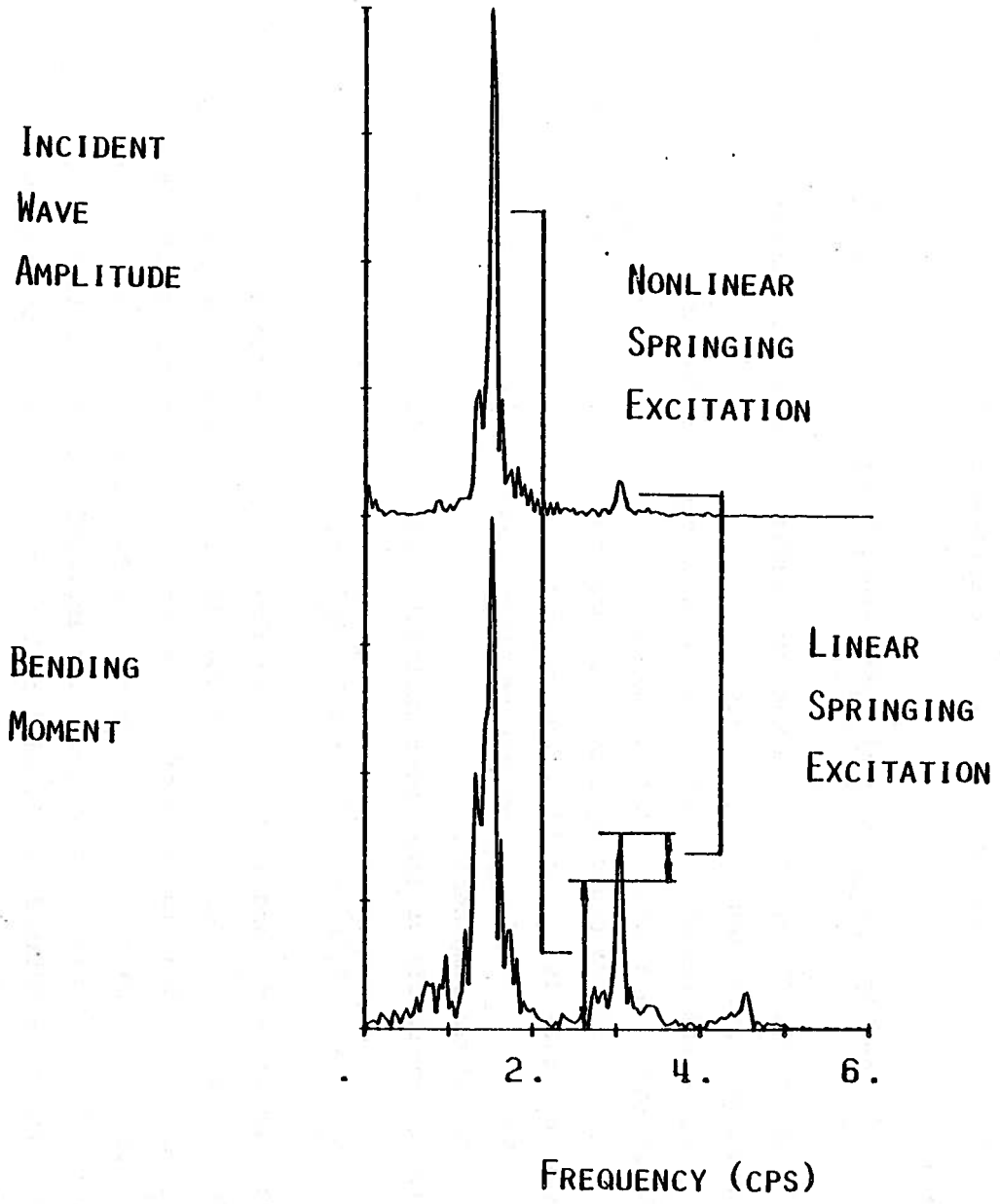

FIGURE 25: NONLINEAR ANALYSES OF SHIP SPRINGING

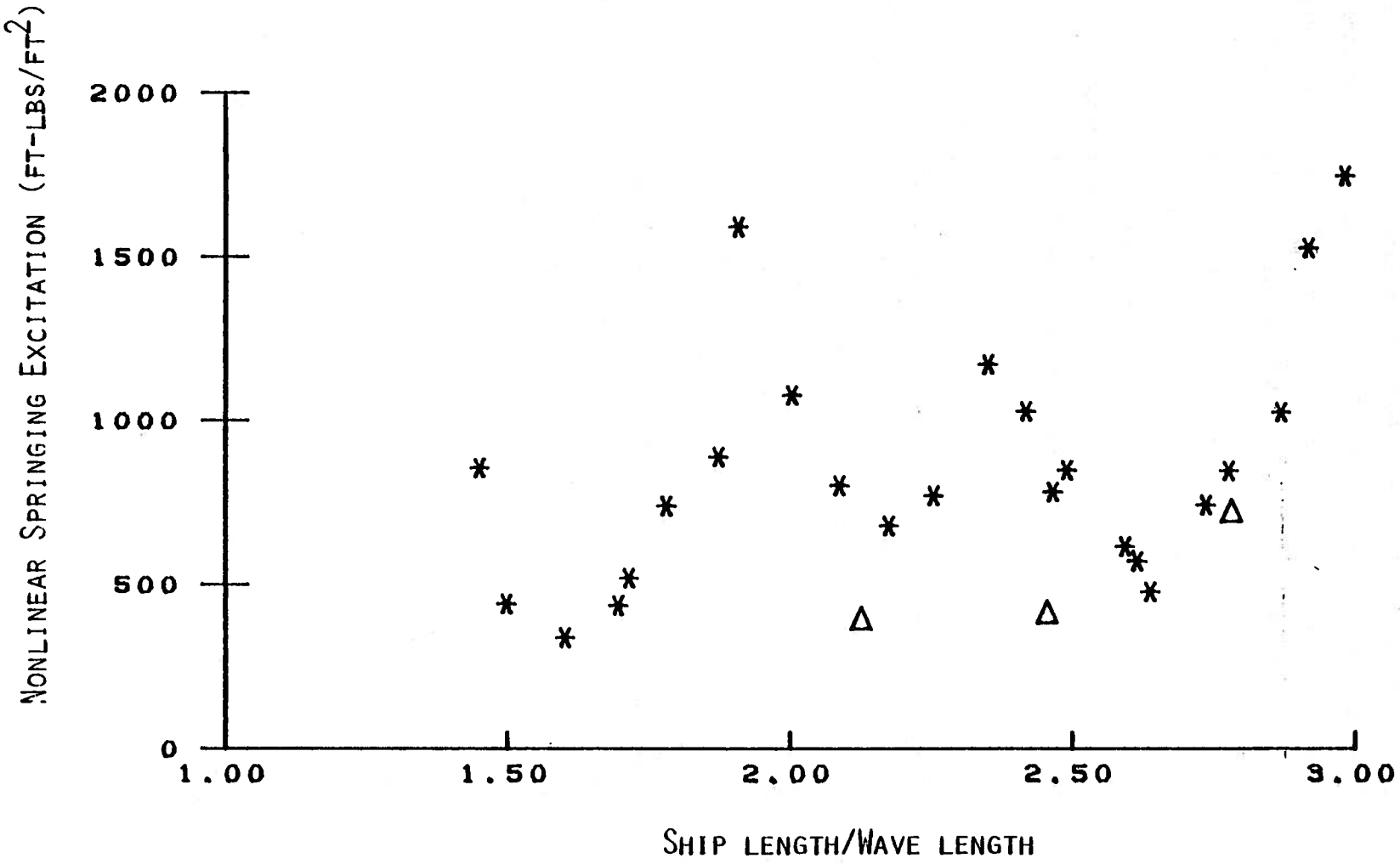

FIGURE 26: MODEL HARMONIC SPRINGING EXCITATION AS A FUNCTION OF SHIP TO FUNDAMENTAL WAVE LENGTH. MODEL FREE TO HEAVE AND PITCH.

wave amplitude was increased. The data seems to indicate that the amplitude of the excitation oscillates with periods of half the ship length to wave length ratio. However, there are not enough data points to draw any definite conclusions. This is one area where additional research is recommended.

The long-wave springing response also showed non-linear behavior. However, most of the effects were measurable only at resonance. This was a result of the large magnification factor which had a value greater than twenty. The excitation tests have demonstrated that there is non-linear exictation over the entire frequency range, but, the non-linear response at the off-resonance frequencies was just too small to be measured.

In summary, we can conclusively state that the springing excitation and response of a Great Lakes bulk carrier has a non-linear component. The extent to which it contributes to the total will depend upon the sea that the vessel is operating in and the dynamic characteristics of the vessel itself. For example, if the natural frequency of the hull corresponds to a frequency of encounter where the linear excitation is small (this might be at a ship length to wave length ratio of 6.15 as shown in Figure 11), then almost all of the response will be non-linear in origin. Conversely, if the resonant frequency occurs at a maximum excitation frequency (a ship length to wave length ratio of 5.6 or 6.6), then the two sources of excitation, non-linear and linear, could be the same order of magnitude. Also, an additional consideration will be the actual frequency content of the sea surface. The available energy at resonance and at sub-harmonics will have a direct bearing on response levels.

Non-Linear Theory of Ship Springing

Under the current contact, little effort has been directed at deriving a new non-linear theory. Most of the work consisted of reading and understanding existing theories. Ohkusu (1979), under sponsorship of this contract, conducted an extensive literature search of work done in Japan. In that country, much of the interest is focused on the non-linear vibrations associated with large amplitude ship motions. This is a somewhat different view than that taken here on the Great Lakes where 1000 foot bulk carrier motions are negligible. However, the non-linear free surface condition, which is the principle cause of the non-linearities, is the same whether one has large amplitude motions or blunt bows scattering incident waves. The literature survey by Ohkusu (1979) reviews the pertinent Japanese works.

References

Belgova, M.A. (1962), "Determination of Overall Bending Moments Caused by Elastive Vibrations of Ships," Leningrad Institute of Water Transport. Issue XXVIII.

Bishop, R., et. al. (1977), "A Unified Dynamic Analysis of Ship Response to Waves," *Roy. Inst. Nav. Arch.* Spring Meeting.

Bongort, K.J. (1979), "Time Series Analysis Program-Users Guide," The University of Michigan, Dept. of Naval Arch. and Marine Eng., NA 574 Project.

Faltinsen, O.M. (1971), "A Rational Strip Theory of Ship Motions: Part 2," The University of Michigan, Dept. of Naval Arch. and Marine Eng., Report No. 113.

Freakes, W., and Keay, K. (1966), "Effects of Shallow Water on Ship Motion Parameters in Pitch and Heave," MIT, Dept. of Naval Arch. and Marine Eng. Report No. 66-7.

Goodman, R.A. (1971), "Wave-Excited Main Hull Vibration in Large Tankers and Bulk Carriers," *Trans. Roy. Inst. Nav. Arch.* 113, pp. 167-184.

Golovato, P. (1959), "A Study of the Transient Pitching Oscillations of a Ship," *JSR*, March, pp. 22-29.

Harding, L. (1976), "The Discrete Fourier Transform," The University of Michigan Computing Center, CC Memo 327.

Hildebrand, F.B. (1956), Introduction to Numerical Analysis, McGraw-Hill Co., Inc., New York, New York.

Hoffman, D., and Van Hoof, R. (1976), "Experimental and Theoretical Evaluation of Springing on a Great Lakes Bulk Carrier," USCG Report CG-D-74.

Jensen, J.J., and Pedersen, T. (1978), "Wave-Induced Bending Moments in Ships - A Quadratic Theory," *Roy. Inst. Nav. Arch.*

Longuet- Higgins, M.S. (1963), "The Effects of Nonlinearities on Statistical Distributions in the Theory of Sea Waves," *JFM*, 17, pp. 459-480.

Maeda, H. (1979), "On the Theory of Coupled Ship Motions and Vibrations," The University of Michigan, Dept. of Naval Arch. and Marine Eng., (to be released).

Noll, M.D. (1980), "Evaluation of SDRC Damping Analysis," CG-B-5-80, U.S. Coast Guard.

Ogilvie, T.F., and Shin, Y-S. (1978), "Integral-Equation Solutions for Time-Dependent Free-Surface Problems," *JSNAJ*, Vol. 143.

Ogilvie, T.F. and Tuck, E.O. (1969), "A Rational Strip Theory of Ship Motions: Part 1," The University of Michigan, Dept. of Naval Arch. and Marine Eng., Report No. 013.

Ohkusu, M. (1979), "A Review of Studies on Springing of Ships in Japan," The University of Michigan, Dept. of Naval Arch. and Marine Eng., (to be released).

Salvesen, N., Tuck, E.O., and Faltinsen, O.M. (1970), "Ship Motions and Sea Loads," *Trans. SNAME,* 78.

Shin, Y-S. (1979), "Three Dimensional Effects on the Hydrodynamic Coefficients and Wave Exciting Forces Used in Predicting Motions of Ships," The University of Michigan, Dept. of Naval Arch. and Marine Eng., Report No. 210.

Thomson, W.T. (1972), Theory of Vibration with Applications, Prentice-Hall, Inc., Englewood Cliffs, New Jersey.

Troesch, A. (1975), "The Diffraction Potential for a Slender Ship Moving Through Oblique Waves," The University of Michigan, Dept. of Naval Arch. and Marine Eng., Report No. 176.

Troesch, A. (1979), "The Diffraction Forces for a Ship Moving in Oblique Seas," *JSR* , Vol 23, No. 2 pp. 127-139.

Tuck, E.O. (1967), "A Simple "Filon-Trapezoidal" Rule," *Math. of Computation.* Vol. XXI, No. 98, pp. 239-241.

Van Gunsteren, F.F. (1974), "Some Further Calculations of Wave-Induced Hull Vibrations," *Proc. Int. Sym. on Dynamics of Marine Vehicles and Structures in Waves,* Univ. College London.

Appendix A: Model Characteristics and Body Plan

CHARACTERISTICS - TOTAL MODEL

Scale	66.67:1
Length Overall, in.	180.00
Length between Perpendiculars, in.	179.93
Beam, in.	18.83
Draft (mean), in.	4.64
Displacement, lbs.	504.8
Longitudinal Center of Gravity, (in. fwd midships)	0.19
Moment of Inertia about Midships, slugs - ft^2	244.62

CHARACTERISTICS - FORE BODY

Length Overall, in.	90.00
Displacement, lbs.	256.7
Longitudinal Center of Gravity, (in. fwd midships)	40.55
Moment of Inertia About Forebody LCG, slugs-ft^2	30.14

CHARACTERISTICS - AFTER BODY

Length Overall, in.	90.00
Displacement, lbs.	248.1
Longitudinal Center of Gravity,(in. aft midships)	41.56
Moment of Inertia about Afterbody LCG, slugs-ft^2	30.88

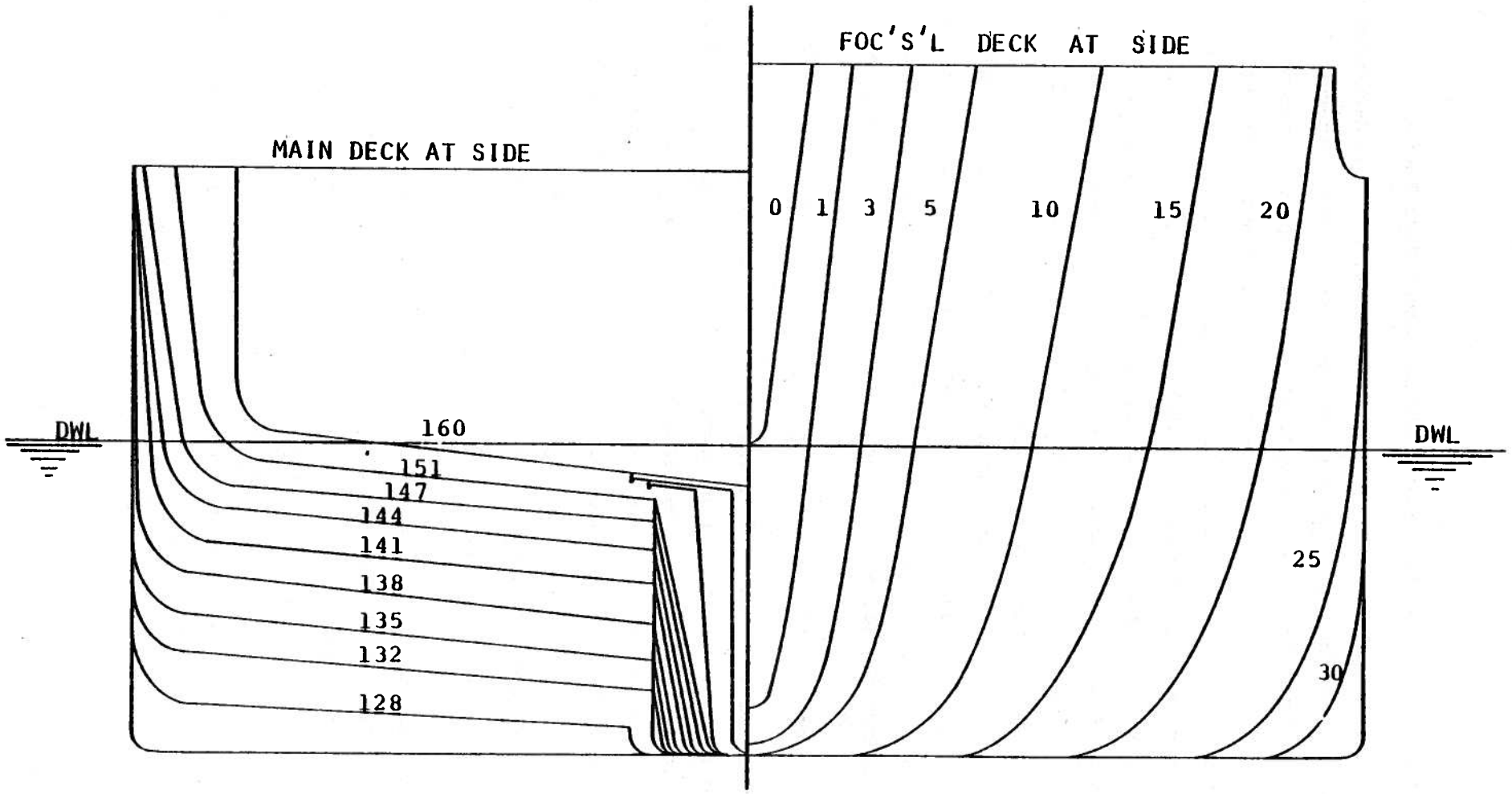

FIGURE A1 : MODEL BODY PLAN (WITH FRAME NUMBERS)

Appendix B: Spring Geometry and Decrement Test Results

This appendix shows the complete results of the decrement tests from which the added mass and damping coefficients were determined.

Figure B-1 shows the working drawing from which the model springs were made. By varying dimension A of that drawing, either a stiff spring or a relatively soft spring could be manufactured. There were six pairs of springs made, ranging in thickness from 0.425 inch to 0.770 inch. The corresponding range of the model natural frequency in water was 13.0 to 18.5 radians per second. This type of spring was used for the decrement and springing response tests. A different experimental configuration was used in measuring the exciting force.

Given the results from a decrement test record as shown in Figure 4, a number of methods were used to determine the added mass and damping terms. Since the model was restrained from heave and pitch and there were no external exciting forces or moments present, equation (3) reduced to the following:

$$\ddot{q}_2(t)(A_{22}+a_{22}) + \dot{q}_2(t)(B_{22}+b_{22}) + q_2(t)[C_{22}+K_s(1+\ell_A/\ell_F)^2] = 0 \qquad \text{(B1)}$$

The various terms have already been defined and those definitions will not be repeated here. The unknowns are the added mass, A_{22}, and damping, B_{22}, terms. (Recall that the mechanical damping, b_{22}, has been measured by vibrating the model in air at a much higher frequency.) The added mass can be simply estimated for preliminary data reduction purposes by reading the frequency of oscillation, ω_o, from the test record. The inertia terms are approximately related to the frequency in the usual way:

$$A_{22}+a_{22} = [C_{22}+K_s(1+\ell_A/\ell_F)^2]/\omega_o^2 \ . \qquad \text{(B2)}$$

The damping can be estimated by measuring the rate of decay of signal. This "logarithmic decrement" technique is described by Thomson (1972). To get more accurate values for A_{22} and B_{22}, methods suggested by Bongort (1979) or Hildebrand (1956) were used. These assumed that the decrement response was the result of a sum of exponential functions. The amplitudes, frequencies, and damping values were chosen such that the functions had a best fit to the experimental data.

Figures B-2 through B-7 show the speed dependency of the added mass and damping coefficients. Figure B-3 is repeated as Figure 5 in the main text. In all of the plots, the added mass remains nearly constant with respect to speed, while the damping coefficient shows a slight increase.

Figures B-8 through B-12 show the frequency dependency of the coefficients for a given Froude number. The Froude numbers ranged from 0.0 to 0.165. As mentionel in the main text, the damping coefficients for the .585 inch spring seem to be unusually high. In the re-test of that particular test condition, as shown in Figure 7 in the section on the short wave experiments, those high values were not repeated.

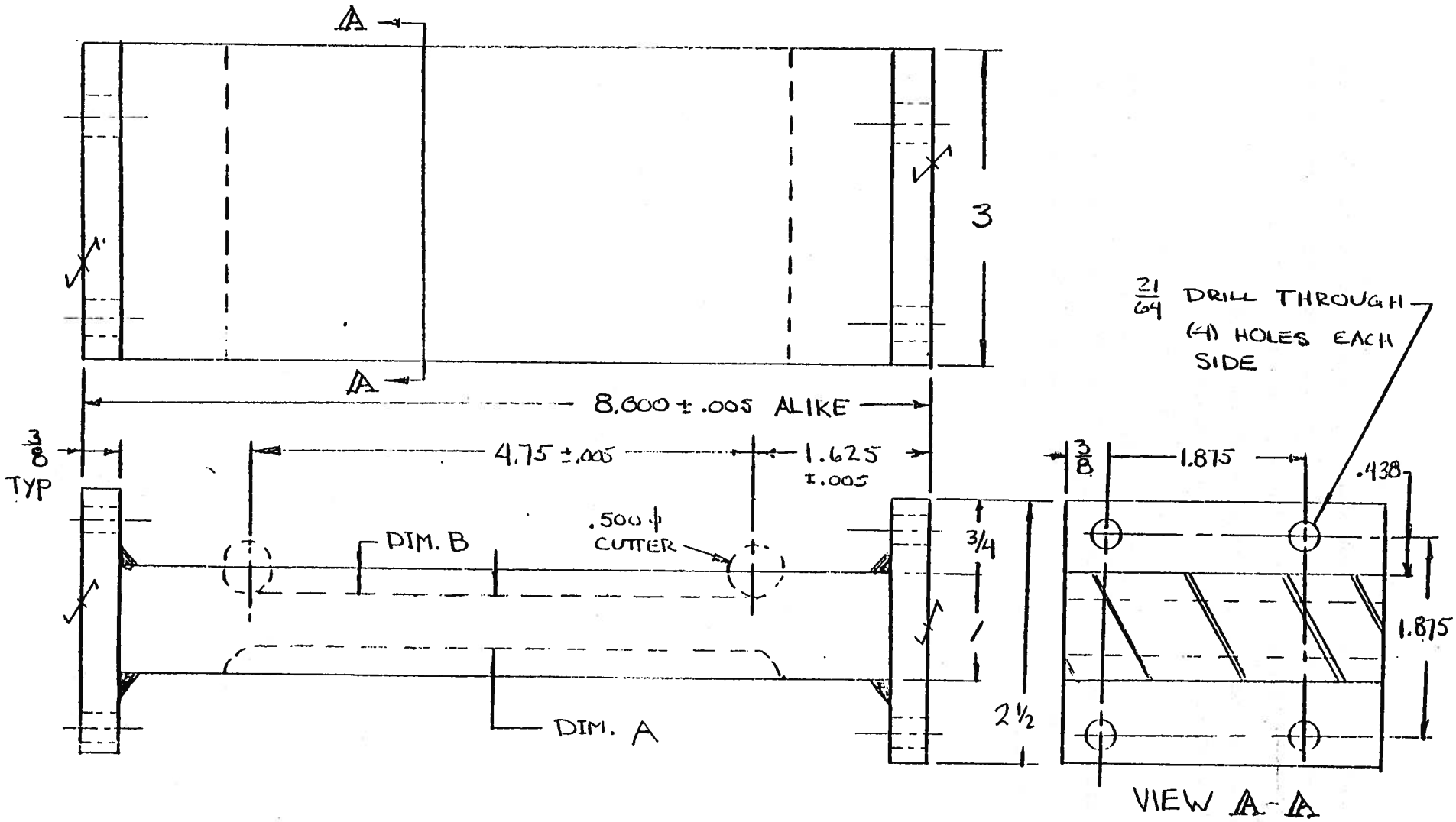

FIGURE B-1 : SPRINGS USED IN THE SPRINGING DECREMENT AND RESPONSE TESTS.

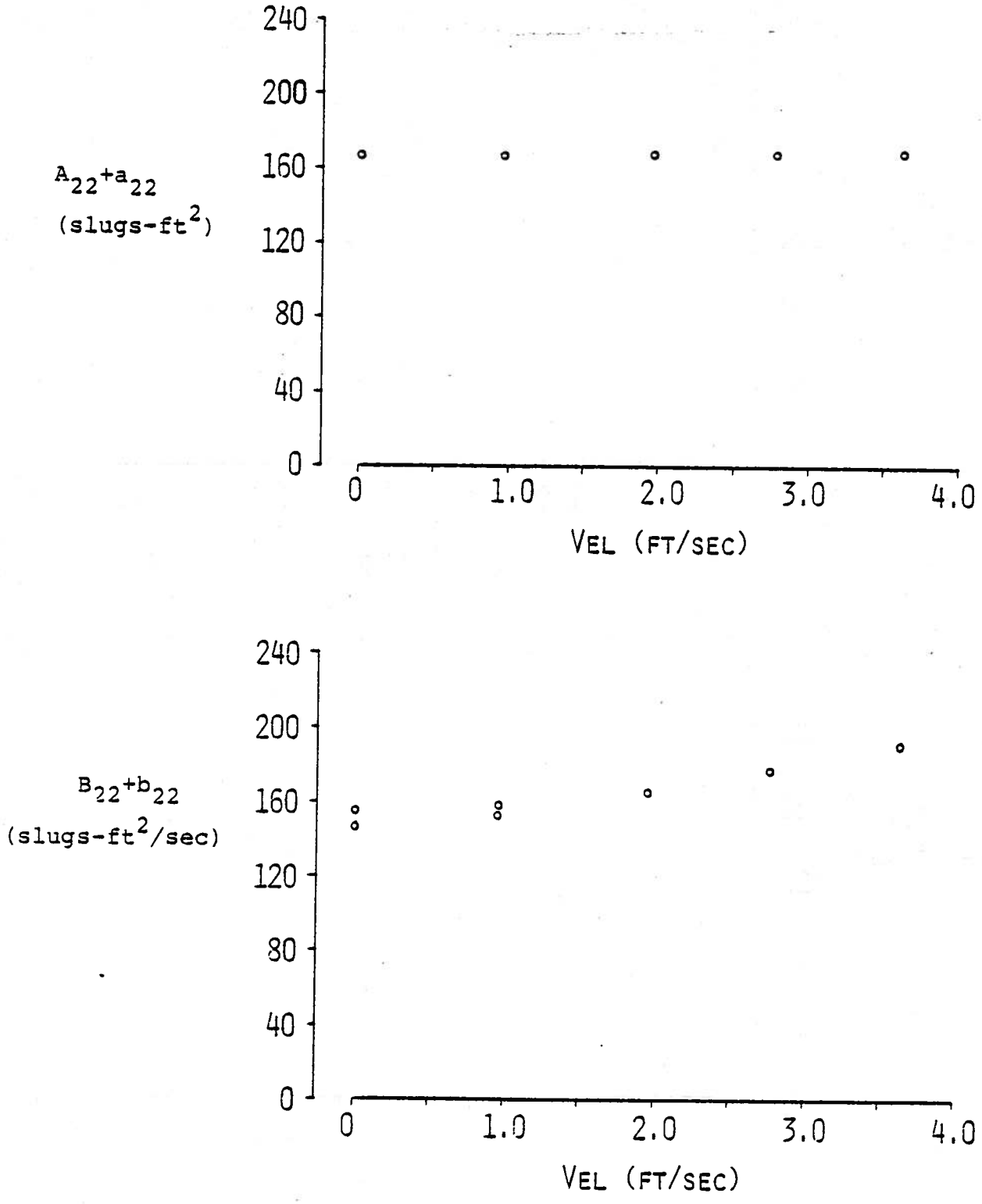

FIGURE B-2: MODEL ADDED MASS AND DAMPING AS A FUNCTION OF SPEED. FREQUENCY OF OSCILLATION $\tilde{=}$2.07 CPS. SPRING THICKNESS = .425 IN.

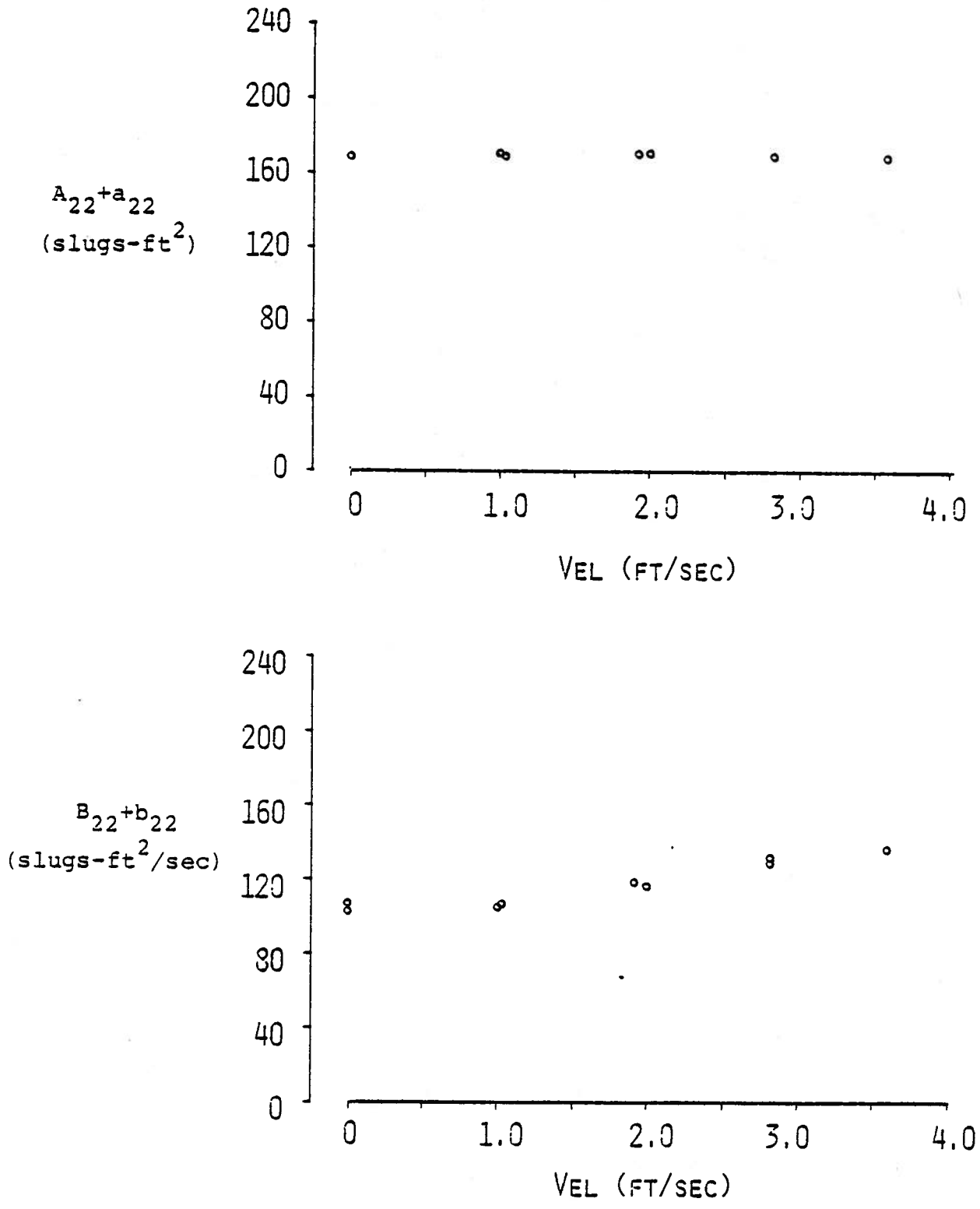

FIGURE B-3: MODEL ADDED MASS AND DAMPING AS A FUNCTION OF SPEED. FREQUENCY OF OSCILLATION ≅ 2.22 CPS. SPRING THICKNESS = .500 IN.

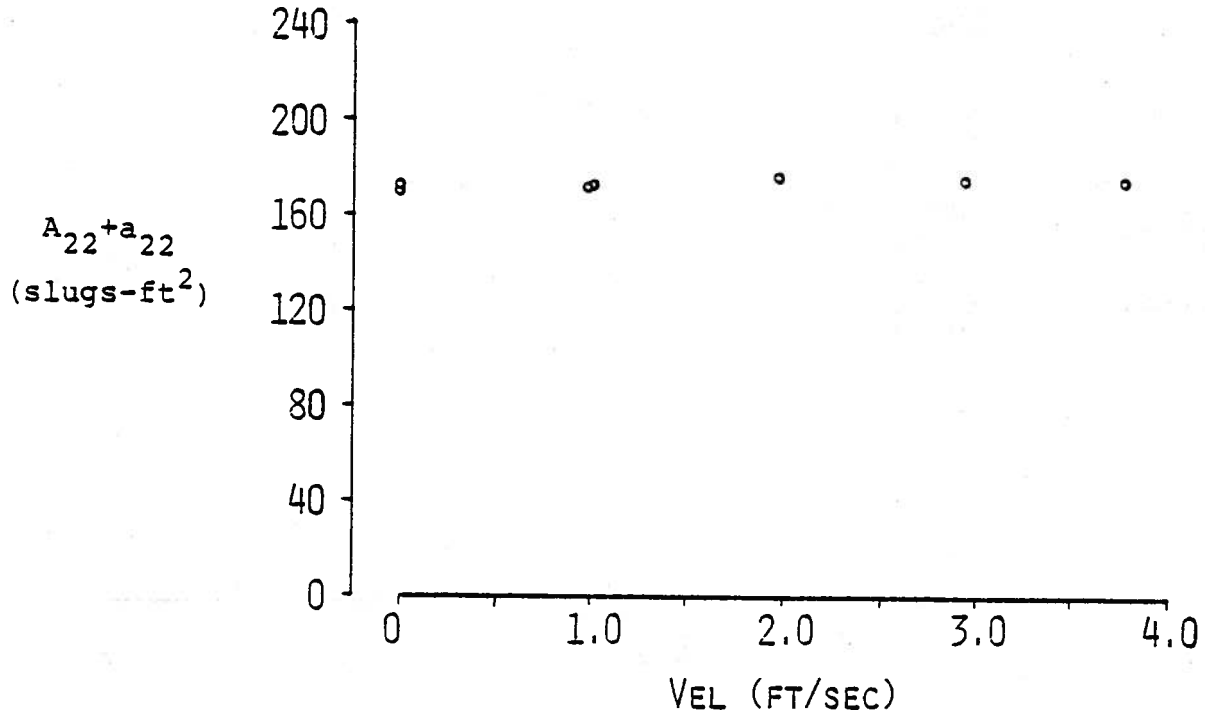

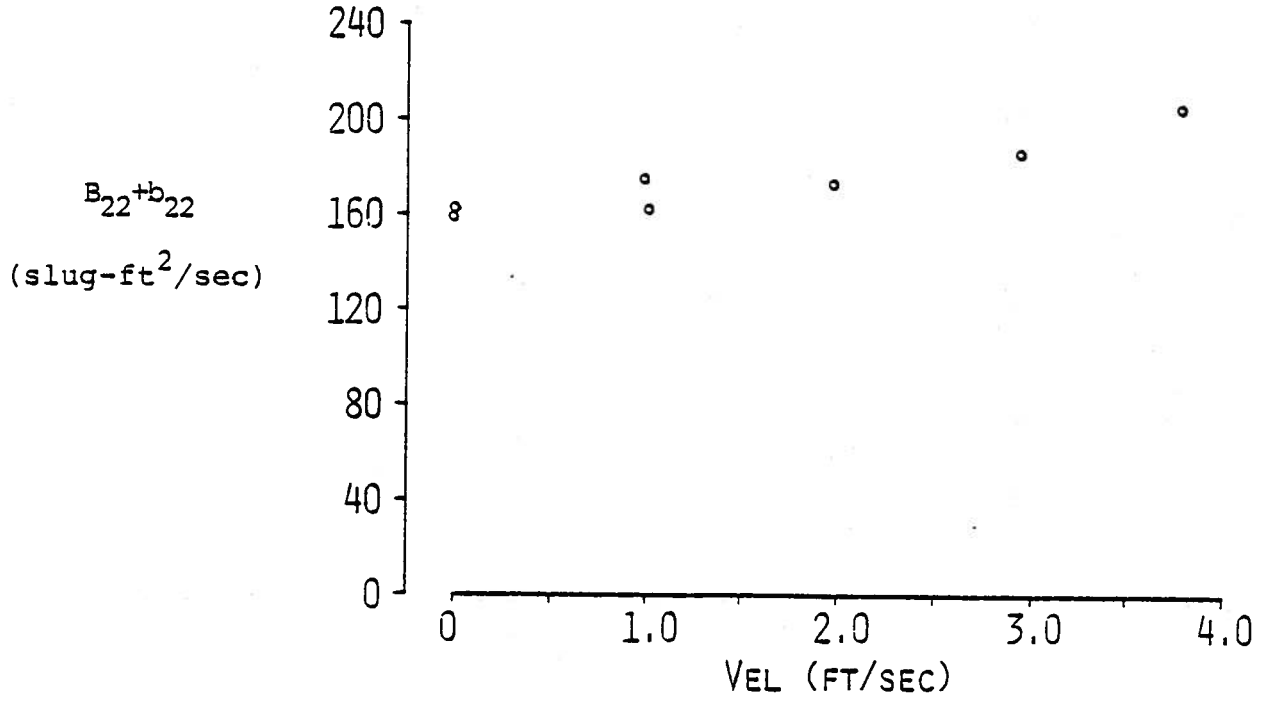

FIGURE B-4: MODEL ADDED MASS AND DAMPING AS A FUNCTION OF SPEED. FREQUENCY OF OSCILLATION $\tilde{=}$ 2.59 CPS. SPRING THICKNESS = .585 IN.

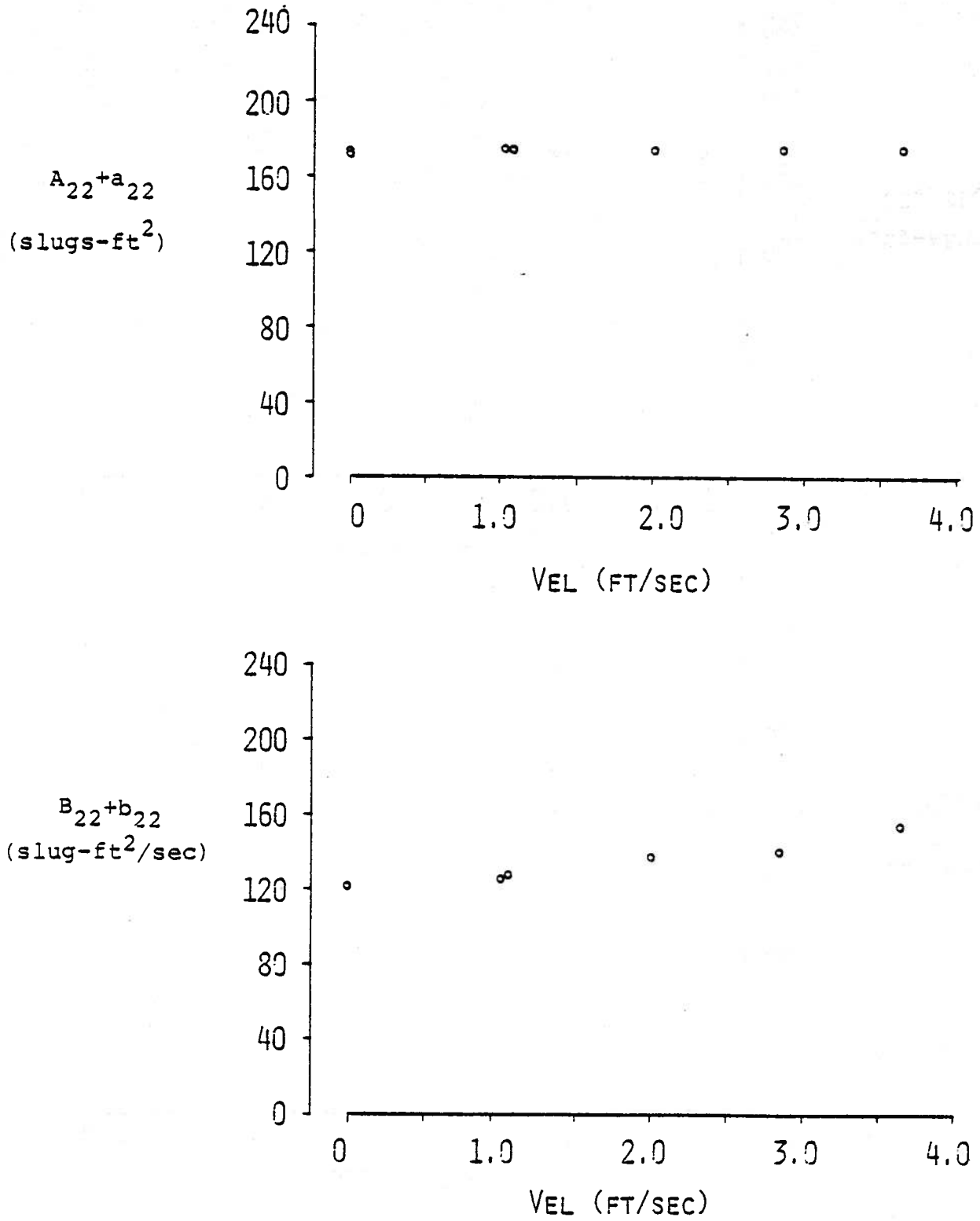

FIGURE B-5: MODEL ADDED MASS AND DAMPING AS A FUNCTION OF SPEED. FREQUENCY OF OSCILLATION $\simeq$ 2.73 CPS. SPRING THICKNESS =.645 IN.

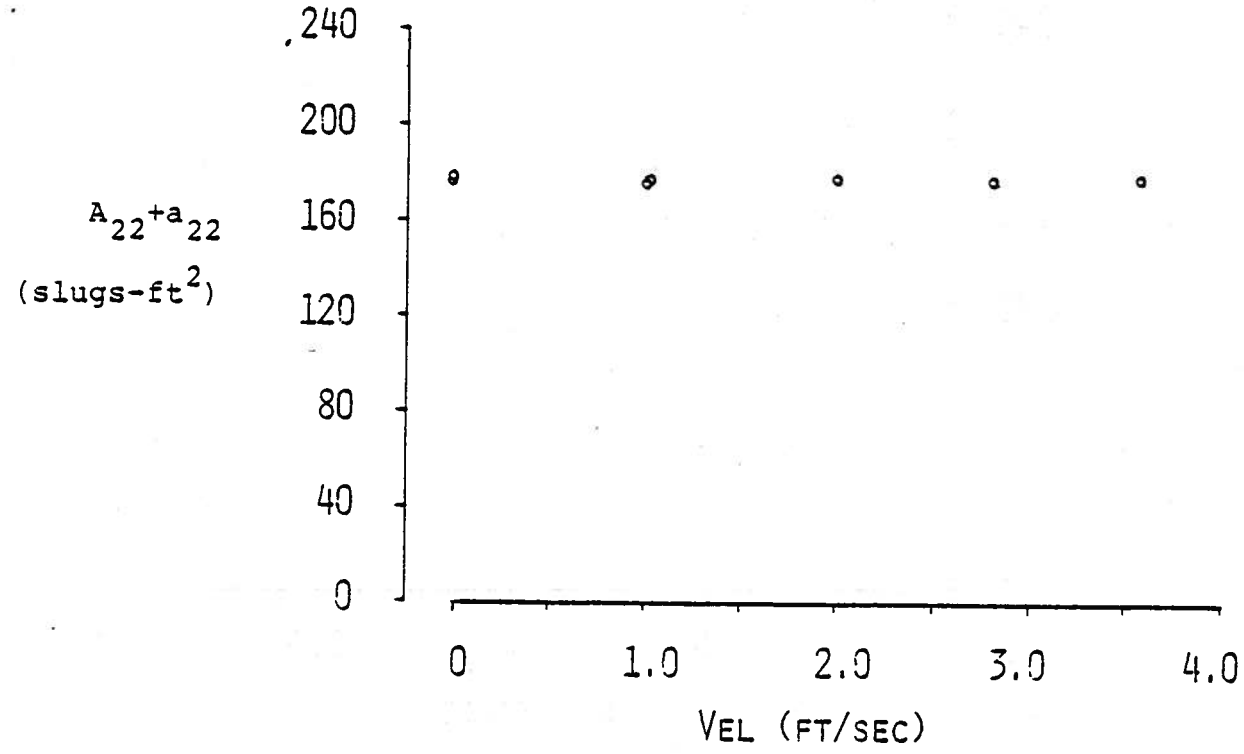

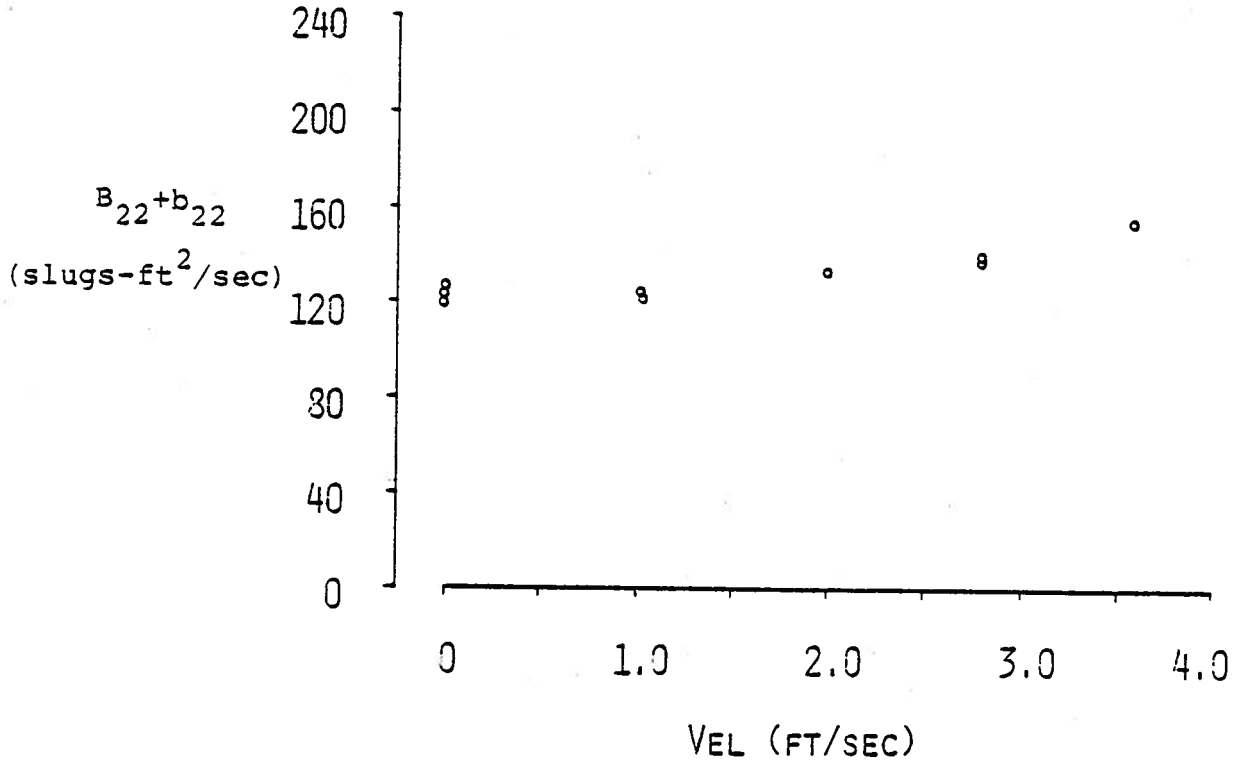

FIGURE B-6: MODEL ADDED MASS AND DAMPING AS A FUNCTION OF SPEED. FREQUENCY OF OSCILLATION $\cong$ 2.84 CPS. SPRING THICKNESS = .710 IN.

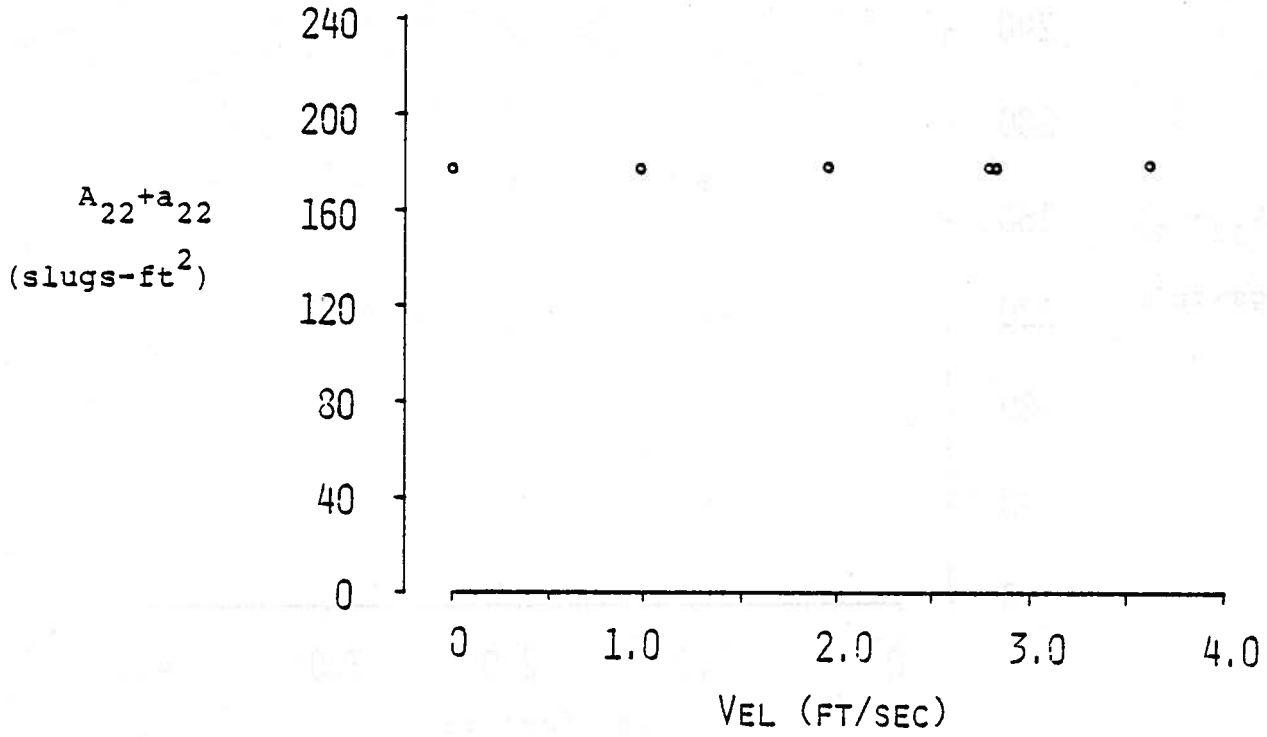

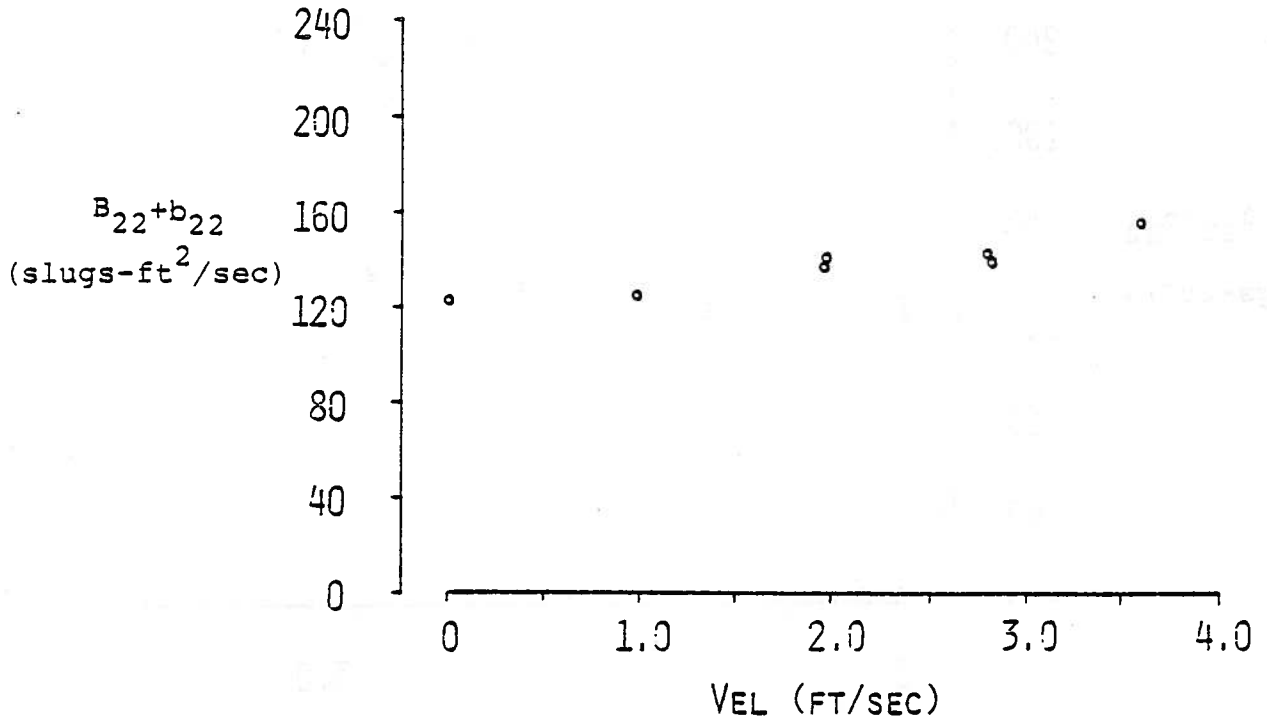

FIGURE B-7: MODEL ADDED MASS AND DAMPING AS A FUNCTION OF SPEED. FREQUENCY OF OSCILLATION $\simeq$ 2.94 CPS. SPRING THICKNESS = .770 IN.

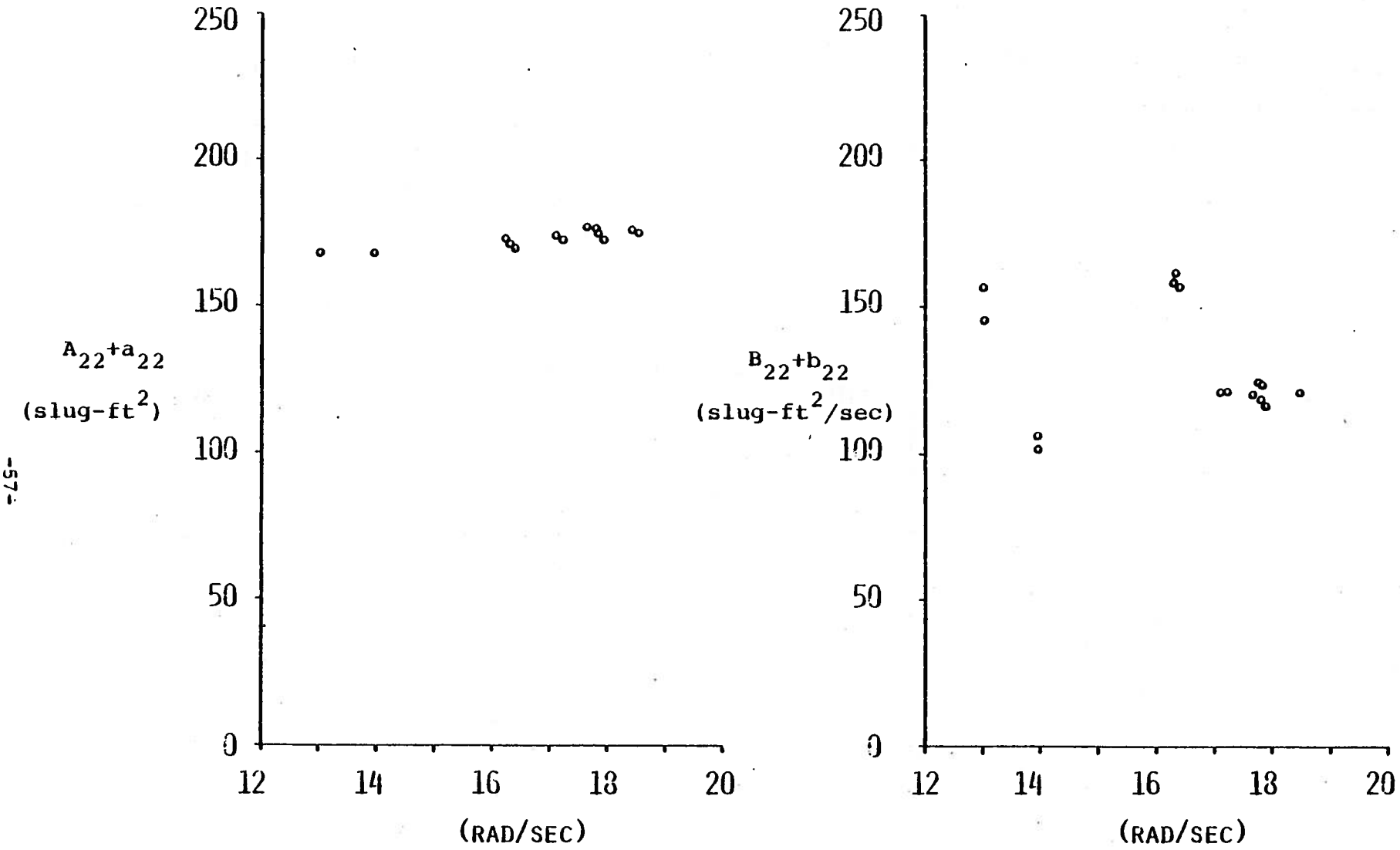

FIGURE B-3: MODEL ADDED MASS AND DAMPING AS A FUNCTION OF FREQUENCY. MODEL FROUDE NUMBER $\simeq$ 0.0

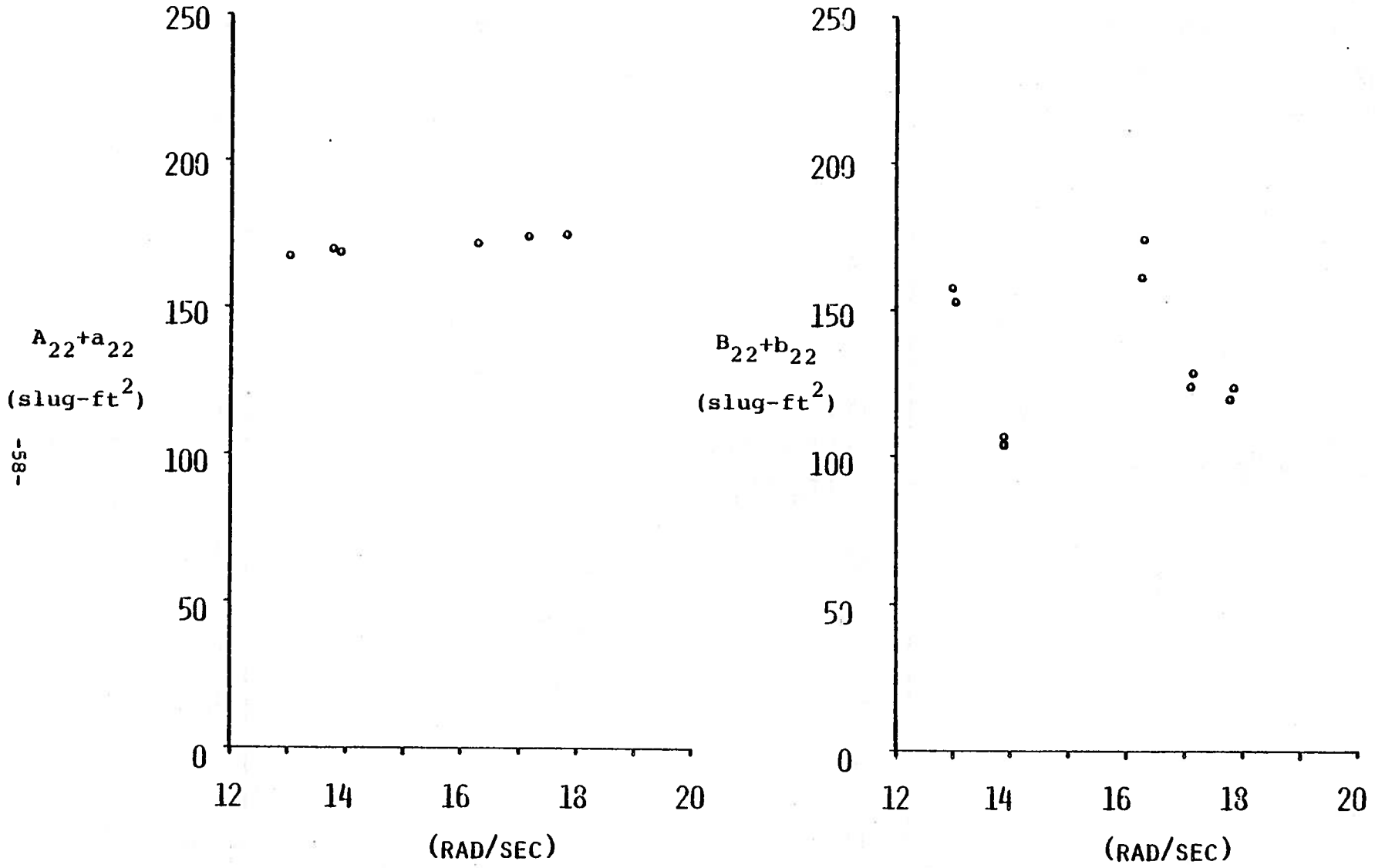

FIGURE B-9: MODEL ADDED MASS AND DAMPING AS A FUNCTION OF FREQUENCY. MODEL FROUDE NUMBER $\tilde{-}$ 0.045

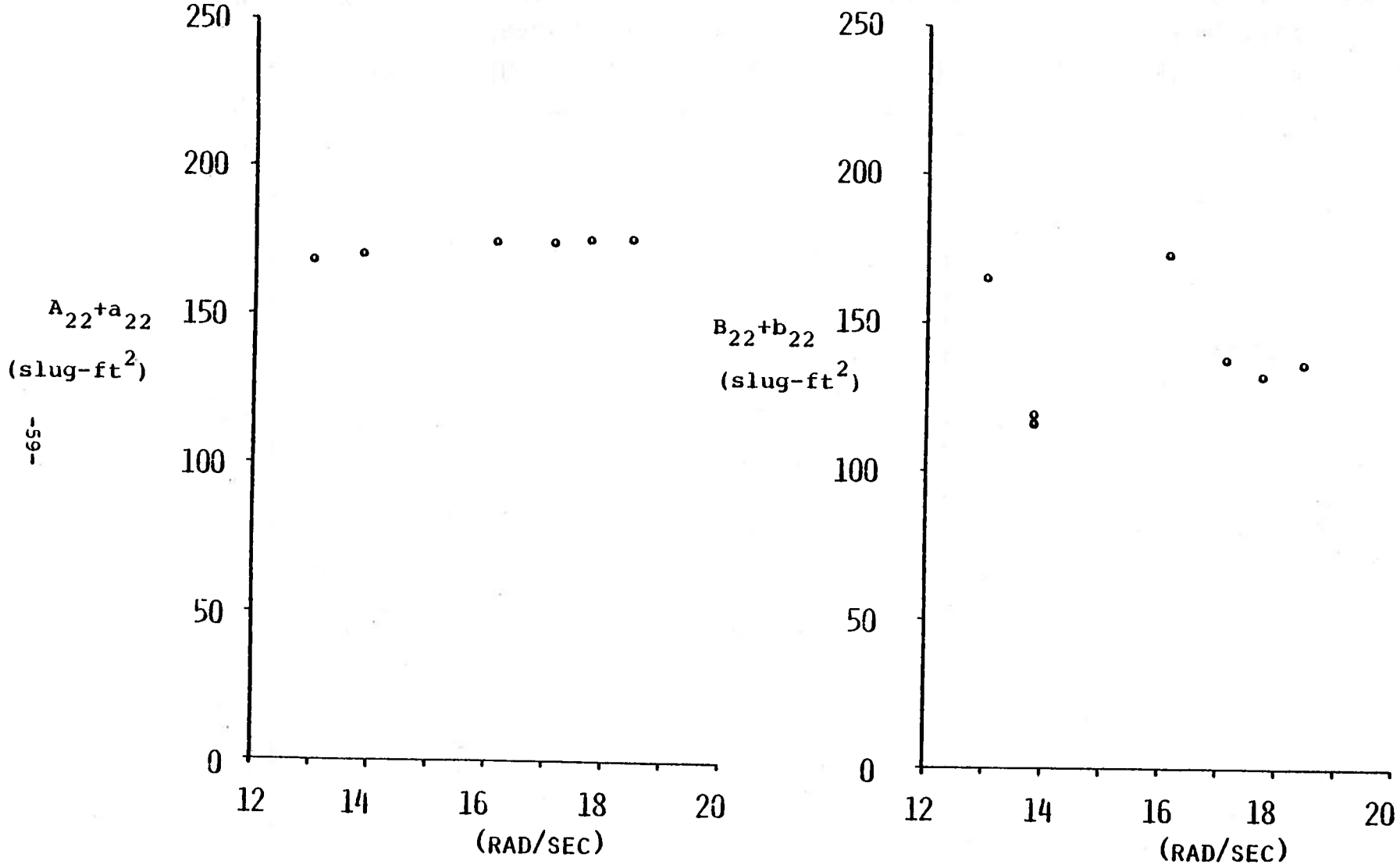

FIGURE B-10 : MODEL ADDED MASS AND DAMPING AS A FUNCTION OF FREQUENCY. MODEL FROUDE NUMBER $\tilde{=}$ 0.090

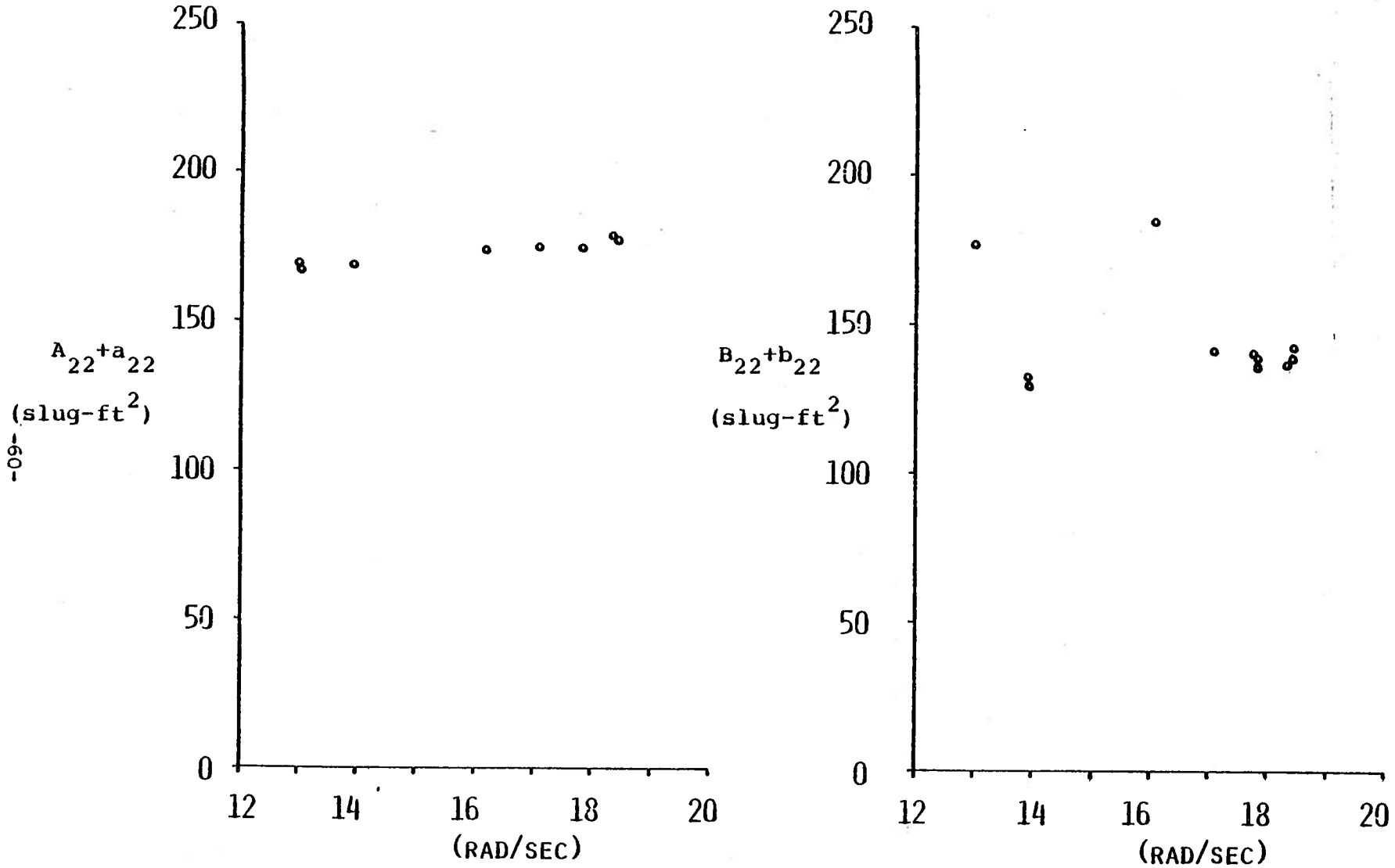

FIGURE B-11: MODEL ADDED MASS AND DAMPING AS A FUNCTION OF FREQUENCY. MODEL FROUDE NUMBER ≃ 0.128

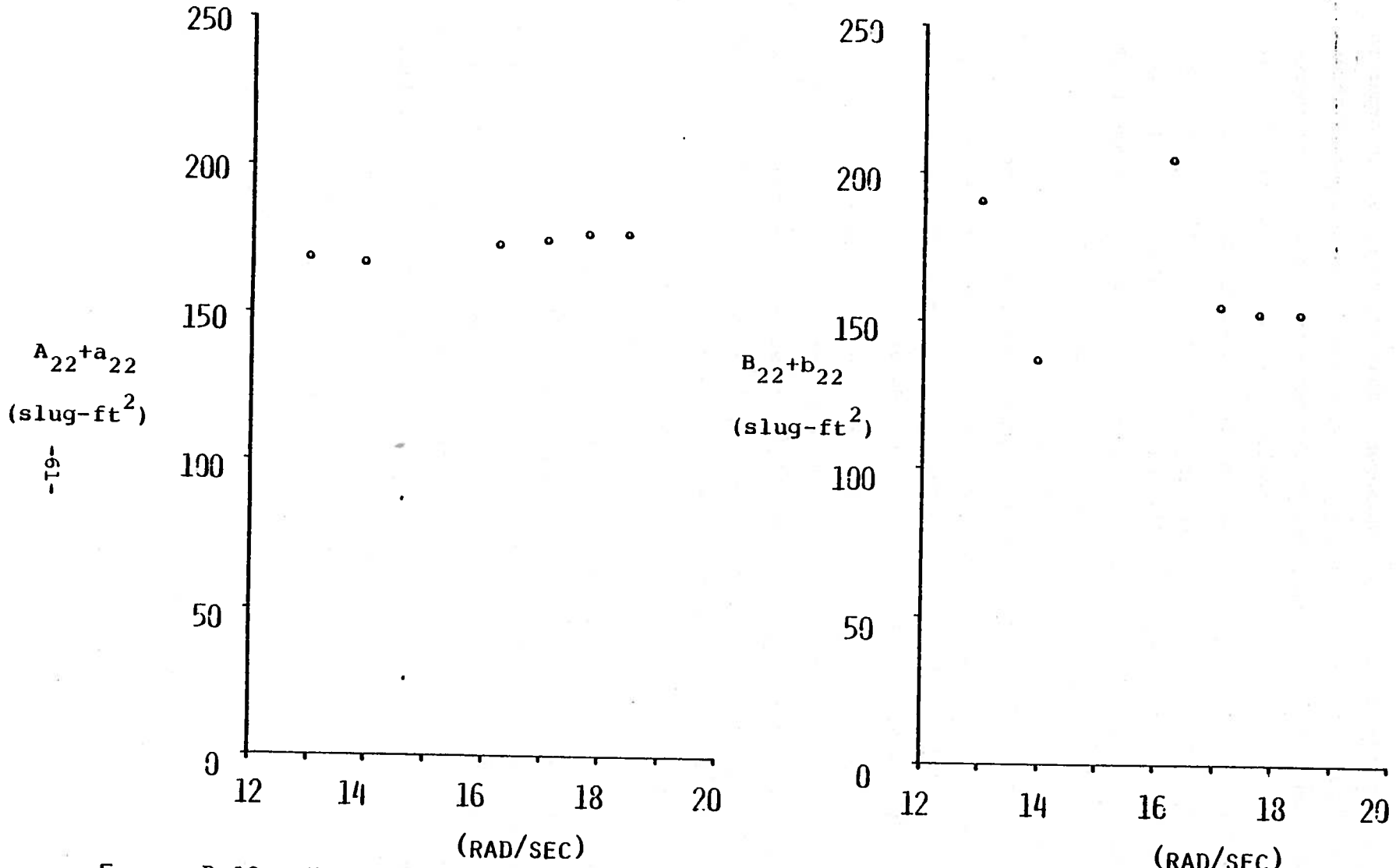

FIGURE B-12: MODEL ADDED MASS AND DAMPING AS A FUNCTION OF FREQUENCY. MODEL FROUDE NUMBER $\simeq$ 0.165

Appendix C: Experimental Springing Excitation and Data Analysis

There were three major requirements that had to be met in order to successfully measure and analyze the experimental springing excitation. First, the model had to be rigid in the sense that it would not appreciably respond (i.e. deflect) to incident waves. This would mean that all of the dynamic terms of equation (3) in the main text would be approximately equal to zero. If the model were perfectly rigid though, no excitation could be measured since no strain would exist. The second requirement was having a wave maker that would generate regular, short waves. To adequately understand the excitation mechanism in both the linear and non-linear case , it was necessary to excite the model one frequency at a time. The third requirement was for a accurate frequency analysis of both the input (the incident waves) and the output (the springing excitation). This was desirable in the linear analysis and absolutely essential in the non-linear analysis.

Figure B1 shows a sketch of the spring used in the decrement and springing response tests. If the thickness of spring is made sufficiently large, then the natural frequency of the model would be high enough not to interfere with the excitation frequency corresponding to the frequency of encounter of the incident waves. (When a mechanical system is to be used to measure a time varying quantity, it is generally felt that the stiffness of the system should be such that the natural frequency of the system is at least five times that of any of the frequencies to be measured. This will reduce the influence of any dynamic effects to or below 4%.) However, a very thick spring makes it impracticable to measure any strain for the magnitude of bending being considered. Consequently, another technique to measure the springing excitation was devised. Equation (3) of the main text shows that if there are no dynamic responses, then the generalized springing excitation, E_2, is proportional to the bending moment at midships, M_o. A device was constructed such that a force some distance above the waterline was measured. See Figure C1.

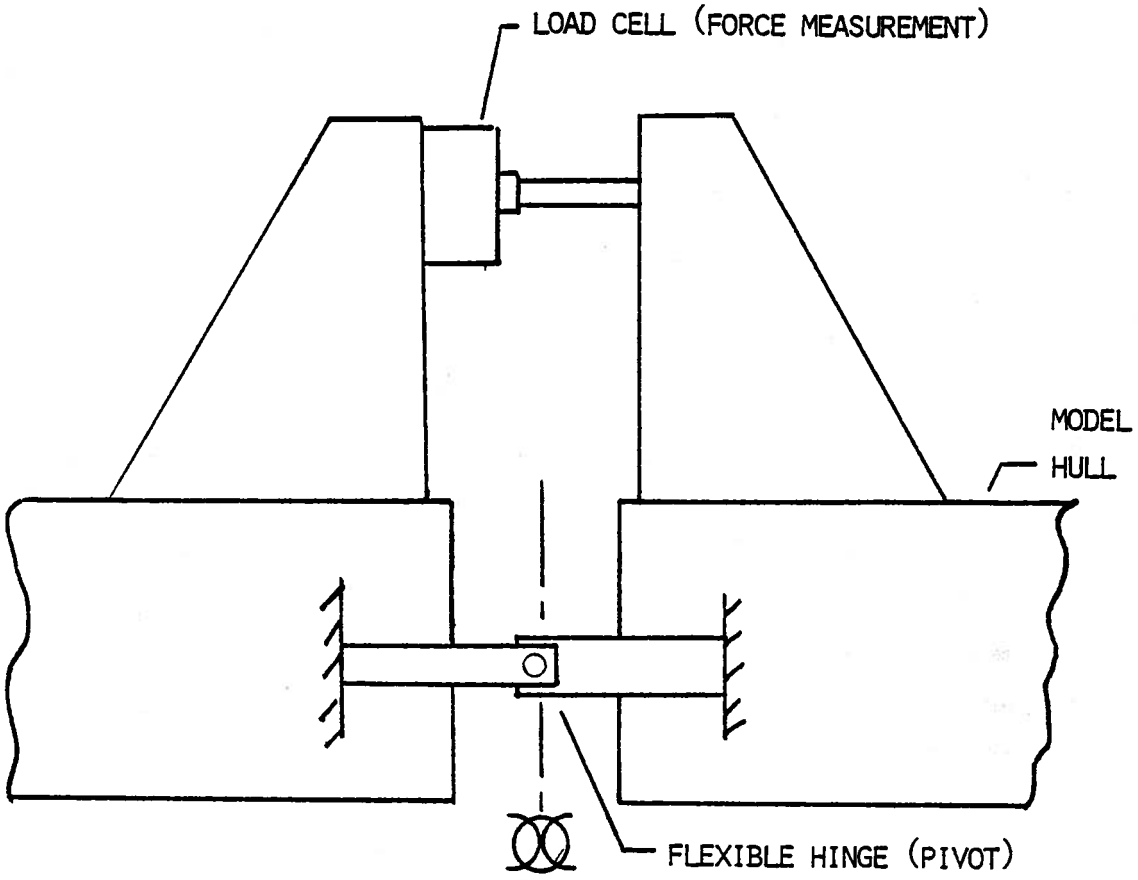

FIGURE C-1 : MECHANISM FOR MEASURING THE SPRINGING EXCITATION.

A flexible hinge was put in the location where the springs would normally go. This hinge provided no resisting moment. Since the distance from the hinge to the load cell can be measured, the bending moment at mid ships can be found. This particular configuration proved an effective way of measuring the exciting moment. With this configuration, the natural frequency of the model in water was approximately 16 cps. This was at least five times greater than any of the test frequencies.

The springing excitation tests (and also the springing response tests) were conducted in wave systems generated by a wave maker oscillating at only

one frequency per test. This is the same way that regular wave model tests would be done. However, since these short waves were slightly irregular, they were analyzed in the same manner as transients tests. In particular, the record describing the incident wave and resultant bending moment showed a signal that started from a zero or mean position, went through a dynamic response and, ideally, returned to the same zero or mean position. The zero start and end conditions meant that the Fourier Transform of the record could be successfully taken. Figure C2 shows such a record. The top record represents the incident wave signal and bottom record represents the bending moment signal. The horizontal scale is the elapsed time in seconds. In principle, all frequencies were present in the incident wave. However, most of the useful information was concentrated in a narrow band around the fundamental frequency of encounter; in this particular case, around 1.5 cps.

The records shown in Figure C2 were digitally filtered before Fourier analyzed. The Fast Fourier Transform (FFT) algorithms used in the Fourier analysis are described by Harding (1976). The actual numerical values of the FFT for the particular record shown in Figure C2 are given in Table C1. The first column is the frequency in cycles per second. The second and third columns are the FFT gain and phase of the wave amplitude. The forth and fifth columns are the FFT gain and phase of the midship bending moment, M_o. The sixth and seventh columns are the gain and phase of the transfer function. The gain in each case must be multiplied by the appropriate conversion factor in order to get the proper units. The phase is in degrees and is restricted to ± 180°. A plot of the gains of the incident wave and bending moment tabulated in Table C1 is shown in Figure C3. It is repeated in the main text as Figure 10. From Table C1, the fundamental frequency of encounter is easily established. By inspection, it occurs between 1.49 and 1.54 cps. Notice that the response of the bending moment at harmonics (3.035 and 4.527 cps) can be read. Also notice the amount of scatter in the transfer function gain. This scatter was the primary reason for restricting attention to the region around the fundamental frequency of encounter when considering the linear response.

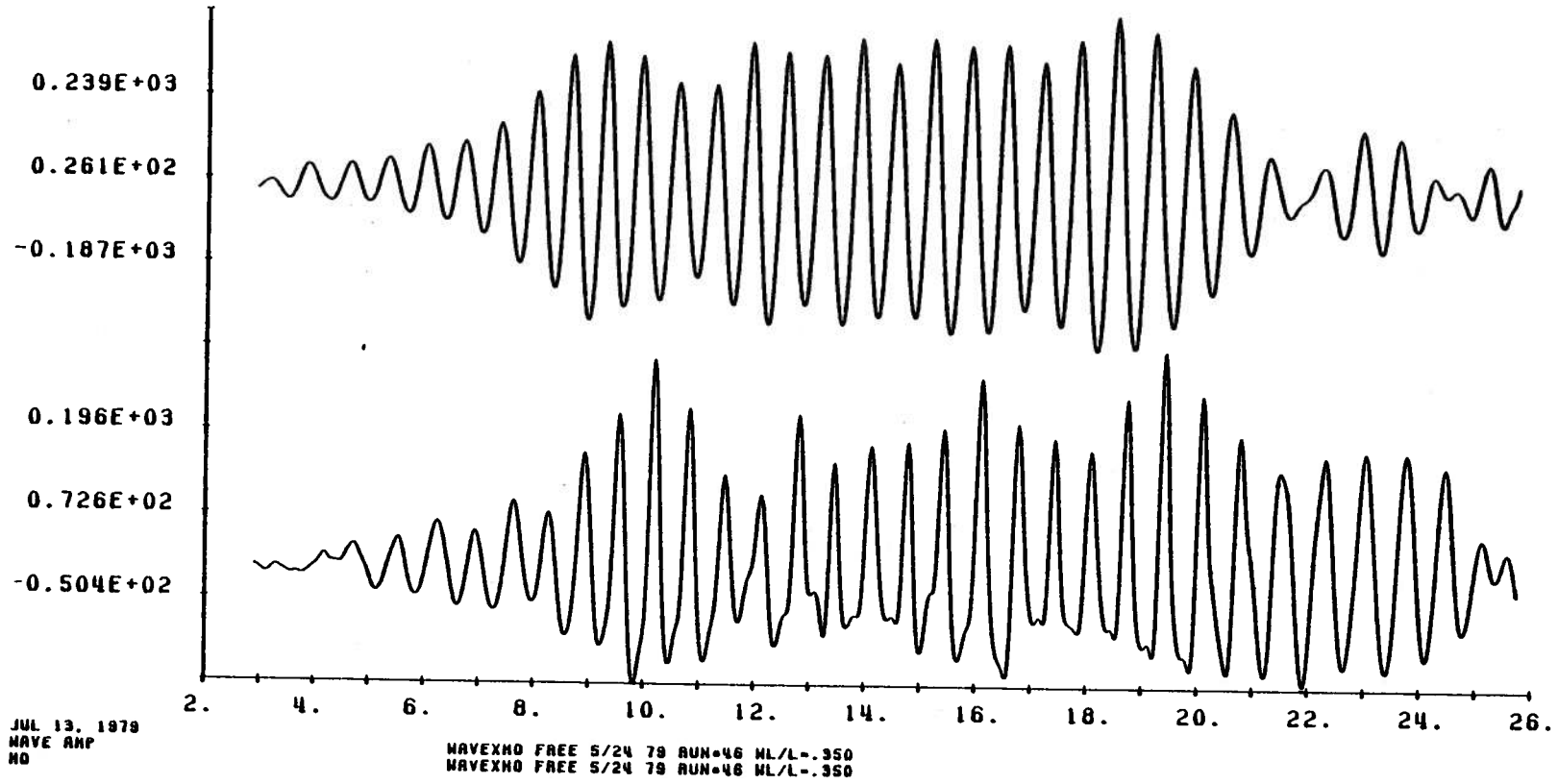

FIGURE C-2: TIME HISTORIES OF TYPICAL INCIDENT WAVE AND BENDING MOMENTS.

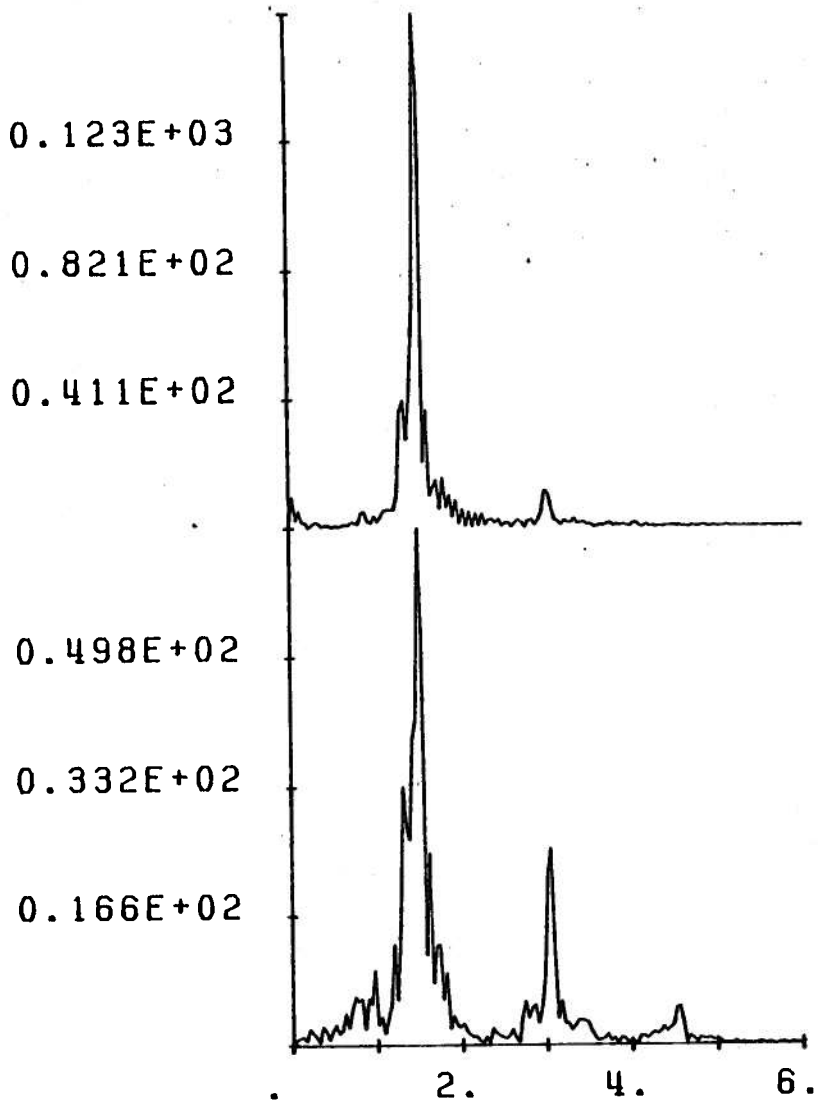

FIGURE C-3: EXAMPLE OF THE FOURIER ANALYSIS OF THE INCIDENT WAVE AND RESULTING SPRINGING EXCITATION.

TABLE C1

EXAMPLE OF FFT OF WAVE AMPLITUDE AND BENDING MOMENT

-- VARIABLE DUMP --

VAR #	VARIABLE LABEL
3	WAVE AMP
4	WAVE AMP
5	MO
6	MO
7	WAVE AMP
9	WAVE AMP

	EXPERIMENT LABEL
-FFT GAIN	WAVEXMO FREE 5/24 79 RUN#46 WL/L=.350
-FFT PHASE	WAVEXMO FREE 5/24 79 RUN#46 WL/L=.350
-FFT GAIN	WAVEXMO FREE 5/24 79 RUN#46 WL/L=.350
-FFT PHASE	WAVEXMO FREE 5/24 79 RUN#46 WL/L=.350
TRANSFR GAIN	WAVEXMO FREE 5/24 79 RUN#46 WL/L=.350
TRANSFR PHAS	WAVEXMO FREE 5/24 79 RUN#46 WL/L=.350

0.0	2.957E+00	1.800E+02	7.083E-01	0.0	2.396E-01	-1.800E+02
0.051	1.139E+01	3.116E+01	1.745E+00	-8.506E+00	1.533E-01	-2.967E+01
0.102	4.946E+00	-1.601E+01	9.675E-01	3.821E+01	1.956E-01	5.422E+01
0.154	1.878E+00	4.103E+01	9.092E-01	-3.016E+01	4.941E-01	-7.120E+01
0.205	2.851E+00	9.905E+01	3.194E+00	-5.191E+01	1.117E+00	-1.510E+02
0.257	1.931E+00	8.044E+01	9.755E-01	4.236E+01	5.052E-01	-3.808E+01
0.309	1.668E+00	-1.214E+02	9.796E-01	1.206E+02	5.875E-01	-1.180E+02
0.360	2.001E+00	7.517E+01	2.800E+00	-3.480E+01	1.399E+00	-1.100E+02
0.412	1.433E+00	7.520E+01	2.044E+00	4.942E+01	1.427E+00	-2.578E+01
0.463	3.486E-01	2.851E+01	1.546E+00	1.263E+02	4.550E+00	9.780E+01
0.514	1.573E+00	1.775E+01	3.063E-01	-2.449E+01	1.948E-01	-4.224E+01
0.566	2.329E-01	-4.615E+01	1.517E+00	8.965E+01	5.363E+00	1.349E+02
0.617	1.460E+00	-1.938E+01	3.445E+00	-1.228E+02	2.360E+00	-1.034E+02
0.669	2.688E+00	3.436E+01	1.996E-01	-9.387E+00	7.391E-02	-4.374E+01
0.720	1.945E+00	3.501E+01	7.729E+00	-8.548E+01	3.980E+00	-1.205E+02
0.772	1.926E+00	9.577E+01	9.291E+00	2.966E+01	4.823E+00	-5.711E+01
0.823	2.168E+00	-1.244E+02	5.022E+00	1.171E+02	2.317E+00	-1.185E+02
0.874	6.950E+00	-3.055E+01	3.357E+00	-1.054E+02	4.002E-01	-7.483E+01
0.926	4.185E+00	9.141E+01	1.140E+01	9.621E+01	2.725E+00	4.793E+00
0.977	6.288E-01	-1.530E+02	6.763E+00	-7.905E+01	1.076E+01	7.401E+01
1.029	6.89?E+00	2.563E+01	6.002E+00	8.102E+01	9.705E-01	5.539E+01
1.080	1.583E+00	1.325E+02	3.219E+00	1.019E+02	2.033E+00	-3.050E+01
1.132	1.225E+01	4.672E+01	8.474E+00	1.168E+02	6.986E-01	7.004E+01
1.183	7.315E+00	-3.830E+01	1.673E+01	4.718E+01	2.288E+00	8.548E+01
1.235	1.401E+01	6.997E+01	1.419E+01	1.296E+02	1.012E+00	3.966E+01
1.286	2.994E+01	1.901E+01	2.579E+01	6.483E+01	9.908E-01	4.582E+01
1.337	4.699E+01	-5.832E+01	3.272E+01	1.363E+00	6.964E-01	6.029E+01
1.389	4.216E+01	-1.173E+02	3.620E+01	-2.379E+01	8.609E-01	9.349E+01
1.440	5.414E+01	1.615E+02	4.715E+01	-8.859E+01	9.708E-01	1.098E+02
1.492	1.799E+02	4.086E+01	8.478E+01	-1.706E+02	4.713E-01	1.485E+02
1.543	1.897E+02	-1.555E+02	6.969E+01	-2.377E+01	3.673E-01	1.318E+02
1.595	2.391E+01	-1.393E+02	1.026E+01	1.260E+01	4.293E-01	1.529E+02
1.646	1.929E+01	-1.801E+01	1.863E+01	1.495E+02	1.021E+00	1.675E+02
1.698	1.491E+01	4.114E+01	1.779E+01	-1.424E+02	1.193E+00	1.765E+02
1.749	2.047E+01	8.326E+01	1.559E+01	-6.052E+01	7.611E-01	-1.438E+02
1.800	1.673E+01	1.267E+02	3.759E+00	1.649E+01	2.246E-01	-1.102E+02
1.852	1.091E+01	-1.164E+02	8.012E+00	-1.685E+02	7.342E-01	-5.209E+01
1.903	8.938E+00	-2.090E+01	5.272E+00	-1.149E+02	5.898E-01	-9.398E+01
1.955	8.978E+00	7.120E+01	4.029E+00	-6.465E+01	4.488E-01	-1.350E+02
2.006	4.651E+00	-1.263E+02	4.631E+00	-1.659E+02	9.956E-01	-3.956E+01
2.058	4.036E+00	2.385E+01	2.667E+00	-6.458E+01	6.607E-01	-8.982E+01
2.109	2.982E+00	1.539E+02	3.391E+00	-1.409E+02	1.177E+00	6.527E+01
2.160	3.976E+00	-4.770E+01	2.435E+00	-2.034E+01	6.125E-01	-3.263E+01
2.212	2.775E+00	8.126E+01	1.963E+00	-1.245E+02	7.076E-01	1.542E+02
2.263	3.239E+00	-7.777E+01	2.141E+00	-1.340E+02	6.733E-01	-2.620E+01
2.315	3.024E+00	1.099E+02	1.409E+00	-1.528E+02	4.655E-01	9.730E+01
2.366	2.584E+00	-3.647E+01	2.106E+00	-1.377E+01	8.109E-01	1.670E+01
2.418	2.986E+00	1.552E+02	2.929E+00	-1.354E+02	9.908E-01	6.942E+01

TABLE C1

(CON'T.)

2.469	2.315E+00	-9.223E-01	1.242E+00	-1.565E+02	5.366E-01	-1.555E+02
2.521	1.769E+00	-1.565E+02	5.739E-01	1.278E+02	3.243E-01	-7.566E+01
2.572	1.273E+00	8.248E+01	2.576E+00	-6.047E+01	2.023E+00	-1.429E+02
2.623	1.385E+00	-3.738E+01	1.837E+00	-1.410E+02	1.326E+00	-1.036E+02
2.675	2.453E+00	-1.279E+02	9.687E-01	1.027E+02	3.950E-01	-1.295E+02
2.726	2.426E+00	1.329E+02	6.717E+00	-3.896E+01	2.768E+00	-1.718E+02
2.778	1.088E+00	5.051E+01	5.874E+00	-1.106E+02	5.397E+00	-1.611E+02
2.829	2.852E+00	-5.428E+01	7.807E+00	1.725E+02	2.737E+00	-1.332E+02
2.881	1.994E+00	-1.728E+02	3.003E+00	4.676E+01	1.506E+00	-1.405E+02
2.932	4.207E+00	1.328E+02	5.850E+00	6.262E+00	1.390E+00	-1.266E+02
2.984	9.069E+00	5.462E+01	1.756E+01	-6.014E+01	1.937E+00	-1.148E+02
3.035	1.663E+01	-1.152E+02	3.526E+01	1.632E+02	2.120E+00	-9.156E+01
3.086	7.331E+00	4.125E+01	1.527E+01	-1.920E+01	2.083E+00	-6.046E+01
3.138	3.594E+00	4.582E+01	6.665E+00	8.357E+00	1.855E+00	-3.746E+01
3.189	1.053E+00	1.457E+02	3.686E+00	1.504E+02	3.501E+00	4.721E+00
3.241	2.329E+00	-1.578E+02	4.900E+00	-1.489E+02	2.104E+00	8.914E+00
3.292	2.319E+00	-1.157E+02	3.234E+00	-1.030E+02	1.394E+00	1.271E+01
3.344	3.178E+00	-3.913E+01	3.842E+00	-2.680E+01	1.209E+00	1.233E+01
3.395	1.675E+00	6.869E+01	3.478E+00	1.204E+02	2.076E+00	5.171E+01
3.447	2.456E+00	1.571E+02	5.045E+00	-1.345E+02	2.054E+00	6.842E+01
3.498	1.324E+00	-9.441E+01	2.573E+00	-2.983E+01	1.943E+00	6.559E+01
3.549	9.701E-01	6.634E+01	1.775E+00	-1.674E+02	1.829E+00	1.263E+02
3.601	2.378E-01	-1.021E+01	7.132E-01	-6.996E+01	2.999E+00	-5.975E+01
3.652	5.502E-01	-3.500E+01	1.100E+00	-1.638E+02	1.999E+00	-1.288E+02
3.704	2.923E-01	1.395E+02	2.139E+00	-8.084E+01	7.318E+00	1.397E+02
3.755	1.045E+00	-6.944E+01	1.118E+00	-1.685E+02	1.071E+00	-9.903E+01
3.807	6.476E-01	1.441E+02	1.190E+00	-7.904E+01	1.699E+00	1.368E+02
3.858	4.869E-01	-1.253E+02	1.764E+00	-1.351E+02	3.623E+00	-9.910E+00
3.909	5.953E-02	-2.110E+01	1.351E-01	4.499E+01	2.270E+00	1.361E+02
3.961	4.909E-01	-7.501E+01	1.127E+00	-9.600E+01	2.296E+00	-2.099E+01
4.012	7.983E-01	-1.606E+02	9.657E-01	-1.499E+02	1.210E+00	1.070E+01
4.064	1.380E+00	9.959E+01	2.738E-01	-4.110E+01	1.984E-01	-1.407E+02
4.115	4.898E-01	-4.817E+01	2.074E+00	-8.917E+01	4.242E+00	-4.100E+01
4.167	4.684E-01	-7.229E+01	1.866E+00	-1.535E+02	3.985E+00	-8.126E+01
4.218	7.660E-01	1.216E+02	1.071E+00	1.165E+02	1.398E+00	-5.129E+00
4.270	3.665E-01	-4.550E+01	2.171E+00	-5.100E+01	5.922E+00	-5.502E+00
4.321	2.313E-01	1.583E+02	2.865E+00	-1.091E+02	1.239E+01	9.261E+01
4.372	4.021E-01	-1.503E+02	2.565E+00	1.687E+02	6.380E+00	-4.101E+01
4.424	3.217E-01	3.583E+01	2.207E+00	1.209E+02	6.862E+00	8.509E+01
4.475	6.492E-01	1.410E+02	2.864E+00	2.785E+01	4.412E+00	-1.131E+02
4.527	5.484E-01	-6.315E+01	6.644E+00	-7.745E+01	1.212E+01	-1.430E+01
4.578	5.025E-01	1.062E+02	4.399E+00	1.314E+02	8.754E+00	2.518E+01
4.630	3.366E-01	-1.048E+02	1.190E+00	-1.223E+02	3.505E+00	-1.753E+01
4.681	9.567E-02	3.113E+01	1.899E+00	-9.178E+01	2.205E+01	-1.229E+02
4.733	3.633E-01	6.041E+01	3.006E-01	-4.434E+01	8.274E-01	-1.047E+02
4.784	4.321E-01	-1.273E+02	7.354E-01	1.412E+02	1.702E+00	-2.156E+01
4.835	2.351E-01	1.501E+02	1.400E+00	-1.581E+02	5.956E+00	5.177E+01
4.887	4.372E-01	2.399E+01	1.497E+00	-9.119E+01	3.402E+00	-1.152E+02
4.938	3.970E-01	-1.031E+02	3.836E-01	1.485E+00	9.663E-01	1.046E+02
4.990	1.190E-01	1.330E+02	9.957E-01	-1.702E+02	8.378E+00	5.678E+01
5.041	1.525E-01	9.234E-01	9.544E-01	-1.016E+02	6.258E+00	-1.025E+02
5.093	2.879E-01	-4.377E+01	4.164E-01	-1.330E+02	1.446E+00	-9.427E+01
5.144	1.471E-01	-8.633E+01	7.533E-01	-1.071E+02	5.122E+00	-2.073E+01
5.195	5.045E-01	1.507E+02	5.033E-01	-1.799E+02	9.976E-01	2.337E+01
5.247	3.310E-01	-9.414E+01	8.406E-01	-1.145E+02	2.539E+00	-3.034E+01
5.298	2.336E-01	-1.384E+02	5.099E-01	-1.409E+02	2.178E+00	-2.597E+00
5.350	1.390E-01	-1.784E+01	6.012E-01	-1.317E+02	4.326E+00	-1.139E+02
5.401	1.530E-01	1.068E+02	5.352E-01	-1.391E+02	3.505E+00	1.140E+02
5.453	3.677E-01	-9.439E+01	4.398E-01	-1.040E+02	1.196E+00	-1.359E+01
5.504	2.416E-02	-9.308E+01	7.664E-01	-1.171E+02	3.172E+01	-2.406E+01

TABLE C1

(CONT'T.)

5.556	9.965E-02	-9.429E+01	6.272E-01	-1.507E+02	6.294E+00	-5.645E+01
5.607	3.936E-02	-3.913E+01	3.135E-01	-1.273E+02	7.966E+00	-9.815E+01
5.658	1.196E-01	-1.737E+02	6.406E-01	-1.157E+02	5.432E+00	5.799E+01
5.710	1.759E-01	-1.185E+02	7.809E-01	-1.316E+02	4.438E+00	-2.311E+01
5.761	1.001E-01	6.395E+00	3.092E-01	-1.769E+02	3.078E+00	1.768E+02
5.813	1.124E-01	1.498E+02	3.892E-01	-8.463E+01	3.453E+00	1.255E+02
5.864	1.056E-01	-1.622E+02	8.485E-01	-1.089E+02	8.038E+00	5.331E+01
5.916	1.752E-01	-1.250E+02	6.733E-01	-1.311E+02	3.842E+00	-5.125E+00
5.967	1.337E-01	-1.114E+02	6.589E-01	-1.592E+02	4.927E+00	-4.781E+01
6.019	1.241E-01	1.387E+02	8.180E-02	-7.994E+01	6.590E-01	1.413E+02
6.070	1.126E-01	-4.204E+01	9.481E-01	-1.166E+02	8.420E+00	-7.457E+01
6.121	1.001E-01	-1.674E+02	3.054E-01	-1.422E+02	3.061E+00	2.526E+01
6.173	7.486E-02	-1.340E+02	4.194E-01	-1.470E+02	5.603E+00	-1.304E+01
6.224	1.188E-02	-1.293E+02	5.613E-01	-1.298E+02	4.725E+01	-4.806E-01
6.276	4.358E-02	-1.789E+02	4.296E-01	-1.236E+02	9.857E+00	5.527E+01
6.327	9.063E-02	-1.361E+02	4.206E-01	-1.255E+02	5.217E+00	1.059E+01
6.379	4.120E-02	-1.518E+02	4.606E-01	-1.359E+02	1.118E+01	1.587E+01
6.430	5.267E-02	-1.371E+02	5.032E-01	-1.315E+02	8.030E+00	5.583E+00
6.481	4.296E-02	-1.354E+02	4.427E-01	-1.246E+02	1.031E+01	1.085E+01
6.533	3.808E-02	-1.661E+02	4.182E-01	-1.345E+02	1.098E+01	3.150E+01
6.584	6.460E-02	-1.327E+02	4.348E-01	-1.308E+02	6.730E+00	1.877E+00
6.636	3.054E-02	-1.455E+02	4.326E-01	-1.333E+02	1.420E+01	1.221E+01
6.687	4.659E-02	-1.345E+02	4.397E-01	-1.311E+02	9.438E+00	3.449E+00
6.739	4.049E-02	-1.355E+02	4.245E-01	-1.323E+02	1.048E+01	3.267E+00
6.790	5.469E-02	-1.491E+02	4.347E-01	-1.316E+02	7.950E+00	1.758E+01
6.842	4.111E-02	-1.390E+02	4.270E-01	-1.321E+02	1.039E+01	6.944E+00
6.893	5.103E-02	-1.390E+02	4.245E-01	-1.322E+02	9.319E+00	6.872E+00
6.944	4.162E-02	-1.449E+02	4.190E-01	-1.329E+02	1.009E+01	1.204E+01
6.996	4.600E-02	-1.423E+02	4.156E-01	-1.327E+02	9.033E+00	9.581E+00